2011

INCREASED BMP SIGNALING DECREASES EPITHELIAL OVARIAN CANCER TUMOUR GROWTH ON THE CHICK CAM BY INHIBITING ANGIOGENESIS

Jason Matthew Reed

INCREASED BMP SIGNALING DECREASES EPITHELIAL OVARIAN CANCER TUMOUR GROWTH ON THE CHICK CAM BY INHIBITING ANGIOGENESIS

(Spine title: Active BMP signaling decreases EOC angiogenesis on chick CAM)

(Thesis format: Monograph)

By

Jason Reed

Graduate Program in Anatomy and Cell Biology

A thesis submitted in partial fulfillment
of the requirements for the degree of
Master of Science

The School of Graduate and Postdoctoral Studies
The University of Western Ontario
London, Ontario, Canada

THE UNIVERSITY OF WESTERN ONTARIO
SCHOOL OF GRADUATE AND POSTDOCTORAL STUDIES

CERTIFICATE OF EXAMINATION

Supervisor

Dr. Trevor Shepherd

Co-Supervisor

Dr. Gabriel DiMattia

Supervisory Committee

Dr. Alison Allan

Dr. John Lewis

Examiners

Dr. Kaiping Yang

Dr. Martin Sandig

Dr. Peeyush Lala

The thesis by

Jason Matthew Reed

entitled:

Increased BMP Signaling Decreases Epithelial Ovarian Cancer Tumour Growth on the Chick CAM by Inhibiting Angiogenesis

is accepted in partial fulfillment of the
requirements for the degree of
Master of Science

Date_____

_____
Chair of the Thesis Examination Board

ABSTRACT

Current limitations regarding the treatment of metastatic epithelial ovarian cancer (EOC) are attributed to our poor overall understanding of its progression due to the limited number of appropriate model systems. To this end, I have characterized EOC tumour growth and angiogenesis using the innovative chick chorioallantoic membrane (CAM) model system. Bone morphogenetic protein (BMP) signaling has been implicated in multiple processes of EOC metastasis, although its role in tumour angiogenesis has never been assessed. I found an inverse correlation between the level of BMP signaling in mouse EOC cells and their abilities to induce angiogenesis both *in vitro* using HUVEC tube formation assays and *in vivo* using a chick CAM angiogenesis collagen onplant assay. These results support the further implementation of the chick CAM as an important tool to study EOC metastasis. Additionally, the putative anti-angiogenic role of BMP4 signaling from my work highlights potential future implications for this pathway in prognostics and treatment of EOC.

Keywords: Bone Morphogenetic Protein, Chick Chorioallantoic Membrane, Epithelial Ovarian Cancer, Angiogenesis, Tumour Formation, Metastasis

ACKNOWLEDGEMENTS

I would like to thank my supervisor, Dr. Trevor Shepherd, and my co-supervisor, Dr. Gabriel DiMattia, for giving me the opportunity to work on such an exciting project. I would never have been able to reach the goals that I was hoping to achieve when I started my research without the tremendous guidance that I have received from both of you over the past two years.

I would also like to thank the other members of my supervisory committee: Dr. Alison Allan, and Dr. John Lewis. Your insights and suggestions were greatly appreciated, and were essential to guiding my project in the positive direction that it has taken.

Dr. Lewis has also been very accommodating in giving me the opportunity to work with the chicks and imaging equipment in his lab. Specifically, I would like to thank Amber Ablack, Laura Fung, and Hon Leong in the Lewis lab. You were very kind for taking the time to teach me how to use the equipment in your lab and how to perform all of the chick CAM assays.

I would also like to thank Yudith Ramos-Valdés for creating the mouse ovarian cancer GFP clones that have been essential for completing many of my experiments. In addition to Yudith, I want to say thank you to the other members of the Shepherd/DiMattia lab: Teresa Peart and Rohann Correa. Your friendship, encouragement, and advice have all been instrumental in the completion of my degree.

TABLE OF CONTENTS

LIST OF FIGURES

LIST OF ABBREVIATIONS

ALK	activin receptor-like kinase
AMEM	Alpha Modification of Eagles' Medium
Apc	adenomatous polyposis coli
BAMBI	BMP and activin receptor membrane bound inhibitor
BBE	bovine brain extract
BCC	basal cell carcinoma
Bcl	B-cell lymphoma
bHLH	basic helix-loop-helix
BMP	bone morphogenetic protein
BMPER	BMP binding endothelial regulator
BMPR	bone morphogenetic protein receptor
BRAF	v-raf murine sarcoma viral oncogene homolog
BRCA	breast cancer associated gene
BSA	bovine serum albumin
BTIC	brain tumour-initiating cell
CA-125	cancer antigen 125
CAM	chorioallantoic membrane
CA-MSC	ovarian carcinoma-associated mesenchymal stem cell
cDNA	complimentary deoxyribonucleic acid
c-Myc	v-myc myelocytomatosis viral oncogene homolog
co-Smad	common mediator mothers against decapentaplegic
Cox2	cyclooxygenase-2

CRC-SC	colorectal cancer stem cell
CSC	cancer stem cell
c-Ski	v-ski sarcoma viral oncogene homolog
CTNNB1	catenin (cadherin-associated protein), beta 1
DMEM	Dulbecco's Modified Eagle's Medium
DMSO	dimethyl sulfoxide
DNA	deoxyribonucleic acid
E	embryonic day
EGM	endothelial cell complete growth medium
EGTA	ethylene glycol tetraacetic acid
EHS	Engel-Holm-Swarm
EOC	epithelial ovarian cancer
EMT	epithelial-mesenchymal transition
ERK	extracellular signaling regulated kinase
FBS	fetal bovine serum
FU	fluorouracil
GBM	glioblastoma
GDF	growth and differentiation factor
GFAP	glial fibrillary acidic protein
GFP	green fluorescent protein
GNP	granule neuron progenitor
HA	hemagglutinin
HCC	hepatocellular carcinoma

HMEC	human microvascular endothelial cell
HRP	horseradish peroxidase
HUVEC	human umbilical vein endothelial cell
ID	inhibitor of DNA binding
IL8	interleukin-8
JNK	Jun N-terminal kinase
KRAS	v-Ki-ras2 Kirsten rat sarcoma viral oncogene homolog
MAF	malignant ascites fluid
MAPK	mitogen-activated protein kinase
MIS	Müllerian inhibiting substance
MISRII	Müllerian inhibiting substance type II receptor
MMP	matrix metalloproteinase
MOSE	mouse ovarian surface epithelium
mRNA	messenger ribonucleic acid
MSCV PIG	murine stem cell virus Puro IRES GFP
MSX	msh homeobox
Myo10	myosin x
NF-κB	nuclear factor kappa-light-chain-enhancer of activated B cells
OSCC	oral squamous cell carcinoma
OSE	ovarian surface epithelium
PARP	poly ADP ribose polymerase
PBS	phosphate-buffered saline
PCR	polymerase chain reaction

PI3KCA	phosphoinositide-3-kinase, catalytic, alpha polypeptide
PKC	protein kinase C
PMSF	phenylmethanesulfonylfluoride
Pten	phosphatase and tensin homolog
PVDF	polyvinylidene difluoride membrane
Rb	retinoblastoma protein
RNA	ribonucleic acid
R-Smad	receptor-activated mothers against decapentaplegic
SCID	severe combined immunodeficiency
SDS-PAGE	sodium dodecyl sulphate polyacrylamide gel electrophoresis
SEM	standard error of the mean
siRNA	small interfering ribonucleic acid
sL1	soluble adhesion protein-1
Smad	mothers against decapentaplegic
Smurf	SMAD specific E3 ubiquitin protein ligase
Src	sarcoma (Schmidt-Ruppin A-2) viral oncogene homolog
SV40 TAg	simian virus 40 large T antigen
TBS	Tris-buffered saline
TBS-T	Tris-buffered saline-Tween 20
TGFβ	transforming growth factor-beta
TP53	tumour protein p53
TSP	thrombospondin
ULA	ultra-low attachment

VEGF	vascular endothelial growth factor
VSVG	vesicular stomatitis virus glycoprotein

CHAPTER ONE

INTRODUCTION

1.1 Overview of ovarian cancer

1.1.1 Prevalence and mortality

Ovarian cancer is the seventh most common type of cancer in women, and it is estimated that there were 2,600 new cases of ovarian cancer in Canada this past year. This represents 3% of the 83,900 total new cases of cancer among women in Canada in 2010 (Canada 2010). Although this is a fairly small percentage of the total number of new cancer incidences, ovarian cancer is the most lethal gynecologic cancer in the western world, and is responsible for more deaths than endometrial and cervical cancer combined (Ozols, Bookman et al. 2004). This is highlighted by the fact that it was the fifth deadliest cancer in terms of mortality in women, and accounted for approximately 5% of the 36,200 cancer related deaths among females in Canada in 2010 (Canada 2010). Although much research has gone into developing treatments for ovarian cancer, there was only a 0.5% decrease in mortality rates among women with ovarian cancer in Canada between 1996 and 2005. Conversely, other cancers such as lung and breast cancer have mortality rates that have decreased by over 2% during the same period of time.

1.1.2 Detection and screening for ovarian cancer

These recent successes in declining mortality rates for other cancers such as lung and breast has been largely attributed to important advancements with respect to early

detection and treatment (Canada 2010). Unfortunately, ovarian cancer is not usually detected during its early stages due to a low specificity of recognizable signs and symptoms (Goff, Mandel et al. 2007). The most common symptoms that women report before they are diagnosed with ovarian cancer are pelvic and abdominal pain, bloating and an increased size of abdomen, increased frequency of urination, and a low desire to eat for periods of at least 1 year preceding diagnosis. Therefore, patients and physicians will often attribute many of these symptoms to other general gynecological concerns such as menstrual problems, aging, or menopause (Argento, Hoffman et al. 2008).

The most common methods that are currently used clinically to detect ovarian cancer are transvaginal ultrasounds, and the measurement of blood circulating marker CA-125 (Argento, Hoffman et al. 2008), which is an antigen that is expressed by the coelomic epithelium (Jacobs and Menon 2004). However, there are several processes other than ovarian cancer that can disrupt the coelomic epithelium such as pregnancy, appendicitis, ovarian cysts, and endometriosis, thereby complicating the interpretations of CA-125 blood test results (Cragun 2011). As well, CA-125 can be elevated in other cancers such as pancreatic, uterine, and lung cancer. Overall, CA-125 is expressed in approximately 50% of early stage ovarian cancers. However, there is a large frequency of false positives and false negatives in CA-125 screening, which suggests that this screening method is not specific or sensitive enough to be used as a definitive tool to diagnose ovarian cancer. The other common screening method that is used to detect ovarian cancer is transvaginal ultrasounds, which attempt to differentiate benign from malignant masses (Cragun 2011). Although this screening method is argued to be the most effective current method for detecting early stage ovarian cancer, it is only able to

distinguish between benign and malignant lesions between 68-81% of the time. Pelvic exams can also be used in an attempt to distinguish between a normal ovary and one that possesses early premalignant lesions, but studies show that these exams are only able to distinguish between the two 45% of the time.

With respect to assessing a woman's risk of developing ovarian cancer, high-risk populations with a family history of ovarian cancer may be screened for germline mutations such as *BRCA1* and *BRCA2*, as women with these mutations have a dramatically increased risk of developing ovarian cancer (Antoniou, Pharoah et al. 2003). However, screening for these mutations is only an assessment of risk, and does not provide a diagnosis of ovarian cancer.

Due to the limited ability of all of these methods to effectively diagnose ovarian cancer at early stages, only 19% of new ovarian cancer cases are diagnosed at early stages when tumours are still localized to the ovary, whereas approximately 70% of new ovarian cancer cases are diagnosed at advanced stages when the cancer has already metastasized outside of the ovaries to distant sites within the peritoneal cavity (Jemal, Siegel et al. 2008). Unfortunately, once ovarian cancer has metastasized outside of the ovaries, standard therapies are much less effective. This can be seen by the fact that although the five-year survival rate for ovarian cancer patients who are diagnosed with early localized disease is 92%, it decreases to 30% in patients who are not diagnosed until the cancer has metastasized to distant sites outside of the ovaries. High mortality in ovarian cancer has also been partly attributed to having one of the highest average ages at initial diagnoses, with a median age of 63 years (Ozols, Bookman et al. 2004). As a result of the current limitations relating to early ovarian cancer detection and the high mortality

associated with these limitations, it is essential to develop better early detection and screening methods, as well as prevention strategies. One way that this may eventually be achieved is by gaining a thorough understanding of the molecular mechanisms and factors that are essential to the development of ovarian cancer.

1.1.3 Origins of ovarian cancer

Epithelial ovarian cancer (EOC) accounts for approximately 90% of all human ovarian malignancies, and is believed to originate from the ovarian surface epithelium (OSE) (Auersperg, Wong et al. 2001). However, there is also recent evidence to suggest that EOC may have alternative origins in the fallopian tubes, which are in close proximity to the ovaries (Medeiros, Muto et al. 2006; Levanon, Crum et al. 2008; Karst and Drapkin 2010). Germ cell ovarian cancers account for 5% of human ovarian malignancies, and stromal cell origins account for the remaining 5% of ovarian cancers (Shield, Ackland et al. 2009). The OSE consists of a single layer of flat-to-cuboidal mesothelial cells with few distinguishing features, and is separated from the stroma of the ovary by an intermediate basement membrane (Auersperg, Wong et al. 2001). Functionally, the OSE is responsible for the transportation of molecules to and from the peritoneal cavity, and is also involved in the processes of ovulatory rupture and subsequent repair.

Although the etiology of ovarian cancer is not completely understood, there are several theories that have attempted to explain why EOC may originate from the OSE, which are centered around data indicating that the risk of an individual developing EOC positively correlates with their number of lifetime ovulatory events (Ozols, Bookman et

al. 2004). The best supported theory over the past several decades relating to this data is the incessant ovulation hypothesis (Fathalla 1971) . This hypothesis suggests that the repetitive rupturing of the OSE that occurs during ovulation results in rapid cell proliferation during postovulatory repair. The repetition of this process over time may lead to mutations in OSE cells, which could eventually lead to the formation of tumour cells. The second common hypothesis is the gonadotropin hypothesis (Ozols, Bookman et al. 2004). It suggests that the increases in pituitary gonadotropins at the start of each ovulation and that can persist for years after menopause can stimulate OSE cells in inclusion cysts within the ovary, which may lead to mutations in OSE cells (Konishi, Kuroda et al. 1999).

There have also been recent studies suggesting alternative origins of EOC other than the OSE. For example, it has been suggested that high grade serous ovarian carcinomas may originate from the fallopian tubes. This is based partly on observations that ovarian carcinomas have little resemblance to OSE cells, and instead have a closer resemblance to the epithelium of the fallopian tube (Levanon, Crum et al. 2008). Additionally, studies have examined the ovaries and fallopian tubes of *BRCA1*$^{+}$ women at high risk for ovarian cancer who had bilateral salpingo-oophorectomies. Upon examination, it was found that early stage serous carcinomas were found in several patients in sections of the fallopian tubes, whereas none were found in the ovaries (Medeiros, Muto et al. 2006). Therefore, it is suggested that since the fallopian tube and particularly the fimbria have a close proximity to the ovaries and are exposed to the same microenvironment, transformed fallopian tube epithelial cells may shed into the

peritoneal cavity or migrate to the ovaries during the early stages of cancer progression (Karst and Drapkin 2010).

1.1.4 Subtypes of epithelial ovarian cancer

There are several subtypes of epithelial ovarian cancer that can be distinguished upon initial diagnosis based on tumour cell morphology. The four most common histological subtypes of ovarian cancer are serous, clear cell, endometrioid, and mucinous carcinomas (Cho and Shih Ie 2009). Each of these subtypes is unique in terms of incidence, genetic mutations, appearance, and response to treatment. Serous carcinomas account for approximately 70% of all EOC cases, clear cell account for 10%, endometrioid account for 7%, and mucinous account for 3%. Additionally, serous carcinomas are further classified into high-grade serous and low grade serous, with high-grade serous accounting for over 90% of serous carcinomas.

Each subtype of ovarian cancer also has characteristic mutations that are frequently associated with it. For example, high-grade serous carcinomas often have *BRCA1* or *BRCA2* and *TP53* mutations (Gilks and Prat 2009), low-grade serous carcinomas are associated with *BRAF* or *KRAS* mutations, and clear cell carcinomas frequently have *PIK3CA* mutations. As well, endometrioid carcinomas have the highest frequency of *CTNNB1* mutations, and mucinous carcinomas are often associated with mutations in *KRAS* (Cho 2009; Gilks and Prat 2009). With respect to prognosis, high-grade serous and clear cell are usually associated with a very poor prognosis, while endometrioid and mucinous are generally associated with more favourable outcomes relative to high-grade serous (Gilks and Prat 2009).

1.1.5 Progression of epithelial ovarian cancer

During the early stages of EOC progression, tumours are confined to either one, or both ovaries (Naora and Montell 2005) (Figure 1.1). The canonical method of epithelial cancer metastasis involves the escape of cells from the primary tumour and the intravasation of these cells into the bloodstream, where they travel through the circulation and extravasate to metastasize at secondary sites (Chambers, Groom et al. 2002). However, unlike most other carcinomas, metastasis of EOC cells through the bloodstream is rare (Allen, Porter et al. 1987). Instead, malignant cells are shed from the primary tumour directly into the peritoneal cavity as EOC progresses. These cells can then exist individually, or as multi-cellular aggregates of EOC cells called spheroids. Individual cells and spheroids are both capable of seeding metastases (Zietarska, Maugard et al. 2007), but spheroid formation is hypothesized to be an intermediate survival mechanism for EOC cells during dissemination (Shield, Ackland et al. 2009). Once they are shed, EOC cells are transported by peritoneal fluid, and directly disseminate throughout the abdominal cavity where they can metastasize to form secondary tumours at regional and distant sites (Naora and Montell 2005). Common sites of metastasis within the abdominal cavity include the uterus, fallopian tubes, omentum, and the diaphragm.

Additionally, the formation of ascites fluid within the abdominal cavity is usually associated with this process of peritoneal dissemination (Naora and Montell 2005). The buildup of this fluid contributing to the transportation of EOC cells is thought to be a combination of several factors including blockage of the lymphatic system that results in

Figure 1.1 Epithelial ovarian cancer metastasis and progression

As ovarian cancer progresses, (A) malignant cells shed from the surface of the ovaries directly into fluid within the peritoneal cavity. These cells can either exist as individual cells, or can aggregate to form spheroids. The individual cells or spheroids will then be transported by ascites fluid throughout the peritoneal cavity where they (B) can form secondary metastases at sites such as the fallopian tubes and omentum (A- adapted from Shield, K. et al. 2009, B – adapted from Naora, H. and D.J. Montell 2005).

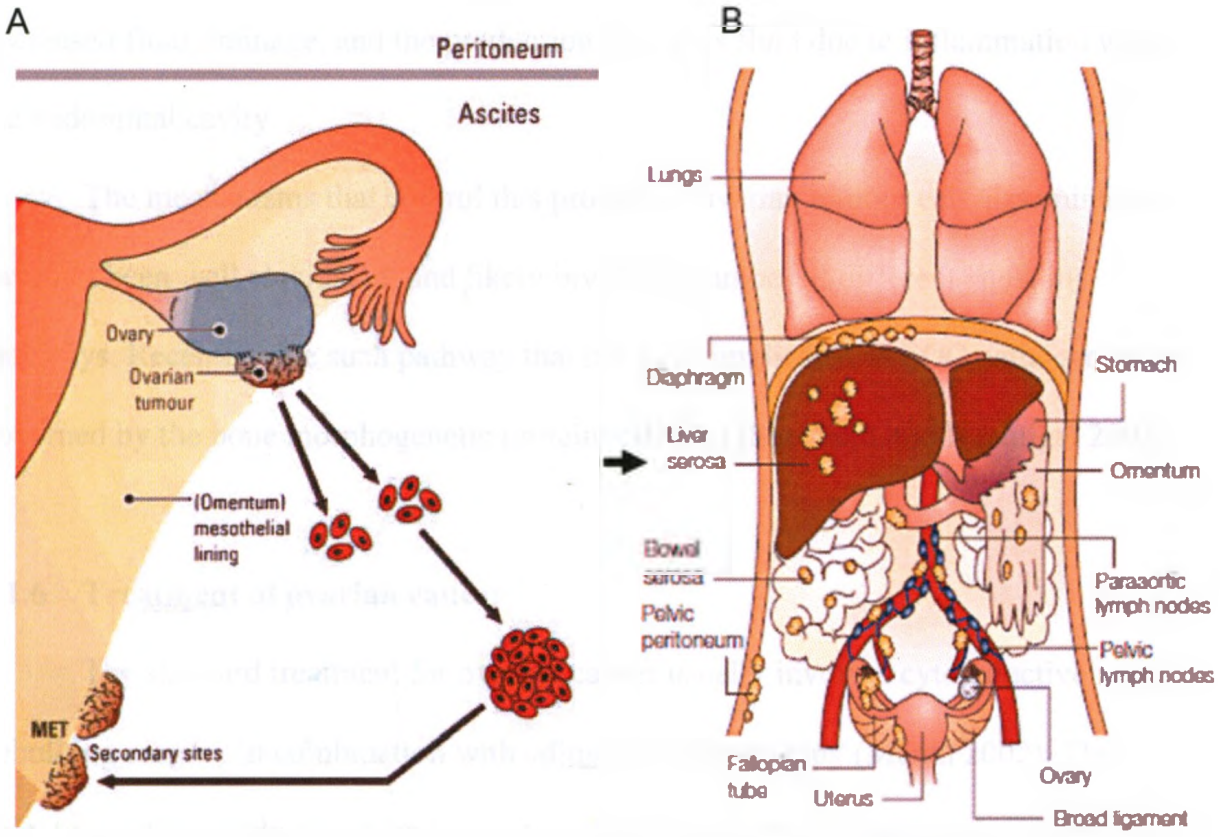
A
Peritoneum
Ascites
Ovary
Ovarian tumour
(Omentum) mesothelial lining
MET
Secondary sites
B
Lungs
Diaphragm
Liver serosa
Bowel serosa
Pelvic peritoneum
Stomach
Omentum
Paraaortic lymph nodes
Pelvic lymph nodes
Fallopian tube
Uterus
Ovary
Broad ligament

decreased fluid drainage, and the production of excess fluid due to inflammation within the abdominal cavity.

The mechanisms that control this process of ovarian tumour cell dissemination have not been well elucidated, and likely involve a number of different signaling pathways. Recently, one such pathway that has been implicated in EOC pathogenesis is governed by the bone morphogenetic proteins (BMPs) (Shepherd and Nachtigal 2003).

1.1.6 Treatment of ovarian cancer

The standard treatment for ovarian cancer usually involves cytoreductive debulking surgery in combination with adjuvant chemotherapy (Mutch 2002). The objectives of cytoreductive surgery are to reduce tumour burden, determine staging, and to determine histological subtype. The reduction of initial tumour burden is very important in ovarian cancer because it is associated with survival advantages. This is seen by the fact that patients with residual tumours that are less than 2 cm have an average survival time of 40-45 months, whereas patients with residual tumours that are greater than 2 cm have an average survival time of only 12-16 months. After cytoreductive surgery, patients are usually treated with intravenous combination chemotherapy of a platinum as well as a taxane-containing agent, which is usually carboplatin-paclitaxel (Gardner and Jewell 2011). However, the majority of patients will recur within 18 months (Han, Lin et al. 2009). Recently, phase III clinical trials suggest that intraperitoneal administration of platinum-taxane chemotherapy may be more effective that intravenous administration (Armstrong, Bundy et al. 2006). As well, neoadjuvant chemotherapy can also be administered to patients prior to optimal debulking surgery

(Bilici, Salepci et al. 2010). The purpose of administering chemotherapy before surgery is to reduce tumour burden in order to increase the likelihood of optimal surgical debulking and therefore increase median survival time.

The buildup of ascites fluid is another symptom of ovarian cancer that needs to be considered in ovarian cancer treatment. This is because recurrent malignant ascites can cause painful and unpleasant symptoms that decrease the quality of life of patients, and can also cause serious complications such as bowel perforation in extreme cases (Jatoi, Giordano et al. 2005). Therefore, repeated paracentesis of ascites fluid from the abdominal cavity may be required as often as every 9-10 days (Mackey and Venner 1996) in order to minimize these symptoms and complications.

Currently, the major focus of clinical trials for ovarian cancer treatment involves targeted biologic agents. For example, poly ADP ribose polymerase (PARP) inhibitors such as Olaparib are currently in phase II clinical trials (Audeh, Carmichael et al. 2010). As well, the anti-angiogenic agent Bevacizumab that targets the vascular endothelial growth factor (VEGF) pathway has demonstrated response benefits to treatment in phase III clinical trials (Jelovac and Armstrong 2011).

1.2 The bone morphogenetic protein signaling pathway

1.2.1 Organization of the bone morphogenetic protein signaling family

The transforming growth factor β (TGFβ) signaling pathway superfamily is involved in diverse cellular processes including developmental processes, adult tissue homeostasis, and also plays complex roles in many diseases (Moustakas and Heldin 2009). For example, misregulation of this pathway can result in tumour development

(Massague 2008). The human TGFβ family consists of 33 members, which are subdivided into families (Moustakas and Heldin 2009). These are the TGFβ, growth and differentiation factor (GDF), activins, nodal, and BMP families of ligands. The BMP family is the largest subgroup within the TGFβ superfamily of ligands, and contains over 20 members that have been identified in humans (Blitz and Cho 2009).

Based on their sequence similarities and functions, the BMPs are generally divided into at least 4 groups. These groups are BMP 2/4, BMP 5/6/7/8a/8b, BMP 9/10, and BMP 12/13/14 (Bragdon, Moseychuk et al. 2011). The BMPs were originally identified for their ability to induce ectopic bone and cartilage formation (Blanco Calvo, Bolos Fernandez et al. 2009). However, they are involved in many other processes such as embryonic patterning and development, tissue homeostasis and regeneration, as well as various diseases (Wagner, Sieber et al. 2010). For example, functions that have been associated with BMP4 specifically include the formation of teeth, bones, limbs, lungs, and eyes from the mesoderm (Thawani, Wang et al. 2010). Additionally, BMP4 is involved in dorsal-ventral patterning and craniofacial development, as well as repairing bone. Although there is a large degree of diversity among the functions and expression patterns of the BMPs, there are many compensatory functional overlaps (Hebert, Hayhurst et al. 2003). For example, it has been shown that BMP2 and BMP4 can compensate for one another in some aspects of development such as with patterning of the dorsal telencephalic midline that eventually gives rise to distinct structures in the adult brain in mammals.

The BMPs are expressed in many tissues in human adults. For example, BMP4 has been shown to be expressed in skeletal muscle, brain, heart, kidney, lung, pancreas,

liver, spinal cord, as well as several other tissues (Bragdon, Moseychuk et al. 2011). With respect to the ovaries, BMP4 has been shown to be expressed in almost all major ovary cell types including oocyte, granulosa, theca, and ovarian surface epithelium cells (Erickson and Shimasaki 2003).

1.2.2 Activation and regulation of bone morphogenetic protein signaling

Of all of the families within the TGFβ superfamily, the BMP family is the most complex with respect to how it is activated and modulated (Hebert, Hayhurst et al. 2003). BMP signaling involves type I (ALK2, ALK3, ALK6) and type II (BMPRII) transmembrane serine/threonine kinase receptors (Blanco Calvo, Bolos Fernandez et al. 2009). In the absence of a signal, these receptors are separated in the plasma membrane. The process of BMP signaling begins when a BMP ligand binds to a BMPRII receptor (Waite and Eng 2003) (Figure 1.2), which results in the recruitment of a type I receptor to form a heteromeric complex. This causes the BMPRII receptor to transphosphorylate the type I receptor at its glycine/serine-rich domain, which results in its activation. Once the type I receptor is activated, it has the ability to bind to several intracellular proteins that are responsible for transducing the signal to the nucleus, which are the Smad proteins. The activated type I receptor subsequently phosphorylates BMP-specific receptor-activated Smads (R-Smads 1, 5, 8), which causes the R-Smad to dissociate from the receptor complex into the cytoplasm. The phosphorylated R-Smads can then form homo- or heterodimers, and then associate with a common mediator Smad (co-Smad4). Finally, the activated R-Smad/Smad4 complex translocates to the nucleus, where it regulates the

Figure 1.2 The bone morphogenetic protein signaling pathway

Activation of canonical Smad-dependent BMP signaling begins with the binding of BMP ligands to transmembrane receptor complexes. This binding leads to BMP-specific R-Smad phosphorylation, formation of an R-Smad/co-Smad4 complex, and translocation of this complex to the nucleus where it affects the expression of different target genes (adapted from Waite and Eng 2003).

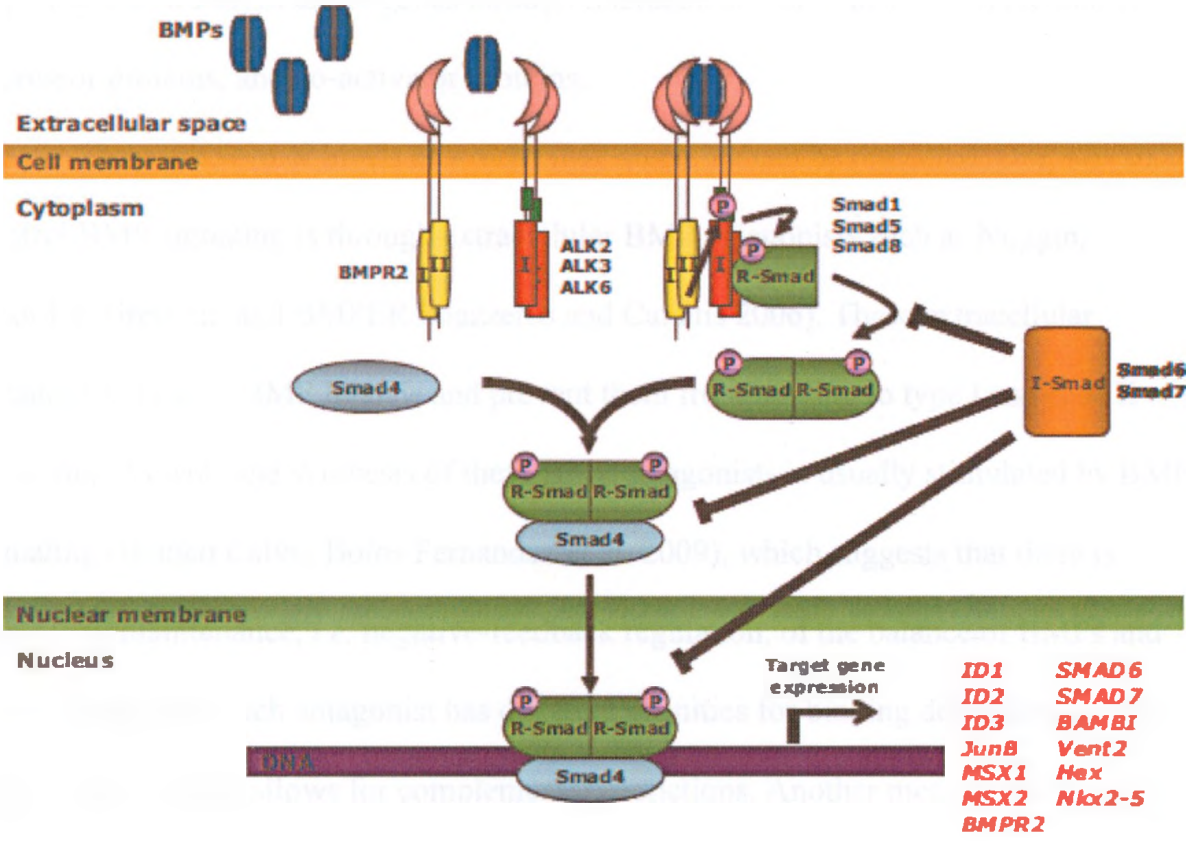
BMPs
Extracellular space
Cell membrane
Cytoplasm
BMPR2
ALK2
ALK3
ALK6
Smad1
Smad5
Smad8
R-Smad
Smad4
R-Smad R-Smad
I-Smad
Smad6
Smad7
Nuclear membrane
Nucleus
DNA
Target gene expression
ID1
ID2
ID3
JunB
MSX1
MSX2
BMPR2
SMAD6
SMAD7
BAMBI
Vent2
Hex
Nkx2-5

expression of different target genes through interactions with transcription factors, co-repressor proteins, and co-activator proteins.

There are several levels at which BMP signaling can be regulated. One way to control BMP signaling is through extracellular BMP antagonists such as Noggin, Chordin, Gremlin, and BMPER (Gazzerro and Canalis 2006). These extracellular antagonists bind to BMP ligands and prevent them from binding to type I and type II receptors. As well, the synthesis of these BMP antagonists is usually stimulated by BMP signaling (Blanco Calvo, Bolos Fernandez et al. 2009), which suggests that there is controlled maintenance, *i.e.* negative-feedback regulation, of the balance of BMPs and their antagonists. Each antagonist has different affinities for binding depending on the BMP ligand, which allows for complementary functions. Another mechanism of inhibiting BMP signaling is through inhibitory Smads 6 and 7 (Imamura, Takase et al. 1997). These Smads can bind to the type I receptor, and therefore compete with R-Smads for activation. Smad6 can also bind to phosphorylated Smad1 to prevent it from forming a complex with Smad4. Another level of regulation is the pseudoreceptor BMP and activin receptor membrane bound inhibitor (BAMBI) (Blanco Calvo, Bolos Fernandez et al. 2009). BAMBI is a transmembrane protein that is similar to type I receptors, and therefore functions as a decoy receptor to limit signaling. BMP signaling can also be regulated by Smad-ubiquitination regulatory factors 1 and 2 (Smurf1 and Smurf2), which can bind to Smads 1 and 5 in order to initiate proteasomal degradation (Izzi and Attisano 2004). Finally, transcriptional co-repressors in the nucleus can prevent the activation of target genes by BMPs. For example, *c-Ski* is a transcriptional co-repressor that can be incorporated into Smad DNA binding complexes, which prevents them from interacting

with co-activators and initiating the transcription of target genes (Akiyoshi, Inoue et al. 1999).

Although these descriptions of BMP signaling involving the Smad proteins is the canonical and most studied aspect of the BMP signaling pathway, BMPs can also induce Smad-independent signaling. For example, BMP signaling has been shown to induce p38 mitogen-activated protein kinase (p38 MAPK) phosphorylation (Nakamura, Shirai et al. 1999), extracellular signaling regulated kinase (ERK) activation (Montesano 2007), c-Jun N-terminal kinase (JNK) activation (Hocevar, Brown et al. 1999), and protein kinase C (PKC)-dependent pathway activation (Hay, Lemonnier et al. 2001). Conversely, the R-Smads and Smad4 can be activated by kinases in other pathways such as Erk1 and Erk2, p38, and JNK (Blanco Calvo, Bolos Fernandez et al. 2009).

One of the transcription factor families that has been established as BMP-regulated target genes are the inhibitors of DNA binding (ID) proteins, of which there are 4 known members of this family (ID1-ID4) (Pesce and Benezra 1993). All of the ID family members contain a highly conserved helix-loop-helix domain that mediates physical interactions with basic helix-loop-helix (bHLH) transcription factors that control gene expression (Benezra, Davis et al. 1990). Since the IDs do not have a DNA binding domain, heterodimeric complexes that are formed between the IDs and transcription factors cannot bind DNA. Therefore, these proteins can have a significant regulatory effect on gene expression. These proteins are known to play important roles in embryogenesis and organogenesis (Lyden, Young et al. 1999), cell differentiation and proliferation (Norton 2000), control of cell cycle progression, apoptosis (Norton and Atherton 1998), and angiogenesis (Benezra, Rafii et al. 2001). As well, there are

functional redundancies and some similar temporal and spatial expression patterns among the 4 ID proteins (Norton 2000). In the adult, these proteins are expressed at low levels in normal tissues, but their expression is often deregulated in tumours (Mern, Hasskarl et al. 2010). For example, the IDs have been shown to be upregulated in several human cancers such ovarian (Shepherd and Nachtigal 2003), lung (Cheng, Tsai et al. 2011), prostate (Forootan, Wong et al. 2007), and breast cancers (Yang, Liu et al. 2010).

1.2.3 Bone morphogenetic protein signaling in cancer

Although many of the BMPs have been implicated in the promotion or inhibition of cancer development (Thawani, Wang et al. 2010), I will be focusing on studies involving BMP4, and to a lesser extent, its subfamily member BMP2. There are several lines of evidence *in vitro* and *in vivo* attributing pro-tumourigenic as well as anti-tumourigenic properties to BMP4 in numerous types of cancer. BMP4 is overexpressed in many cancers such as melanoma (Rothhammer, Poser et al. 2005), hepatocellular carcinoma (Maegdefrau, Amann et al. 2009), colon adenocarcinoma (Deng, Makizumi et al. 2007), and multiple myeloma (Grcevic, Kusec et al. 2010). However, BMP4 has been shown to exhibit decreased expression relative to normal tissues in cancers such as prostate cancer (Spanjol, Djordjevic et al. 2010), and retinoblastoma (Haubold, Weise et al. 2010).

There is a large body of evidence *in vitro* suggesting that BMP4 signaling increases cancer cell proliferation, increases migration, increases invasion, decreases apoptosis, and induces expression of EMT markers. Treatment of the human DAOY cerebellar primitive neuroectodermal tumour medulloblastoma cell line with either BMP2

or BMP4 induced an anti-apoptotic effect based on immunohistochemistry (Iantosca, McPherson et al. 1999). In other studies, tissue sections of osteosarcomas that were removed from patients were evaluated to look at BMP2 and BMP4 expression (Arihiro and Inai 2001). It was found that BMP2 and BMP4 expression strongly correlated with the tendency of these tumours to metastasize to bone in patients. Abnormal duct organization and ductal lumen obliteration represent some of the early stages of breast cancer progression. When mouse J3B1A mammary epithelial cells were treated with BMP4, they were unable to form any recognizable ductal lumen, thus contributing to the tumourigenic progression of these cells (Montesano, Sarkozi et al. 2008). Another study using J3B1A cells has shown that treatment with BMP4 significantly increases proliferation (Montesano 2007). Similarly, GH3 prolactinoma cells that were treated with BMP4 exhibited increased cell proliferation (Paez-Pereda, Giacomini et al. 2003). The expression of c-Myc oncoprotein was also increased in these BMP4-treated GH3 cells, while treatment with the BMP inhibitor noggin decreased proliferation and expression of c-Myc. In human LAPC-4 and LAPC-9 prostate cancer cells, treatment with noggin resulted in decreased cell migration (Feeley, Gamradt et al. 2005). A study involving NCI H929 and Thiel human myeloma cell lines investigated the role of BMP4 signaling in apoptosis (Grcevic, Kusec et al. 2010). These cell lines were treated with the proteasome inhibitor Bortezomib alone or in combination with BMP4. Results demonstrated that cells treated with BMP4 were partially protected from the apoptotic effects induced by Bortezomib. BMP4 also has an important role in tumourigenesis in hepatocellular carcinoma (HCC). The HepG2, Hep3B, and PLC human HCC cell lines in addition to primary human HCC cells isolated from patients were transfected with antisense BMP4

expression plasmids or siRNA against BMP4 (Maegdefrau, Amann et al. 2009). Knockdown of BMP4 resulted in a decrease in both cell migration and invasion through Matrigel. With respect to the Panc-1 human pancreatic cancer cell line, treatment with BMP4 induces epithelial-mesenchymal transition (EMT) (Hamada, Satoh et al. 2007). This was seen by the fact that these treated cells exhibited decreased expression of E-cadherin, and increased expression of vimentin. It was suggested that these effects on EMT induction are mediated through an increase in homeobox gene transcription factor MSX2 expression. MSX2 has been previously shown to be a target gene of BMP signaling (Hussein, Duff et al. 2003), and enhances EMT in pancreatic cancer cells (Satoh, Hamada et al. 2008). Additionally, these BMP4-treated Panc-1 cells had enhanced cell motility (Hamada, Satoh et al. 2007). HCT116 human colorectal cancer cell line clones have also been transfected with BMP4 over-expression plasmid (Deng, Makizumi et al. 2007). These BMP4 overexpressing clones show increased resistance to serum-starving induced apoptosis (Deng, Makizumi et al. 2007). These cells also displayed enhanced migration and invasion through Matrigel. Noggin treatment reversed all of these tumourigenic effects in HCT116 cells. Another study examining human colorectal cancer by using the SW480 cell line shows that the stable transfection of BMP4 plasmid in these cells results in the upregulation of vimentin expression (Deng, Ravikumar et al. 2009).

These pro-tumourigenic effects of BMP signaling have also been assessed *in vivo*. For example, GH3 prolactinoma cells that were stably transfected with noggin and injected into nude mice formed tumours that were smaller based on volume, and these tumours also had reduced c-Myc oncoprotein expression (Paez-Pereda, Giacomini et al.

2003). Additionally, studies subjected SCID mice to tibial injections with LAPC-9 prostate cancer cells that were transduced with retrovirus that contained noggin-cDNA (Feeley, Gamradt et al. 2005). Mice that were injected with these noggin-overexpressing LAPC-9 cells formed significantly smaller osteoblastic lesions when viewed on radiographs (Feeley, Gamradt et al. 2005).

There is a growing body of evidence *in vitro* suggesting that the BMPs, particularly BMP4, play important roles as tumour suppressors. For example, treatment with BMP2 or BMP4 inhibits proliferation of mouse cerebellar granule neuron progenitor (GNP)-like medulloblastoma cells (Zhao, Ayrault et al. 2008) . The effects of BMP2 and BMP4 treatment have also been evaluated in primary human glioblastoma (GBM) cells. Treatment with BMP2 or BMP4 did not induce cell death or apoptosis *in vitro* in these cells (Piccirillo, Reynolds et al. 2006). However, BMP4 treatment, and to a lesser extent BMP2 treatment, significantly decreased the proliferation of GBM cells. Relative to non-treated cells, BMP treatment also led these cells to become more differentiated as seen by cell morphology and increases in the fluorescence signaling intensity of glial fibrillary acidic protein (GFAP). In another study, human glioma U251 cells that were transfected with BMP4 plasmid exhibited decreased proliferation (Liu, Tian et al. 2010). Upon BMP4 treatment of 9 different breast cancer lines, all cell lines exhibited significant growth inhibition relative to vehicle-treated cells (Ketolainen, Alarmo et al. 2010) (Ketolainen, Alarmo et al. 2010). Another study that investigated the relationship between BMP signaling and breast cancer used MDA-MB-231 breast cancer cells, and treatment of these cells with BMP4 resulted in a significant decrease in the migratory and invasive abilities of these cells (Shon, Kim et al. 2009). These effects were likely

mediated through decreased mRNA expression of matrix metalloproteinase 9 (MMP 9), which is an enzyme that is in part responsible for the degradation of surrounding extracellular matrix components during invasion and metastasis. Treatment of human A549 epithelial ling cancer cells with BMP4 led to a more senescent phenotype (Buckley, Shi et al. 2004) . In another study involving A549 lung cancer cells, BMP4-treatment led to decreased p-ERK and Bcl2, supporting decreased proliferation and increased potential for apoptosis, as well as decreased invasiveness. Similarly, studies with siRNA-mediated knockdown of BMP4 in A549 and NCI-H460 non-small cell lung cancer cells showed increased proliferation, as well as decreased senescence (Su, Zhu et al. 2009). Treatment with exogenous BMP4 decreased proliferation and increased apoptosis in ANBL-6, OH2, and IH1 human myeloma cell lines (Hjertner, Hjorth-Hansen et al. 2001). In this same study, freshly isolated primary multiple myeloma cancer cells from several patients that were immediately treated with BMP4 exhibited increased apoptosis. Treatment of 8 retinoblastoma cell lines with recombinant human BMP4 results in an increase in apoptosis (Haubold, Weise et al. 2010). Also, primary human basal cell carcinoma (BCC) cells that were isolated from patient tumours and subsequently treated with recombinant human BMP4 exhibited decreased cell proliferation (Sneddon, Zhen et al. 2006). Similarly, primary human BCC cells in this study that were treated with recombinant mouse BMP inhibitor Gremlin-1 exhibited increased cell proliferation. Using human AtT-20 pituitary corticotroph tumour cells, it was shown that treatment with BMP4 inhibited cell proliferation (Giacomini, Paez-Pereda et al. 2006). Finally, human NTERA2 teratocarcinoma cells that were treated with exogenous BMP4 exhibited a decrease in cell proliferation and increased apoptosis (Nishanian, Kim et al. 2004).

There has also been a small number of studies *in vivo* supporting BMP signaling as an anti-tumourigenic pathway. For example, mouse cerebellar GNP-like medulloblastoma cells were transfected with BMP4 and were allografted into immunocompromised athymic mice (Zhao, Ayrault et al. 2008). Tumours formed in these mice were much smaller than allografts of cells transfected with a control vector. When BMP4-saturated polyacrylic beads where co-injected with GBM cells into mice, the mice developed smaller, more confined lesions, and survived for a significantly longer period of time compared to controls (Piccirillo, Reynolds et al. 2006). Another study showed that BMP4-treated A549 cells that were injected into nude mice formed much smaller tumours based on volume (Buckley, Shi et al. 2004). Also, stably transfecting human AtT-20 pituitary corticotroph tumour cells with expression vectors for noggin or a dominant-negative form of BMP4 and injecting them into nude mice corresponded to increased tumourigenicity as measured by tumour volume (Giacomini, Paez-Pereda et al. 2006). Finally, BMP4-treated human NTERA2 cells that were injected into immunodeficient mice formed smaller tumours relative to controls based on tumour volume (Nishanian, Kim et al. 2004).

BMP4 has recently been shown to have an effect on cancer stem cells, or cancer initiating cells. One study used primary colorectal cancer stem cells (CRC-SCs) that were selected from primary patient tumour samples based on CD133 expression (Lombardo, Scopelliti et al. 2011). Although BMP4 is usually expressed in colorectal cancer, it was not detected in the CRC-SCs (Lombardo, Scopelliti et al. 2011). *In vitro*, CRC-SCs form spheres of aggregated cells, whereas differentiated colorectal cancer cells lack this ability. Treatment of CRC-SCs with exogenous BMP4 induced cell differentiation based

on immunohistochemical staining for the expression of $CK20^+$ cells. Phase contrast microscopy also confirmed that these cells differentiated as evidenced by larger, polygonal colon cells. The effect of BMP4 treatment on CRC-SC response to chemotherapy was also evaluated. Tumours that were formed in immunocompromised mice by CRC-SC sphere injections were treated with oxaliplatin and 5-fluorouracil (5-FU) alone or in combination with BMP4-loaded heparin acrylic beads. Combination treatment with BMP4 sensitized the tumours to chemotherapy as measured by tumour size after treatment. Also, another study investigated the role of BMP4 in brain tumour-initiating cells (BTICs) of human GBMs (Piccirillo, Reynolds et al. 2006). Treatment of primary adult human GBM cells with exogenous BMP4 significantly reduced the pool of BTICs by approximately 50% in GBM cell populations as measured by sorting for $CD133^+$ cells from culture.

Overall, these differing and often contrasting reports on the numerous roles of BMP4 in cancer highlight the fact that BMP signaling may have unique roles in the process of tumourigenesis on a cancer-specific basis. Additionally, BMP signaling may have different roles even within the same type of cancer depending on the stage of the disease. Therefore, it is essential to study the roles of BMP4 signaling in an EOC-specific context.

1.2.4 Bone morphogenetic protein signaling in ovarian cancer

It has been shown that immortalized normal OSE cells, ovarian cancer cell lines, primary normal OSE cells, and primary EOC cells all express BMP4 mRNA (Shepherd and Nachtigal 2003). However, BMP2 was expressed in a smaller number of samples,

and BMP7 was not expressed in any sample. Mature BMP4 protein was also expressed in primary EOC cells as measured by immunoprecipitation of ^{35}S-Met/Cys radiolabeled BMP4 proteins that were secreted by cells into culture medium. Additionally, all of the samples expressed the intracellular components that are necessary for a functional BMP4 signaling pathway based on mRNA expression. These included type II BMP receptors, as well as type I BMP ALK3 receptors. Type I BMP ALK6 receptors were expressed in the EOC cell lines, but expression was very weak or absent in the primary and immortalized cells. In addition, each group of cells expressed co-Smad4, and R-Smads 1, 5, and 8.

Not only are components of BMP4 signaling present in EOC and OSE cells, but the pathway is also functional (Shepherd and Nachtigal 2003). This was assessed by treating cells *in vitro* with recombinant human BMP4. BMP4 treated cells expressed increased phospho-Smad1 and had enhanced nuclear localization of phospho-Smad1 based on indirect immunofluorescence. BMP-regulated target genes Smad6, Smad7, ID1, and ID3 RNA were all induced by BMP4 treatment. Interestingly, ID1 and ID3 expression were induced approximately 5 fold more in BMP4-treated primary EOC cells relative to induction in BMP-treated normal OSE cells. A similar study has shown that treatment of CaOV3 human ovarian cancer cells with noggin resulted in a decrease in endogenous ID3 mRNA expression in a dose-dependent manner (Shepherd, Theriault et al. 2008). However, treatment of these cells with broader BMP inhibitors that have a weaker affinity for BMP4 did not significantly change ID3 expression, which suggests that ID3 overexpression in human EOC is controlled primarily by autocrine BMP4 signaling.

The CaOV3 and SkOV3 human ovarian cancer cell lines in addition to primary EOC cells that were isolated from ascites fluid were all treated with recombinant human BMP4. With respect to proliferation, BMP4 treatment had no effect (Shepherd and Nachtigal 2003). However, BMP4 treatment led to changes in cell morphology that resembled cell spreading and cells appeared more flattened as opposed to the epithelial-like cobblestone morphology that was representative of untreated cells (Shepherd and Nachtigal 2003; Theriault, Shepherd et al. 2007). As well, primary human ovarian cancer cells and normal OSE cells were treated with human recombinant BMP4 or transduced with an adenovirus expressing constitutively active ALK3 (ALK3QD). These cells were significantly larger in size with respect to area relative to untreated cells based on phase-contrast images (Theriault, Shepherd et al. 2007). One of the functional implications of this cell spreading morphology was seen by the fact that BMP4 treatment led to decreased cell detachment *in vitro* (Shepherd and Nachtigal 2003). Additionally, primary EOC cells that were treated with BMP4 or transduced with ALK3QD showed increased motility (Theriault, Shepherd et al. 2007). Conversely, treatment of these cells with noggin decreased cell motility. However, treatment of normal OSE cells with BMP4 did not affect motility, which suggests that EOC cells have enhanced their motility in response to acquired autocrine BMP signaling. As well, primary EOC cells that were transduced with ALK3QD exhibited an increase in invasive potential *in vitro*. After BMP4 treatment, primary EOC cells exhibited increased expression of Snail and Slug protein. These EMT marker proteins are known to repress E-cadherin (Batlle, Sancho et al. 2000), which exhibited decreased protein expression in BMP4 treated cells. This suggests that BMP4 can induce EMT in primary EOC cells (Theriault, Shepherd et al.

2007). Another study has shown that chordin is underexpressed in EOC tumour samples relative to normal ovarian tissue at the mRNA level (Moll, Millet et al. 2006) . After this discovery, BG1 and PEO14 human ovarian cancer cell lines were transiently transfected with an expression vector for chordin. This chordin overexpression decreased the migration and invasion capabilities of these cells. Additionally, chordin treatment increased the adhesion of EOC cells.

Studies have also implicated BMP signaling in decreasing metastatic potential in ovarian cancer. For example, OVCA429 human ovarian cancer cells were transfected for doxycycline-inducible expression of constitutively-active ALK3QD in order to evaluate the role of BMP signaling in ovarian cancer metastasis (Shepherd, Mujoomdar et al. 2010). Xenografts of these OVCA429 ALK3QD induced clones into athymic nude mice resulted in decreased tumour implantation on peritoneal surfaces. As well, these mice exhibited a decrease in ascites formation. A potential underlying basis for this decrease in metastatic potential was that β1-integrin and β3-integrin mRNA expression was decreased in ALK3QD-expressing cells. These integrin proteins are essential for cell adhesion, and in fact, ALK3QD-expressing cells exhibit reduced cell adhesion to fibronectin and vitronectin *in vitro*. Additionally, OVCA429 ALK3QD-expressing cells had reduced cell cohesion based on their decreased ability to form spheroids in ultra-low attachment plates as measured by decreased size and density of the spheroids in culture. Overall, this paper suggested that although upregulated BMP signaling is advantageous for cells to lose adhesion and exfoliate from the primary tumour, decreased BMP signaling may be important for cells to metastasize and adhere to secondary tumour sites. In an expression study involving BMP2, it was shown that this protein in addition to

BMPR1B and BMPRII was expressed at lower levels in ovarian cancer tumours compared to normal ovarian tissue (Ma, Ma et al. 2010). Additionally, retrospective analyses were completed in which tumour sections obtained from patients were stained for BMP2 and evaluated using immunohistochemistry. A correlation was found suggesting that patients with positive expression of BMP2 in tumours had a significantly increased average 5-year survival rate relative to patients with tumour samples that did not stain for BMP2. Studies investigating the role of BMP signaling in ovarian cancer have also focused on antagonists of this pathway. For example, SKOV3 human ovarian cancer cells were transfected with a vector expressing BAMBI, which is a BMP type I pseudoreceptor (Pils, Wittinger et al. 2010). Upregulated BAMBI expression in these cells led to increased cell proliferation as measured *in vitro*.

Human ovarian carcinoma-associated mesenchymal stem cells (CA-MSCs) have recently been identified and characterized (McLean, Gong et al. 2011). Upon subcutaneous injections of human ovarian cancer SKOV3 cells alone or in combination with either CA-MSCs or healthy donor MSCs into immune-compromised mice, co-injection with CA-MSCs significantly increased tumour size based on weight. As well, culturing ovarian tumour cells in the presence of CA-MSCs resulted in the tumour cells forming large spheroids *in vitro*, which is associated with cancer stem cells (CSCs) (Ernst, Hofmann et al. 2009). Interestingly, *BMP2* and *BMP4* mRNA were significantly upregulated in all human CA-MSC samples (McLean, Gong et al. 2011). Inhibition of BMP signaling with noggin decreased tumour spheroid formation, and prevented CA-MSC cells from stimulating ovarian tumour growth in mice.

1.2.5 Bone morphogenetic protein signaling and angiogenesis

Angiogenesis is one of the hallmarks of cancer along with uncontrolled proliferative signaling, reprogramming of energy metabolism, evasion of growth suppression, resistance to cell death, evasion of immune destruction, replicative immortality, and the activation of invasion and metastasis capabilities (Hanahan and Weinberg 2011). In addition to normal tissues, tumours require access to a blood supply in order to receive oxygen and nutrients, and to excrete waste products and carbon dioxide. During embryonic development, blood vessels can form through one of two processes (Hanahan and Folkman 1996). The first process is vasculogenesis, which involves the formation of new blood vessels through the creation of new endothelial cells from progenitor cells. The second process is angiogenesis, which involves the sprouting of new capillaries from pre-existing blood vessels. In the adult, new blood vessel formation is accomplished predominantly through the process of angiogenesis.

With the exception of transient processes such as wound healing and the female reproductive cycle, vasculature in the adult is usually in a quiescent state (Hanahan and Weinberg 2011). However, the vasculature remains activated during tumour development throughout the process of angiogenesis in order for tumours to be able to survive and grow beyond 1-2 mm in diameter (Bergers and Benjamin 2003). This change in vasculature activity is termed the angiogenic switch, which describes a change in the balance between angiogenic promoters such as VEGF, and angiogenic inhibitors such as thrombospondin-1 (TSP-1) (Hanahan and Folkman 1996).

Interestingly, the blood vessels that are formed by angiogenesis during tumourigenesis differ from blood vessels formed under normal conditions because they

are irregularly shaped and disorganized, unusually large, have extensive branching, and display leakiness (Nagy, Chang et al. 2010). Briefly, this process of angiogenesis in tumours begins with endothelial cells releasing factors that degrade the basement membrane of the vessel walls (Hanahan and Folkman 1996). The endothelial cells near this area of membrane degradation then invade the surrounding stroma and proliferate as a migrating column. Then, these endothelial cells will strop proliferating and differentiate so that they are able to tightly adhere to each other and form a new capillary tube.

The BMP signaling pathway has been shown to be essential in the processes of vasculogenesis and angiogenesis, with BMP2 and BMP4 appearing to be the most important members of the BMP family in this process as evidenced by mouse knockout models (Moser and Patterson 2005). Mouse embryos with inactivated BMP4 display defects in mesoderm formation, which is required for vascular development, and most mice die around embryonic day (E)7.5 (Winnier, Blessing et al. 1995). Some of these mice survive until approximately E9.5, but eventually die and exhibit abnormal vasculature with a reduced number of blood islands. ALK2-deficient mouse embryos die early in development with severe disruption of mesoderm formation that is essential in the formation of mature vasculature (Gu, Reynolds et al. 1999). ALK3-deficient mouse embryos exhibit similar characteristics, and die early in development due to a lack of mesoderm formation (Mishina, Suzuki et al. 1995). As well, mice with heterozygous inactivating mutations of BMP type 2 receptor have an impaired ability to remodel vasculature in response to exposure to prolonged hypoxia (Beppu, Ichinose et al. 2004). The Smads have also been shown to play an important role in angiogenesis during mouse embryonic development. For example, Smad1 null mice die during gestation in part due

to vascular disorganization (Lechleider, Ryan et al. 2001), and mice in which Smad5 is inactivated die during gestation due to vasculature defects and irregular distribution of blood cells (Yang, Castilla et al. 1999). Additionally, Smad4 deficient mice die by E6.5 due to a lack of mesoderm formation (Sirard, de la Pompa et al. 1998). Transcription factors that are targeted by BMP signaling have also been investigated in knockout mice. For example, double knockout $ID1^{-/-}$ $ID3^{-/-}$ mice die before E13.5 (Lyden, Young et al. 1999). Blood vessels in these mice are unable to branch or sprout into the neuroectoderm, and also have defects in the vasculature within the forebrain.

It has been shown both *in vitro* and *in vivo* that human endothelial cells involved in blood vessel formation possess an intact and functional BMP signaling pathway, and there is direct evidence that BMP signaling plays a role in the process of angiogenesis (Valdimarsdottir, Goumans et al. 2002). Using Matrigel tube formation angiogenesis assays with human microvascular endothelial cells (HMECs), it was shown that BMP4 enhanced angiogenesis (Rothhammer, Bataille et al. 2007). In mouse osteoblast cells, exogenous treatment of BMP4 *in vitro* induced angiogenesis due to an increase in VEGF-A protein production (Deckers, van Bezooijen et al. 2002). However, BMP4-induced angiogenesis treatment was abrogated when VEGF-A antibody was added to these osteoblast cells, suggesting that BMP4-induced angiogenesis is mediated in part by VEGF-A. Ectopic BMP4 signaling in zebrafish embryos induced the expression of VEGF and VEGF receptor 2 mRNA in embryonic endothelial and blood precursor cells (He and Chen 2005). As well, treatment of human retinal pigment epithelial cells with BMP4 led to an increase in VEGF secretion in a dose and time-dependent manner (Vogt, Unda et al. 2006). Transient transfections of endothelial cells from human colon, mouse

aorta, and mouse heart with constitutively-active ALK3, Smad1, or Smad5 were shown to stimulate cell migration and tube formation (Valdimarsdottir, Goumans et al. 2002). Interestingly, ectopic expression of Id1 also stimulated tube formation, while treatment with antisense Id1 blocked the BMP-induced effects on tube formation. Other than VEGF and Id1, relatively little is known about downstream target genes that are affected by BMP signaling that have a role in angiogenesis (Ren, Charles et al. 2007). Recently, gene expression profiling of BMP-treated mouse intraembryonic endothelial cells highlighted *Cox2* as a gene that is strongly upregulated by BMP stimulation. Inhibition of Cox2 blocked the BMP-induced increases in endothelial cell proliferation and tube formation. Similar microarray studies have also shown that *Myo10* is strongly upregulated in BMP-treated mouse endothelial cells, with inhibition of Myo10 decreasing BMP-induced tube formation on Matrigel (Pi, Ren et al. 2007).

Although these studies highlight a role for BMP signaling in the activation of angiogenesis, there are also several conflicting reports that implicate BMP signaling in the inhibition of angiogenesis. In a mouse model where retina were subjected to hypoxia in order to stimulate neovascularization, BMP4-mRNA expression was drastically decreased (Mathura, Jafari et al. 2000). Likewise, primary cultures of human retinal pericytes exhibited increased expression of BMP4 antagonist chordin-like 1 mRNA in response to hypoxia. Angiogenesis assays using human umbilical vein endothelial cells (HUVECs) were done using exogenous BMP4 alone, exogenous chordin-like 1 alone, or in combination. BMP4 treatment significantly inhibited angiogenesis (Kane, Godson et al. 2008) . While chordin-like 1 did not have a significant effect on its own, it modulated the inhibitory effect of BMP4 on angiogenesis when added in combination. BMP4

signaling has also been implicated in studies *in vivo* looking at the process of microvascular remodeling, which includes the formation of new blood vessels as well as the regression of others. When BMP4 was injected transcorneally into postnatal day 8 rats, the number of apoptotic endothelial cells was significantly increased in dissected pupillary membranes (Kiyono and Shibuya 2003). Conversely, the addition of noggin or BMP4-specific neutralizing antibody increased the number of surviving capillary cells by 4-6 fold. BMP4 has also been shown to induce apoptosis of primary human capillary venous endothelial cells in a dose-dependent manner *in vitro* (Kiyono and Shibuya 2006). However, human arterial endothelial cells were not affected by BMP4 treatment initially. Interestingly, mRNA levels of inhibitory Smads 6 and 7 were strongly correlated with BMP4-induced apoptosis resistance in these cells, and knockdown of inhibitory Smad expression with siRNA caused sensitization of endothelial cells to BMP4 stimulation.

BMP antagonists have also been implicated in angiogenesis. Increasing doses of BMPER increased HUVEC sprouting, which was inhibited when BMPER was silenced (Heinke, Wehofsits et al. 2008). These results were also confirmed with *in vivo* experiments where BMPER protein addition to the surface of the chick chorioallantoic membrane (CAM) increased the density of the capillary network and average diameter of blood vessels. As well, using a subcutaneous mouse Matrigel plug assay, increased BMPER enhanced endothelial cell invasion. Interestingly, BMPER lost its proangiogenic capacity at higher concentrations both *in vitro* and *in vivo*, which suggests the presence of a feedback mechanism to modulate endothelial cell functions in a dose-dependent manner, or off-target effects such as the inhibition of additional low-affinity ligands. Another BMP antagonist, Gremlin, has been shown to increase blood vessel formation *in*

vivo when gelatin sponge implants containing Gremlin were placed on the surface of the chick CAM (Mitola, Moroni et al. 2008). Specifically, Gremlin induces angiogenesis by inducing angiopoietin-1 expression in endothelial cells through the activation of NF-κB.

1.2.6 Bone morphogenetic protein signaling and tumour angiogenesis

With respect to tumour growth, the BMPs have been implicated in enhancing angiogenesis in several different types of cancer. BMP2 has been the most extensively studied with respect to the role of BMPs in angiogenesis and tumour formation (Langenfeld and Langenfeld 2004; Raida, Clement et al. 2005; Bieniasz, Oszajca et al. 2009). For example, co-injection of A549 lung cancer cells and recombinant BMP2 into athymic nude mice resulted in the formation larger tumours that had a significant increase in the number of blood vessels relative to control injections (Langenfeld and Langenfeld 2004). The inhibition of BMP2 signaling with noggin or BMP2 antisense oligonucleotides resulted in decreased blood vessel formation in these tumours. Similar effects of BMP2 have been observed in breast cancer, as athymic nude mice that were injected with BMP 2 stably-transfected MCF-7 human breast cancer cells exhibited developed tumours with high vascularization (Raida, Clement et al. 2005). Furthermore, it was shown in this study that BMP2 upregulates p38 MAPK phosphorylation and Id1 expression in HUVECs, which suggests potential mechanisms by which BMP2 can achieve its effects on tumour angiogenesis. As well, it has been shown that BMP2 mRNA is positively correlated with VEGF mRNA in lung cancer patients (Bieniasz, Oszajca et al. 2009).

BMP4 has also been shown to play a role in tumour angiogenesis. Mel Im melanoma cells that were stably transfected with antisense BMP4 or noggin expression vector had a decreased ability to induce endothelial cell tube formation (Rothhammer, Bataille et al. 2007). As well, when these transfected cells were injected into athymic nude mice, resultant tumours had a decrease in blood vessel density. In Hep3 human HCC cells, BMP4 expression was significantly increased when hypoxia was induced *in vitro* (Maegdefrau, Amann et al. 2009) . Additionally, HCCs that were transfected with siRNA against BMP4 and co-cultured with HMECs resulted in a significantly decreased ability to induce angiogenesis.

The role of the BMP signaling pathway has also been assessed indirectly in $Id1^{+/-}$ $Id3^{-/-}$ mice. In these mice, reduced Id expression resulted in small tumour growth from injected breast cancer cells, and these tumours regressed within 2 weeks relative to the much larger tumours that were formed in wild-type mice (Lyden, Young et al. 1999). Tumour growth in $Id1^{+/-}$ $Id3^{+/+}$ was intermediate between wild-type and $Id1^{+/-}$ $Id3^{-/-}$ mice, clearly indicating a dose-dependency of Id protein function on tumour angiogenesis. These results were consistent for injections of B6RV2 lymphoma cells, and B-CA breast cancer cells into Id-deficient mice where differences in tumour growth were attributed to poor vascularization due to decreased branching and sprouting of blood vessels compared to wild-type mice.

Due to numerous studies that have been discussed above implicating BMP signaling in tumour angiogenesis, components of the BMP signaling pathway have been established as potential targets for anti-angiogenic therapy in some cancers. For example, the heparin sulfate proteoglycan mimetic drug WSS25 has been shown to inhibit human

microvascular endothelial cell tube formation in Matrigel angiogenesis assays (Qiu, Yang et al. 2010). Mechanistically, WS225 was shown to exert its effects by blocking BMP2/Smad/Id1 signaling. This result was confirmed *in vivo*, as WSS25 treatment of nude mice that were injected with hepatocellular carcinoma cells exhibited decreased tumour growth due to the inhibition of angiogenesis.

In rare instances, BMPs have been shown to either have no effect on angiogenesis, or decrease angiogenesis in tumours. For example, there was no significant difference in VEGF and IL-8 expression levels upon recombinant human BMP2 treatment of UMSCC-1 and UMSCC-74A human oral squamous cell carcinoma (OSCC) cells (Gao, Tong et al. 2010). This result was confirmed *in vivo*, as there was no difference in blood vessel density of OSCC tumours formed from cells that were infected with adenovirus expressing BMP-2 before being injected into mice. Also, treatment of A549 lung carcinoma cells with BMP4 *in vitro* led to decreased expression of VEGF protein, which contributed to the formation of smaller tumours that were formed in nude mice (Buckley, Shi et al. 2004). Additionally, the BMP antagonist gremlin is believed to play a pro-angiogenic role in specific cancers. For example, injection of human adenocarcinoma HEC-1-B cells into nude mice showed very strong gremlin expression in highly vascularized areas of the tumour, whereas expression was much lower in other parts of the tumour (Stabile, Mitola et al. 2007). Despite the fact that the majority of the current literature supports the BMPs as pro-angiogenic factors with respect to tumourigenesis, these examples of BMPs having anti-angiogenic effects highlight the importance of studying BMP signaling relating to tumour angiogenesis in a cancer-specific context. Specifically, the role of BMP signaling in angiogenesis has never been

reported in EOC. Therefore, our findings will shed light on the potentially unique role of BMP4 signaling on mouse EOC angiogenesis.

1.3 Models of cancer

1.3.1 Mouse models of epithelial ovarian cancer

Although there have been other animal models such as rat (Davies, Auersperg et al. 1998), rabbit (Coppola, Saunders et al. 1999), and hen (Johnson 2009) models of ovarian cancer, this discussion will focus on mouse models of EOC. Historically, the majority of animal models of ovarian cancer have involved xenografting human ovarian cancer cells into immunodeficient mice such as severe combined immunodeficient (SCID) and athymic nude mice (Cho 2009). These xenografts have been administered by subcutaneous implantation (Downer, Jones et al. 2001), intraperitoneal injections (Shepherd, Mujoomdar et al. 2010), and by orthotopic implantations into the mouse ovarian bursa (Greenaway, Henkin et al. 2009).

Alternatively, mouse cell lines were created from studies in which mouse ovarian surface epithelial cells were passaged repeatedly *in vitro*. Late passage cells then spontaneously transformed and were able to form ovarian tumours when injected into both immunocompromised and immunocompetent mice (Roby, Taylor et al. 2000). From this study, the spontaneously-transformed clone ID8 has been generated, which has been shown to express constitutively active Src (Pengetnze, Steed et al. 2003). There is another mouse ovarian cancer cell line that has been created by transfecting SV40 TAg into primary cultures of mouse ovarian surface epithelium (MOSE) cells, which were then able to form tumours when injected into nude mice (Kido and Shibuya 1998). However,

additional mouse EOC cell lines with specific and known mutations need to be created and characterized so that they can be used in order to gain a more thorough understanding of EOC.

There have been some recently developed genetically engineered mouse models of EOC. One of the first transgenic mouse models of EOC was created by expressing the early region of the SV40 TAg gene, and placing it under the transcriptional control of the *MISRII* (Müllerian inhibiting substance type II receptor) gene promoter (Connolly, Bao et al. 2003). These TgMISIIR-TAg transgenic mice develop poorly differentiated ovarian cancer that replicates several key features of human ovarian cancer progression such as tumour dissemination and the formation of ascites. Recently, there have been several mouse models of ovarian cancer that rely on conditional expression of genes through Cre-recombinase mediated excision of specific sequences flanked by *loxP* sites containing these genes (Connolly 2009). This is accomplished by locally administering adenovirus that expresses Cre-recombinase to the mouse ovarian bursa. For example, one study developed LoxP-Stop-LoxP-*Kras* $^{G12D/+}$ *Pten* $^{LoxP/LoxP}$ mice with conditional activation of *Kras* and conditional inactivation of *Pten*, which was the first genetic mouse model of endometrioid EOC; a cell line developed from these mice will be discussed later (Dinulescu, Ince et al. 2005). Another mouse model that develops tumours that are histologically similar to endometrioid EOC is the *Pten* $^{LoxP/LoxP}$ *Apc* $^{LoxP/LoxP}$ mouse model with conditional inactivation of the *Pten* and *Apc* genes (Wu, Hendrix-Lucas et al. 2007). As well, *p53* and *Rb* are conditionally-inactivated in *p53* $^{LoxP/LoxP}$ *Rb* $^{LoxP/LoxP}$ mice, and tumours that are formed in these mice resemble serous EOC (Flesken-Nikitin, Choi et al. 2003).

Ideally, other *in vivo* model systems need to be used in order to complement mouse EOC studies and address some of the limitations of the current xenograft and genetically-engineered mouse models. One such model that has rarely been used to study EOC, but that offers many unique advantages, is the chick chorioallantoic membrane (CAM) model system. I will discuss several characteristics of this model system as well as the few ovarian cancer studies that have utilized this system in order to highlight several of the unique advantages of this model that can be utilized to study EOC.

1.3.2 Chick chorioallantoic membrane

In the developing avian embryo, the chick CAM is a specialized tissue that functions as a lung for the embryo, as it is responsible for gas and nutrient exchange between the embryo and the surrounding atmosphere (Deryugina and Quigley 2008). Initially, the CAM is formed between days 5 and 6 of embryonic development due to the partial fusion of chorion and allantois. It is a very thin structure that usually less than 100 μm in thickness once it is fully formed (Deryugina and Quigley 2008). Histologically, it consists of 3 main layers (Deryugina and Quigley 2008).The first layer is the ectoderm, which is usually attached to the shell membrane and is one or two epithelial cell layers in thickness. This layer eventually develops into the capillary plexus around day 10, which is a network of capillaries that connect arterial and venous blood vessel networks that contribute to a highly vascularized tissue. The middle layer is the mesoderm that also has many blood vessels, of which some are terminal capillaries that end immediately below the ectoderm. This layer also contains stromal components and collagen fibers. Finally, the third and innermost layer is the one-cell layer thick flat endoderm, which separates

the rest of the CAM from the allantoic cavity. Between days 10-15, there are 2 types of inflammatory cells that can present themselves in the embryos (Deryugina and Quigley 2008). The first group is the heterophils, which are the avian equivalent to mammalian neutrophils. The second group of inflammatory cells is the monocytes. Both of these inflammatory cells are sources of growth factors and pro-angiogenic MMPs, and therefore facilitate angiogenic responses.

With respect to cancer, the chick CAM has been used as an *in vivo* model to evaluate angiogenesis (Chim, Qin et al. 2011), primary tumour growth (Gao, Cao et al. 2004), metastasis (Subauste, Kupriyanova et al. 2009), and to screen potential drugs (Shen, Wang et al. 2010). There are several advantages of using the chick CAM model system. For example, until day 11 or 12 of embryonic development when the CAM has expanded to fully envelope the embryo, the CAM vasculature is undergoing maturation through the constant generation of new blood vessels (Deryugina and Quigley 2008). Immediately prior to this time between days 8 and 10, the central portion of the CAM is developed and is very responsive to proangiogenic or antiangiogenic stimuli. Therefore, the CAM is used as a model to test pro- or antiangiogenic compounds (Deryugina and Quigley 2008). Additionally, the lymphoid system of the CAM is not fully formed until the late stages of incubation, and is therefore relatively immunotolerant early in development (Deryugina and Quigley 2008). As a result, the CAM can accept most cell grafts without species-specific limitations, such as human tumour cells. Another benefit of the chick CAM is that growth of tumour xenografts on the surface of the chick CAM is very rapid (Figure 1.3), which is evidenced by the fact that visible tumours grow as early as 4-7 days after tumour cell inoculation. In fact, some tumour cell types under ideal

Figure 1.3 Rapid growth of tumour xenografts in the chick CAM model system

(A) The highly vascularized chick CAM consists of three main layers. Epithelial ovarian cancer cells can be xenografted onto the surface of the chick CAM, and (B) are inoculated at sites where large blood vessels at the surface intersect. Inoculating cells at these sites will increase the probability of successful tumour formation. (C) After 7 days, 1×10^6 MOSERM cells that had been seeded onto the CAM formed a tumour between 1 and 2 mm in diameter. Scale bars: 2 mm.

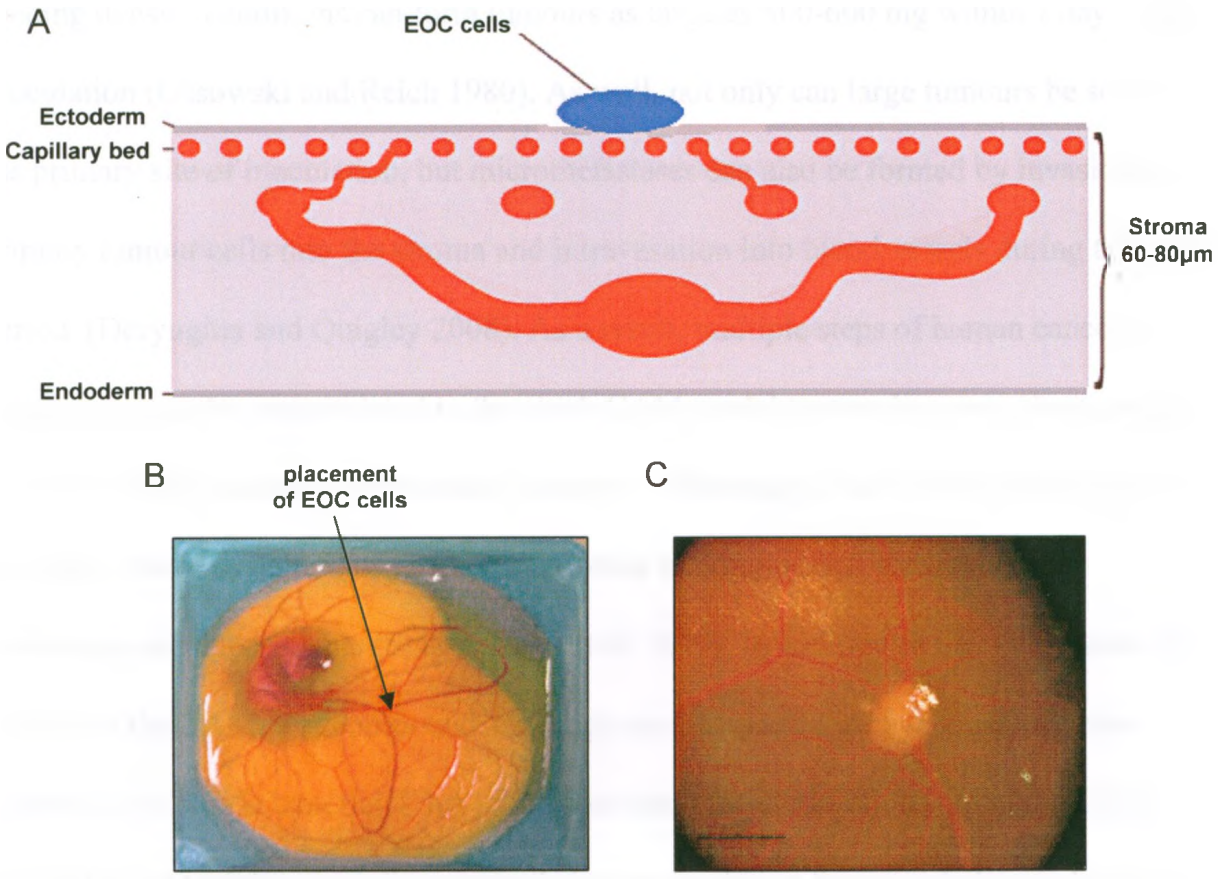
A
EOC cells
Ectoderm
Capillary bed
Stroma
60-80µm
Endoderm
B
placement
of EOC cells
C

seeding density conditions can form tumours as large as 500-600 mg within 7 days after inoculation (Ossowski and Reich 1980). As well, not only can large tumours be seen at the primary site of inoculation, but micrometastases can also be formed by invasion of primary tumour cells into the stroma and intravasation into blood vessels during this time period (Deryugina and Quigley 2008). As a result, multiple steps of human cancer progression can be recapitulated in the chick CAM model system in a very short period of time relative to other *in vivo* model systems. Additionally, the CAM is a very simple and inexpensive system relative to other models, making it ideal for large-scale screenings and experiments (Staton, Reed et al. 2009). In addition to inoculations on the surface of the CAM, test compounds or drugs can be injected intravenously or intra-allantoically. This is beneficial due to the fact that limited excretions out of the CAM allows for the maintenance of compounds in the circulation for extended periods of time. Similarly, the easy accessibility and simplicity of the system also allows for repeated treatments over time to the CAM if required.

However, there are some limitations of using the CAM system, particularly with respect to angiogenesis. First of all, the CAM itself is well vascularized. Therefore can be difficult to distinguish new capillaries from pre-existing capillaries (Staton, Reed et al. 2009). As well, irritation of the CAM during inoculations or injections can cause inflammatory responses which can induce angiogenesis on its own (Deryugina and Quigley 2008). The chick CAM has long been used as a common model system in developmental biology, but has not been as common in the field of cancer research which has largely focused on mouse models in large part due to the ability to genetically engineer these models (Hagedorn, Javerzat et al. 2005). However, relatively new studies

have highlighted techniques that may allow for genetic manipulation of the avian embryo (Pekarik, Bourikas et al. 2003).

There are two ways in which the chick CAM can be prepared in order to perform various assays, which are called the '*in ovo*' and '*ex ovo*' methods. In the *in ovo* method, fertilized eggs are placed in a humidified chamber at 37°C and the embryos are allowed to partially develop (Ribatti, Vacca et al. 1996). Then, a small window can be cut in the eggshell so that the underlying CAM is exposed and accessible. After this, the window is often covered with cellophane tape until the desired assay is performed. In the *ex ovo* method, the embryo and extraembryonic membranes are transferred to a Petri dish in the early stages of development, typically on day 3 or 4 of development (Auerbach, Kubai et al. 1974). The dish is then incubated at 37°C in a humidified chamber until the desired assay is performed. Therefore, the CAM develops in the Petri dish as a flat membrane, and reaches the edges of the dish as it develops (Ribatti, Vacca et al. 1996). While both techniques are considered to be minimally invasive, they both have advantages and disadvantages associated with them. It is argued that the *in ovo* method requires less maintainence during development (Staton, Reed et al. 2009). Additionally, embryos can be maintained to later stages of development using this method. Due to the fact that the entire CAM can be seen with the *ex ovo* method as opposed to only being able to see a small portion of the CAM, multiple xenografts can be placed onto the surface of each CAM (Ribatti, Vacca et al. 1996). Although, there can be loss of embryos within the first 3 days following their transfer to Petri dishes, survival rates after this point are very good and are comparable to the *in ovo* method (Auerbach, Kubai et al. 1974).

The chick CAM has been used to study many types of cancer such as colon cancer (Kim, Hur et al. 2011), gliomas (Auf, Jabouille et al. 2010), and pancreatic cancer (Laklai, Laval et al. 2009). There have also been some studies that have investigated aspects of ovarian cancer using the chick CAM system. For example, Kaempferol is a naturally occurring flavonoid that is found in many fruits and vegetables (Luo, Rankin et al. 2009). It was shown that when OVCAR3 human ovarian cancer cells were treated with Kaempferol, tumour growth of these cells was decreased as measured by tumour weight. Additionally, angiogenesis was decreased in these treated cells as measured using an angiogenesis onplant assay. A very similar study was done which tested the effect of Apigenin on angiogenesis by placing Matrigel onplants containing Apigenin with OVCAR3 cells onto the CAM (Fang, Zhou et al. 2007). Apigenin, which is also a naturally occurring flavonoid, showed anti-angiogenic properties as measured by the number of new blood vessels formed. Studies have shown that soluble L1 adhesion molecule (sL1) protein is expressed at high levels in primary EOC tumour samples (Fogel, Gutwein et al. 2003), and this protein has also been detected at high levels in the ascites fluid of ovarian cancer patients (Gutwein, Stoeck et al. 2005). The effects of sL1 on angiogenesis were then assessed by using the chick CAM angiogenesis onplant assay, and it was shown that sL1 significantly increases angiogenesis on the CAM based on blood vessel density (Friedli, Fischer et al. 2009). Another study used malignant ascites fluid (MAF) that was isolated from ovarian cancer patients using paracentesis (Richardson, Gunawan et al. 2002). Although the MAF contained VEGF, it also contained angiostatin and other anti-angiogenic factors. It was found that application of MAF to the surface of the chick CAM inhibited capillary formation. Other studies have

been used to test the effectiveness of newly synthesized compounds on angiogenesis on the chick CAM before being applied to other model systems. For example, a library of compounds that were designed to be angiogenic inhibitors were applied directly to the surface of the chick CAM, and two compounds were identified to significantly inhibit angiogenesis as measured by blood vessel density (Dings, Chen et al. 2006). These two compounds were then applied to an *in vivo* model in which MA148 human ovarian carcinoma cells were injected into athymic nude mice with or without daily administration of the compounds. It was found that both compounds reduced tumour growth as measured by tumour volume and weight, and these treated tumours were confirmed to have decreased microvessel density. The authors of the study then suggested that their next steps would be to complete ongoing toxicity profiles in mice followed by initiating phase I clinical trials in humans. Overall, the chick CAM can be used as an effective model system to study multiple aspects of tumourigenesis in various types of cancer. These studies that have been described that use the chick CAM to study EOC provide evidence that this system can be effectively utilized for additional EOC experiments. Therefore, my studies will involve using this model system in order to further support its use as an effective tool to study EOC.

1.4 Objectives and experimental rationale

Based on previous data showing that upregulated BMP signaling decreased the ability of EOC tumour cells to metastasize to form secondary nodules upon injection into mice (Shepherd, Mujoomdar et al. 2010), I hypothesize that upregulated BMP signaling in the mouse EOC cell lines will decrease EOC tumour formation on the chick CAM by

decreasing the rate of proliferation, and by inhibiting the angiogenic potential of these cells. This hypothesis will be addressed by completing the following objectives:

A. Characterize proliferation, tumour formation, angiogenesis, and BMP signaling gene expression in MOSERM, MASC2, and 4306 mouse EOC cell lines *in vitro* and on the chick CAM

B. Assess role of altered BMP signaling on EOC tumourigenesis and angiogenesis

C. Assess applicability of the chick CAM as an alternative model system that can be used to study multiple aspects of EOC progression, specifically tumour formation and angiogenesis

One of the important aims of my research is to support the use of the chick CAM as an alternative model system that can be used to study multiple aspects of EOC metastasis. The MOSERM, MASC2, and 4306 mouse EOC cell lines have not been well characterized in the literature. Therefore, given that each of these cell lines formed in mice, I will determine whether these cells will also be able to form tumours in another model system by seeding them onto the chick CAM. I will then further characterize these three mouse EOC cell lines by investigating what mechanism(s) are responsible for the differences in tumourigenic potential that may be seen between the cell lines on the chick CAM.

BMP signaling has been implicated in multiple aspects of EOC tumourigenesis including EMT transition, cell adhesion, motility, and invasive potential *in vitro* (Shepherd and Nachtigal 2003; Moll, Millet et al. 2006; Theriault, Shepherd et al. 2007). It has also been implicated in limiting the ability of EOC cells to form secondary tumour nodules *in vivo* (Shepherd, Mujoomdar et al. 2010). Therefore, I will further characterize

the MOSERM, MASC2, and 4306 cell lines by assessing their relative expression levels of 84 TGFβ/BMP signaling-related genes compared to normal mouse EOC cells. Additionally, I will compare the relative BMP signaling expression levels of the mouse EOC cell lines with one another in order to determine if there are any expression patterns that will correlate with other tumourigenic properties that will be assessed.

Essential to gaining a better understanding of the complex roles that BMP signaling plays in EOC is to alter the expression and activity of this pathway in MOSERM, MASC2, and 4306 cells. One approach to accomplish this is to stably-transfect cells with ALK3QD, which is a constitutively-active type I BMP receptor. BMP signaling will also be altered in parental mouse EOC cell lines by administering short-term treatment of BMP4, BMP antagonist noggin, or BMP receptor type I inhibitor LDN-193189. These methods will allow me us to assess the role of altered BMP signaling on tumour formation on the chick CAM, proliferation, cell survival, and angiogenesis using multiple strategies.

Angiogenesis will be assessed in the ALK3QD clones as well as in the initial characterization of angiogenic potential in the three parental mouse EOC cell lines by using an innovative chick CAM angiogenesis onplant assay. I will therefore have the opportunity to further develop the chick CAM as a model system that can be used to study EOC by utilizing it in these angiogenesis studies as well as in tumour formation studies.

CHAPTER TWO

MATERIALS AND METHODS

2.1 Cell lines

The MOSERM cell line (gift from Dr. Barbara Vanderhyden, University of Ottawa, Ottawa, ON) was derived from mouse ovarian surface epithelial cells isolated from transgenic mice expressing a temperature sensitive mutant of SV40 large T antigen (Yao, Li et al. 2006). These cells were subsequently transfected with plasmids to ectopically express the *Ras* and *Myc* oncogenes. The MASC2 ovarian cancer cell line (gift from Dr. Barbara Vanderhyden, University of Ottawa, Ottawa, ON) was derived from the ascites fluid of mice with metastatic ovarian tumours due to the conditional transgenic expression of SV40 large T antigen specifically in the OSE (Laviolette, Garson et al. 2010). The 4306 ovarian cancer cell line (gift from Dr. Daniela Dinulescu, Brigham and Women's Hospital, Boston, MA) was derived from the ascites fluid of conditional transgenic mice with metastatic ovarian cancer. These mice express oncogenic mutant $Kras^{G12D}$ in addition to having an inactivated *Pten* tumour suppressor gene specifically in the OSE (Dinulescu, Ince et al. 2005).

2.2 Cell culture

The MOSERM and MASC2 murine ovarian cancer cell lines were grown in Alpha Modification of Eagles' Medium (AMEM – Wisent, St. Bruno, QC, Canada) supplemented with 5% Fetal Bovine Serum (FBS – Wisent). The 4306 murine ovarian

cancer cell line was grown in Dulbecco's Modified Eagle's Medium (DMEM – Wisent) supplemented with 5% FBS. MOSERM, MASC2, and 4306 cells were grown in standard tissue culture-treated polystyrene plates (Sarstedt, Montreal, QC). Primary HUVECs (gift from Dr. John Lewis, London Regional Cancer Program, London, ON) were grown in Endothelial Cell Complete Growth Medium (EGM – Lonza, Walkersville, MD) containing 2% FBS and supplemented with 0.4% Bovine Brain Extract (BBE – Lonza). HUVECs were grown and maintained in Cell$^+$ T175 flasks (Sarstedt). Cells were detached from tissue culture plates for passaging with 0.25% Trypsin/1%EDTA solution (Wisent), which would then be deactivated with media containing 5% FBS. Cells were maintained in humidified chambers at 37°C with 95% air and 5% CO_2.

2.3 Establishment of GFP and GFP-ALK3QD clones

MOSERM, MASC2, and 4306 GFP clones were previously created (work completed by Yudith Ramos-Valdés) using a murine stem cell virus (MSCV) retroviral vector. HEK293T cells were used as a packaging cell line, which were transfected using SuperFect® Transfection Reagent (Qiagen, Toronto, ON). At day 1, the SuperFect® Transfection Reagent was added to DMEM along with a MSCV Puro IRES GFP viral vector (MSCV PIG) containing GFP and the Puromycin resistance gene, ψ packaging vector, and vesicular stomatitis virus glycoprotein (VSVG) plasmid. After 24 hours, media on the transfected plates was changed. At day 5, approximately 100μL of virus containing media from the HEK293T transfected plates was added to 6cm plates with the cell lines of interest that were to be infected (MOSERM, MASC2, 4306). After 24 hours, media on these infected plates was changed. Finally, these cells were placed under

Puromycin (BioShop, Burlington, ON) selection pressure at a concentration of 1μg/mL after which time 5 GFP-expressing clones from each of the parental cell lines (MOSERM, MASC2, 4306) were isolated and expanded (worked completed by Yudith Ramos-Valdés).

ALK3QD clones were created by transfecting MOSERM-GFP, MASC2-GFP, and 4306-GFP cells with a pcDNA 3.0 expression vector (Invitrogen, Carlsbad, CA) containing hemagglutinin (HA) -tagged hALK3QD. The ALK3QD (Q233D) BMP type I receptor contains a Q-to-D point mutation in its glycine/serine rich domain at amino acid 233 (Hoodless, Haerry et al. 1996). As a result, this removes the requirement of transphosphorylation by BMPRII due to BMP ligand binding for the BMP type I receptor to be activated. GeneJuice® Transfection Reagent (Novagen, Mississauga, ON) was used in these transfections. Briefly, 15 μL GeneJuice® was added to 300μL of either AMEM (MOSERM GFP and MASC2 GFP cells) or DMEM (4306 cells) followed by the addition of 5 μg HA-tagged hALK3QD pcDNA 3.0 (0.45 μg/μL). This mixture was added to 60mm plates that were going to be transfected, which were then incubated for 72 hours. After this time, cells were placed under G418 (Wisent) selection pressure at concentrations of 800 μg/mL for 10-14 days. After this time, 4 MOSERM, 2 MASC2, and 5 4306 GFP ALK3QD clones were isolated and expanded.

2.4 *In vitro* cell proliferation and survival assays

Cell proliferation was assessed either by cell counting using a haemocytometer, or by alamarBlue® (Invitrogen) proliferation assays. For cell counting, 5000 cells of each cell line were seeded onto 60 mm plates in 5 mL media, and were grown for up to 5 days.

Each day, adherent cells were exposed to trypsin for all approximately 5 minutes, and following cell detachment, the trypsin was inactivated using FBS-containing media. To evaluate total cell number, trypsinized cells were counted using a haemocytometer by averaging 2 haemocytometer counts for each plate.

For alamarBlue® proliferation, 500 cells were seeded into the wells of 96-well plates, and were grown for up to 5 days in 200 μL of media. At each time point (days 0, 1, 2, 3, 4, 5) media was aspirated and replaced with 200 μL of a 1:20 ratio of alamarBlue®: media. The alamarBlue® treated 96-well plates were then incubated at 37°C for 4 hours. At this time, the reactions were measured fluorometrically using a Wallac 1420 Multilabel Counter (Perkin Elmer Wallac, Gaithersburg, MD) with a fluorescence protocol. This protocol uses a fluorescence excitation wavelength of 570 nm, and fluorescence emission at 585 nm in order to quantify fluorescence units.

Cell survival was measured using similar conditions as the alamarBlue® proliferation assay, but with some modifications. For the MOSERM and MASC2 cell lines, 5000 cells were seeded into the wells of a 96-well plate. For the 4306 cell line, 10000 cells were seeded into the wells of a 96-well plate. The cells were then grown for up to 5 days in 200 μL of serum-free media (0% FBS). At each time point (days 0, 1, 2, 3, 4, 5), media was aspirated and replaced with 200 μL of a 1:20 ratio of alamarBlue®: serum-free media. Cell survival was then measured as described above using the Wallac 1420 Multilabel Counter. Seeding densities are based on a preliminary 5 day serum-starving alamarBlue® experiment in which various quantities of cells (2000-10000 cells in 96-well plates) for each line were seeded in order to determine the minimum amount

of cells that had to be seeded in order to be able to achieve a quantifiable fluorescence signal after 5 days.

2.5 RNA isolation and gene expression profiling

RNA isolation from cells grown in monolayer was completed by using an RNeasy Mini Kit (Qiagen) as per manufacturer's instructions. The isolated RNA was then treated using an Amplification Grade DNase I kit (Sigma-Aldrich, Oakville, ON) in order to remove contaminating DNA as per manufacturer's instructions. The quality and quantity of the isolated RNA was determined using a NanoDrop 1000 Spectrophotometer (NanoDrop Products, Wilmington, DE).

Gene expression profiles for the MOSERM, MASC2, and 4306 cell lines were assessed by using a TGFβ/BMP Signaling Pathway RT^2 Profiler PCR Array System (SABiosciences # PAMM-035, Frederick, MD). This array uses 96-well plates that contain optimized primers in each well for genes of interest that are involved in the TGFβ/BMP signaling pathway. The array also contains wells for several housekeeping genes, as well as control wells for PCR performance, RNA quality, and genomic DNA contamination. Briefly, 1 µg DNase-treated RNA was used for first strand cDNA synthesis that was completed using an RT^2 First Strand Kit (SABiosciences) as per manufacturer's instructions. This newly-synthesized cDNA in a volume of 102µL was mixed with RT^2 SYBR® Green/Rox™ qPCR Master Mix (SABiosciences) as per manufacturer's instructions that contained all of the buffers and reagents that are required for real-time PCR (real-time PCR buffer, nucleotides, high-performance HotStart DNA Taq polymerase, ROX® reference dye). Then, 25 µL of the master mix/cDNA mixture

was aliquoted in each of the wells of the 96 well-plates, and plates were run using a Strategene Mx3000P QPCR machine (Agilent Technologies, Cedar Creek, TX). Data analysis of the results was quantified using a PCR Array Data Analysis Web Portal for Excel (SABiosciences).

2.6 Western blotting

Total cellular protein was isolated by first scraping cells from their cell culture plates, and then washing them with cold Dulbecco's Phosphate-Buffered Saline (PBS) (Wisent). These cells were pelleted by centrifugation (5 minutes at 2000 x g), and were then dissolved in lysis buffer (50mM HEPES pH 7.4, 150mM NaCl, 10% glycerol, 1.5mM $MgCl_2$, 1mM EGTA, 10 mM sodium pyrophosphate, 1mM sodium orthovanadate, 10mM NaF, 1mM PMSF, 0.1% SDS, 1% sodium deoxycholate, 1% Triton X-100, and 1X protease inhibitor cocktail (Roche, Mississauga, ON)) for 20 minutes, at which time total cellular protein was clarified by centrifugation (20 minutes at 14000 x g).

The protein concentration of each lysate was determined by Bradford analysis as described previously (Bradford 1976), with some modifications. Briefly, a standard curve was generated using increasing concentrations of Bovine Serum Albumin (BSA) (New England Biolabs, Pickering, ON) by using Protein Assay Dye Reagent Concentrate (Bio-Rad Laboratories, Mississauga, ON). The colourimetric assay was quantified using a Model 3550 Microplate Reader (Bio-Rad Laboratories). Protein samples were then diluted by between 1:100 and 1:1000 in PBS, and 200µL of diluted protein was added to wells in a 96-well plate. 100µL of Protein Assay Dye Reagent that was diluted 2:1 with

PBS was added to each well, and values were quantified using the Model 3550 Microplate Reader. Finally, protein concentration was determined based on interpolation using the standard curve.

Protein extracts (50-90 μg) were resolved by sodium dodecyl sulfate polyacrylamide gel electrophoresis (SDS-PAGE) using 8% or 12% gels. These proteins were transferred to a polyvinylidene difluoride membrane (PVDF – Roche), and were subsequently blocked with 5% skim milk in Tris-buffered saline and Tween 20 (TBST – 10mM Tris-HCl pH 8.0, 150mM NaCl, 0.1% Tween 20) for at least one hour at room temperature. Membranes were washed in TBST and incubated overnight at 4°C in TBST in 5% skim milk with 0.02% NaN_3 and appropriate concentrations of primary antibodies (actin, ID1, ID3, phospho-Smad1/5/8, Smad1, HA high affinity – 1/1000). After this, the membranes were incubated in anti-rabbit horseradish peroxidase (HRP)-linked secondary antibody (1/10,000 - GE Healthcare, Piscataway, NJ) for one hour at room temperature. Membranes incubated with anti-HA high affinity primary antibody were incubated in goat anti-rat HRP-linked secondary antibody (1/25,000 – Thermo Fisher Scientific, Toronto, ON). Immunoreactive bands were visualized by incubating the membranes for five minutes with chemiluminescence detection reagent (ECL Plus – GE Healthcare), exposing them to Hyperfilm™ ECL high performance chemiluminescence film (GE Healthcare), and developing them using a Kodak M35A X-OMAT Processor (Kodak Graphic Communications Company, Toronto, ON).

In some instances, blots were stripped to reprobe with different primary antibodies. Briefly, membranes were incubated with stripping buffer (2% SDS, 100mM β-mercaptoethanol, 62.5mM Tris-HCl pH 6.8) for approximately 45 minutes at 70°C.

The membranes were washed several times in TBST for at least 40 minutes. After this, membranes were reprobed beginning with blocking the membranes with 5% skim milk in TBST for at least one hour at room temperature as described above.

2.7 Antibodies and other reagents

Antibodies against total Smad1 (# 9517) and phospho-Smad 1/5/8 (# 9511) were purchased from Cell Signaling Technologies (Danvers, MA). The antibodies against ID1 (# BCH-1/195-14) and ID3 (# BCH-4/6-1) were purchased from BioCheck Inc. (Foster City, CA). Anti-actin antibody (# A2066) was purchased from Sigma-Aldrich. Anti-HA high affinity antibody (# 11 867 423 001) was purchased from Roche. LDN-193189 BMP type I receptor inhibitor was purchased from Axon Medchem BV (Groningen, The Netherlands). Recombinant human Noggin and BMP4 were both purchased from R&D Systems #6057-NG-025 and 314-BP-010, Burlington, ON). LDN-193189, Noggin, and BMP4 were reconstituted as per product specifications.

2.8 Chick CAM tumour imaging and growth assay

Tumour growth assays on the chick CAM were performed similarly to other studies (Mitchell, Pobre et al. 2010). Fertilized White Longhorn chicken eggs were purchased from McKinley's Hatchery (St. Mary's, Ontario), and incubated in a rotary incubator at 38°C and 80% humidity. At day 4 of development, eggshells were removed and the embryos were carefully placed into weigh boats. Embryos were covered with lids and placed in a humidified stationary air incubator at 38°C and 80% humidity. At day 10 of development, the CAM was gently abraded with sterile filter paper that was

approximately 7 mm in diameter. After 10 minutes, the filter paper was gently removed using jeweler's forceps, and 25uL of cells (1,000,000 cells per 25uL PBS) were inoculated onto the surface of the CAM at the abraded site. Inoculation sites were chosen where large blood vessels intersected on the surface of the CAM, and that were also approximately an equal distance between the embryo and the edge of the weigh boat. The embryos were returned to the humidified stationary air incubator for the remainder of the experiment. After 7 days of incubation (i.e. at day 17 of development), images of tumour nodules were captured using PS Remote (Breeze Systems Ltd, Camberly, UK) and Paint Shop Pro 9 (Jasc Software, Ottawa, ON) with a StereoLumar.V12 fluorescence dissection microscope (Carl Zeiss, Toronto, ON) mated to a Hamamatsu ORCA-ER camera (Digital Imaging Systems Ltd, Buckinghamshire, UK). After imaging, tumours were excised and placed in Formalde-Fresh Solution (Thermo Fisher Scientific) overnight, and were then weighed using a Mettler AE240 digital semi-micro analytical balance (Mettler-Toledo Inc, Columbus, OH).

2.9 *In Vitro* angiogenesis assay

In vitro angiogenesis assays were performed as described previously (Kubota, Kleinman et al. 1988), with some modifications. Matrigel™ Basement Membrane Matrix (BD Biosciences, Mississauga, ON) which is a solubilized basement membrane extracted from Engel-Holm-Swarm (EHS) sarcomas, was diluted 1:2 with chilled EGM. This diluted Matrigel (60µL) was added to wells of a 96-well culture plate, and incubated at 37°C for 1-2 hours to allow for polymerization. HUVECs were plated onto the layer of gelled Matrigel at a concentration of 10,000 cells/50µL EGM, and were co-cultured with

50µL of mouse epithelial ovarian cancer cells (5000 cells/50µL media) in serum-free media. The plates were incubated at 37°C in 5% CO_2/95% air. After 3-6 hours, each well was photographed with an Olympus IX70 inverted microscope using Image-Pro Plus 6.2 (Media Cybernetics Inc., Bethesda, MD). Endothelial tube formation was quantified in each well by counting the number of branch points in 6-12 random fields of view at 100X magnification.

2.10 Chick CAM angiogenesis assay

Angiogenesis assays were performed as described previously (Seandel, Noack-Kunnmann et al. 2001), with some modifications. Briefly, high concentration rat-tail type I collagen (BD Biosciences) in autoclaved H_20 was neutralized with 10X PBS and 0.1N NaOH at a ratio of 8:1:1. The volumes of rat-tail type I collagen/autoclaved water varied to attain a final concentration of neutralized collagen at 2.5 mg/mL. Hepes solution (Sigma Aldrich) was added at a final concentration of 20mM to ensure a stable pH of 7.4. The pH of the final neutralized collagen solution was tested and additional 0.1 N NaOH was added if necessary. Two parts of neutralized collagen solution were combined with one part sterile 1X PBS containing BSA (final concentration 1 mg/mL) as a carrier protein. Finally, cells of interest were incorporated into the collagen at a concentration of 4×10^7 cells per mL.

Thirty microlitres of the final collagen/cell solution were pipetted onto 2 layers of sterile nylon mesh grids (Innovascreen, Halifax, NS). The mesh, which was cut and autoclaved beforehand, was prepared by placing the upper mesh (2mm x 2mm) onto the lower mesh (3mm x 3mm) at a 45^0 angle. For each experimental group, 40 collagen/mesh

onplants were laid onto Parafilm (Pechiney Plastic Packaging Company, Cleveland, OH) in 100 x 100 mm Petri dishes, and placed at 37°C for 3 hrs to allow for collagen polymerization into fibrils. Jeweler's forceps were used to place four onplants onto each CAM of 9-day-old chick embryos. The onplant-bearing embryos were incubated for an additional 3 days, at which time onplant vascularization was quantified. Newly formed vessels were identified by analyzing the upper plane of the onplant with a dissecting microscope. The angiogenic index of the onplants was determined as the percentage of mesh grids that contained newly formed blood vessels out of the total number of grids in the upper mesh. Images were captured using Volocity (Improvision Inc., UK) with a StereoLumar.V12 fluorescence dissection microscope mated to a Hamamatsu ORCA-ER camera.

2.11 Statistical Analyses

Data are expressed in figures as the mean ± standard error of the mean (SEM). When comparing an experimental sample with its matched control, a two-tailed unpaired Student's *t*-test was used. To compare the means among more than two samples, a one-way analysis of variance was used followed by Tukey's *post hoc* analysis. Differences with p values ≤ 0.05 are considered to be statistically significant. These statistical analyses were performed using GraphPad Prism version 3.0 software (GraphPad Software Inc, San Diego, CA).

CHAPTER THREE

RESULTS

3.1 MOSERM and 4306 mouse ovarian cancer cell lines form tumours on the chick chorioallantoic membrane (CAM)

The MOSERM, MASC2, and 4306 mouse ovarian cancer cell lines have not been well characterized either *in vitro* or *in vivo* in the literature. Given that each of these cell lines are able to form tumours in mice, I sought to determine the tumourigenic potential of each cell line in another model system by seeding them onto the chick CAM. The GFP-expressing clones that our lab has previously developed (work by Yudith Ramos-Valdés) were used for this experiment so that cells could be visualized by fluorescence microscopy even if macroscopic tumours were not formed, and to confirm that nodules that were formed were indeed composed of ovarian cancer cells. For each cell line, 1 x 10^6 cells in 25µL were seeded onto the surface of the CAM. After one week, tumour formation was assessed. MOSERM and 4306 cells form macroscopic tumour nodules on the chick CAM that and are consistently larger than 1 mm in diameter (Figure 3.1A). In fact, MOSERM tumours are visibly larger than the 4306 tumours. Since MASC2-GFP cells that were seeded onto the CAM did not form visible tumour nodules, fluorescence images were taken every day after the initial seeding to determine if these cells were present and able to survive on the CAM (data not shown). Although these cells were visible under fluorescence on the CAM up to approximately four days after seeding, they were no longer detectable on the CAM by day 7.

Figure 3.1 MOSERM and 4306 cells form tumours on the chick CAM.

Approximately 1 x 10^6 cells were seeded onto the surface of each chick CAM at embryonic day 11. (A) Brightfield and fluorescent images of the xenograft locations were taken 7 days after the initial seeding at 20X magnification. (B) The tumours were then excised from the surface of the CAM, placed in formalin overnight, and weighed. Error bars represent the standard error of the mean for tumour weight from at least 6 excised tumours per group. Asterisks indicate statistically significant differences between treatments (**p = 0.0087). Scale bars: 2 mm.

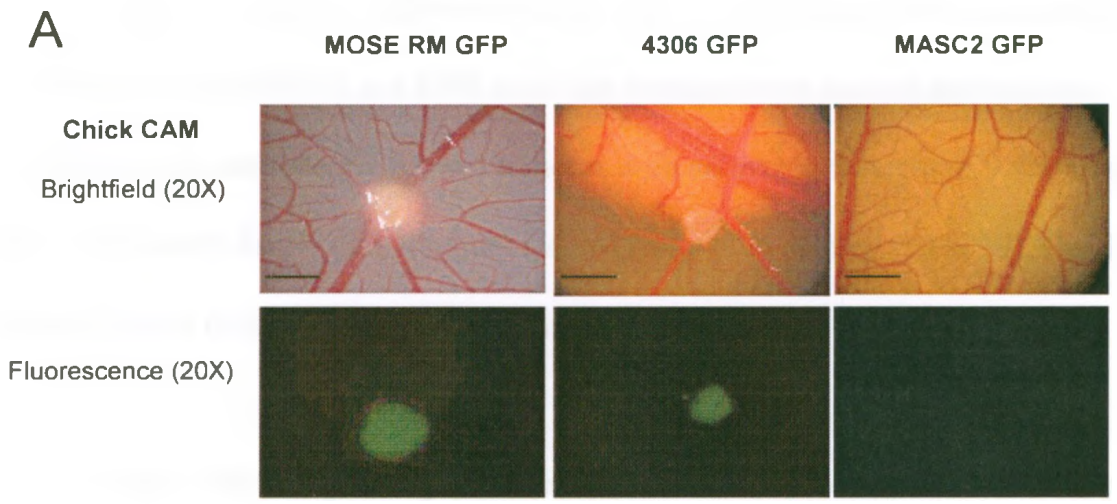
A
MOSE RM GFP
4306 GFP
MASC2 GFP
Chick CAM
Brightfield (20X)
Fluorescence (20X)

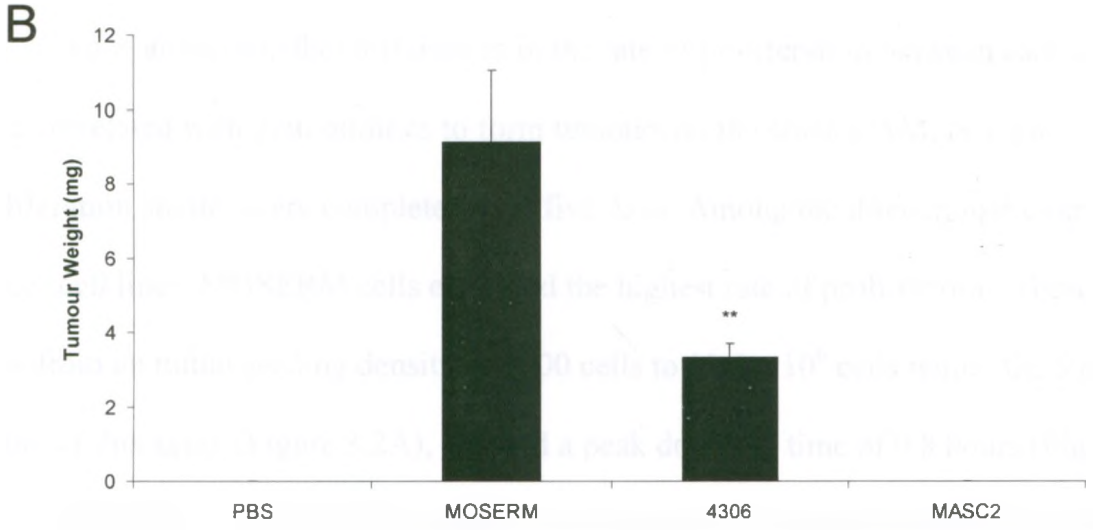
B
Tumour Weight (mg)
12
10
8
6
4
2
0
**
PBS
MOSERM
4306
MASC2

In order to quantify differences in the size of the tumours formed on the chick CAM between MOSERM and 4306 cells, the tumours were excised and weighed. MOSERM cells consistently formed tumours with an average weight of 9.1 ± 1.9mg that were significantly larger than tumours formed from 4306 cells ($p = 0.0019$), which had an average weight of 3.3 ± 0.4mg (Figure 3.1B).

3.2 Tumour forming ability on chick CAM does not correlate with *in vitro* proliferation

To evaluate whether differences in the rate of proliferation between each cell line were correlated with their abilities to form tumours on the chick CAM, *in vitro* proliferation studies were completed over five days. Among the three mouse ovarian cancer cell lines, MOSERM cells exhibited the highest rate of proliferation. These cells grew from an initial seeding density of 5000 cells to 11.5 x 10^6 cells within the 5 day period of this assay (Figure 3.2A), and had a peak doubling time of 9.8 hours (Figure 3.2B). MOSERM cells grew significantly more rapidly than both the MASC2 and 4306 cell lines ($p < 0.001$). Interestingly, MASC2 cells proliferate with a peak doubling time of 11.4 hours, which represented growth from 5000 to 3.5 x 10^6 cells within 5 days. This level of proliferation for MASC2 cells is significantly greater than 4306 cells ($p < 0.05$), which have a peak doubling time of 12.8 hours that represents growth from 5000 to 1.5 x 10^6 cells in 5 days.

Figure 3.2 Differences in the rate of proliferation of mouse EOC cell lines grown *in vitro*.

For each cell line, 5000 cells were seeded onto 60 mm plates and were grown for up to 5 days. At each time point, cells were trypsinized and counted. (A) Values represent the average number of cells between 3 replicates, and 2 haemocytometer counts were performed for each replicate. Bars represent the standard error of the mean for each group at each time point. (B) The peak doubling time for each cell line was calculated in hours by using the formula $T_D = 1/[\ln(N_t/N_o)/t](\ln 2)$ where N_t is the number of cells after the desired time interval (5 days) in the exponential growth phase, N_o is the number of starting cells, and t is the length of the experiment in hours (Mehrara, Forssell-Aronsson et al. 2007).

A

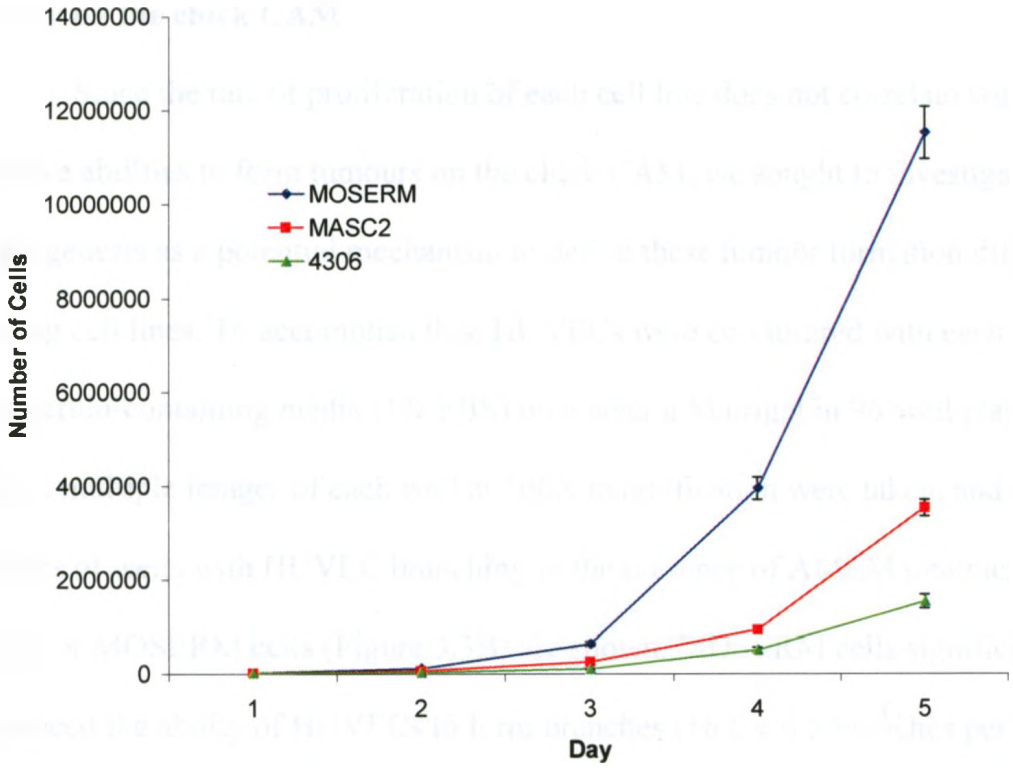

B

Cell Line	Peak Doubling Time (hours)
MOSERM	9.8
MASC2	11.4
4306	12.8

3.3 *In vitro* angiogenesis correlates with mouse EOC cell line tumour-forming ability on the chick CAM

Since the rate of proliferation of each cell line does not correlate with their relative abilities to form tumours on the chick CAM, we sought to investigate angiogenesis as a potential mechanism to define these tumour formation differences among cell lines. To accomplish this, HUVECs were co-cultured with each cell line in low serum-containing media (1% FBS) on a layer a Matrigel in 96-well plates. After 6 hours, multiple images of each well at 100X magnification were taken, and representative images of wells with HUVEC branching in the presence of AMEM treatment (Figure 3.3A) or MOSERM cells (Figure 3.3B) are shown. MOSERM cells significantly enhanced the ability of HUVECs to form branches (16.6 ± 0.5 branches per field of view) relative to AMEM alone (12.4 ± 0.3 branches per field of view; $p = 0.0016$; Figure 3.3C). Co-culture of HUVECs with 4306 cells also significantly enhanced HUVEC branching (10.7 ± 0.2 branches per field of view) compared to DMEM alone (8.0 ± 1.0 branches per field of view; $p = 0.0191$). In contrast, treatment of HUVECs with MASC2 cells did not significantly affect the rate of branching (8.1 ± 1.0 branches per field of view) when compared to AMEM alone (7.8 ± 0.7 branches per field of view).

3.4 *In vivo* angiogenic potential of mouse EOC cells assessed using the chick CAM

The chick CAM has been previously been used as an *in vivo* model system to assess angiogenesis. In order to determine if the abilities of MOSERM and 4306 cell lines to induce angiogenesis *in vitro* can also be detected *in vivo*, chick CAM

Figure 3.3 Angiogenesis as a potential mechanism defining differences in mouse EOC tumour formation on the chick CAM.

1×10^4 human umbilical vein endothelial cells (HUVECs) were plated onto Matrigel and co-incubated with 5000 MOSERM cells, MASC2 cells, or 4306 cells in low serum-containing media (1% FBS) in 96 well plates. After 3-6 hours, angiogenesis was quantified. Angiogenesis is measured by counting the number of branches formed by HUVECs per field of view. Representative images of branches within a field of view in a 96-well plate at 100X magnification are shown for AMEM control (A) and MOSERM cells (B). HUVEC branches are indicated by black arrows. The image for AMEM treatment contains 13 branches, while the image for MOSERM treatment contains 16 branches. (C) Branch counts for each cell line are represented by grey bars, while branch counts for their respective serum-free media treatments are represented by black bars. Error bars represent standard error of the mean for the average number of branches based on at least 4 wells per group. Pairwise comparisons were made within each pair of treatments, and asterisks indicate statistically significant differences within each pair (*p = 0.0191, **p = 0.0016).

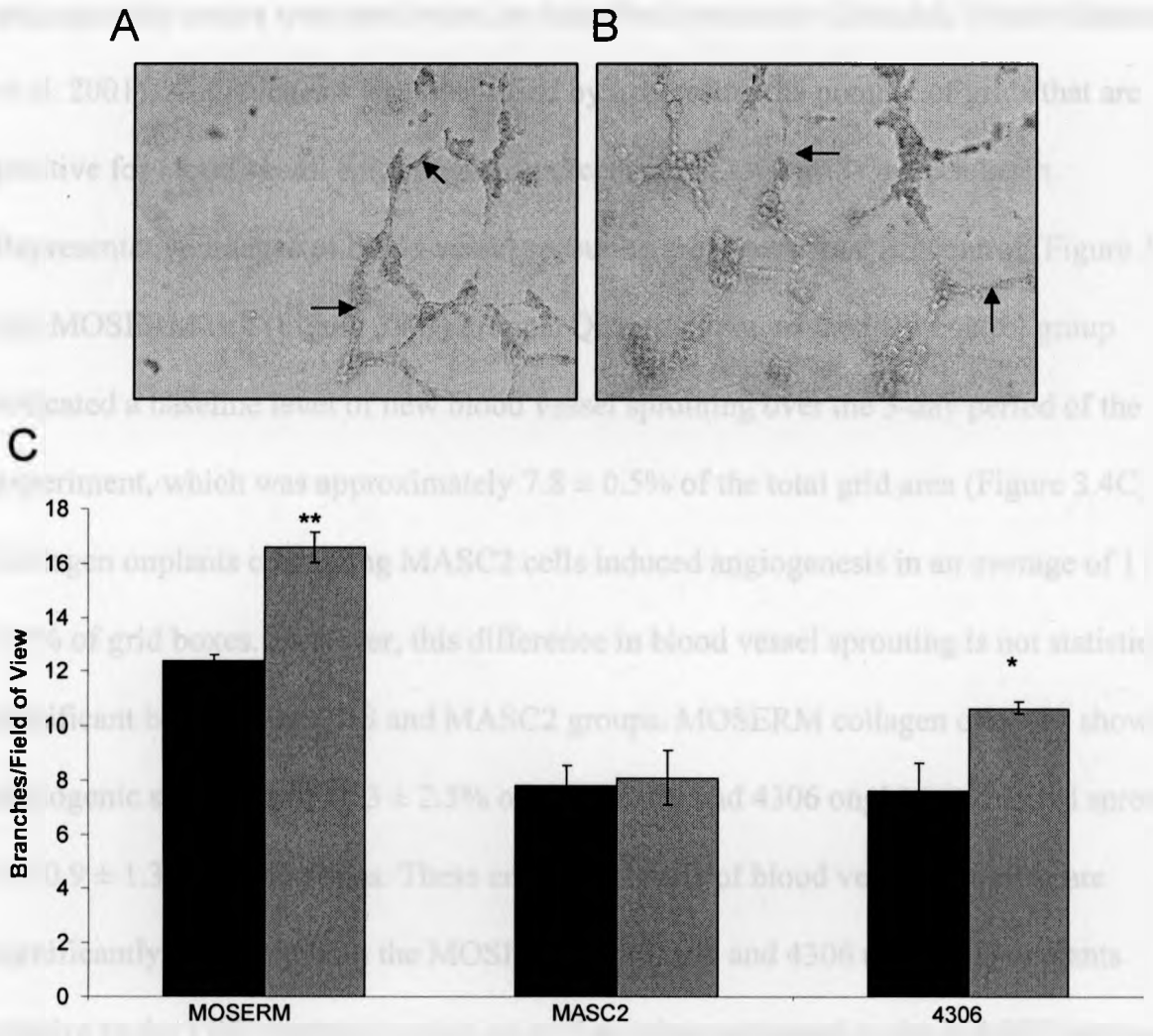
A
B
C
Branches/Field of View
18
16
14
12
10
8
6
4
2
0
**
*
MOSERM
MASC2
4306

angiogenesis assays were performed as described previously (Seandel, Noack-Kunnmann et al. 2001). Angiogenesis was quantified by expressing the number of grids that are positive for blood vessel sprouting as a percentage of total grids in each mesh. Representative images of blood vessel sprouting are shown for PBS control (Figure 3.4A) and MOSERM cell (Figure 3.4B) groups. Quantification of the PBS control group indicated a baseline level of new blood vessel sprouting over the 3-day period of the experiment, which was approximately 7.8 ± 0.5% of the total grid area (Figure 3.4C). Collagen onplants containing MASC2 cells induced angiogenesis in an average of 11.4 ± 1.7% of grid boxes. However, this difference in blood vessel sprouting is not statistically significant between the PBS and MASC2 groups. MOSERM collagen onplants showed angiogenic sprouting in 18.3 ± 2.5% of grid boxes, and 4306 onplants exhibited sprouting in 20.9 ± 1.3% of grid boxes. These enhanced levels of blood vessel sprouting are significantly greater in both the MOSERM ($p < 0.05$) and 4306 ($p < 0.01$) onplants relative to the PBS treatment group, as well as when compared to the MASC2 treatment group ($p < 0.05$). There was no significant difference in the degree of sprouting between the MOSERM and 4306 treatment groups.

3.5 Inverse correlation of mouse EOC cell line BMP4 signaling gene expression and tumour formation on the chick CAM

BMP signaling has been implicated in the progression of ovarian cancer in numerous studies (Shepherd and Nachtigal 2003; Moll, Millet et al. 2006; Theriault, Shepherd et al. 2007; Shepherd, Theriault et al. 2008; Pils, Wittinger et al. 2010; Shepherd, Mujoomdar et al. 2010). Previously, 4306 cells have been shown to possess an intact Müllerian Inhibiting Substance (MIS) signal transduction pathway based on ALK2,

Figure 3.4 Differences in angiogenic potential between mouse EOC cell lines are revealed on the chick CAM.

1×10^5 MOSERM, MASC2, or 4306 cells were embedded in collagen, which was then inserted between two mesh grids and placed on the surface of the chick CAM. After 3 days, angiogenesis was quantified. The degree of new blood vessel sprouting was measured by counting the number of grid boxes within each mesh that were positive for blood vessel sprouting. Representative images with blood vessel sprouting for PBS control (A) and MOSERM cells (B) are shown. Examples of grid boxes that are positive for new blood vessel sprouting are indicated by black arrows. The PBS mesh grid contains 3 of 47 boxes that are positive for blood vessel sprouting (6.4%), while the MOSERM mesh grid contains 6 of 41 boxes that are positive for blood vessel sprouting (17.1%). Note that a positive grid is determined if blood vessel sprouting is present, regardless of how many sprouts are within that grid box. (C) The percentage of grids that were positive for angiogenic sprouting is represented for each treatment group. Error bars represent standard error of the mean for the average percentage of positive grids based on at least 7 mesh grids per group. Different letters represent statistically significant differences among groups ($p < 0.05$).

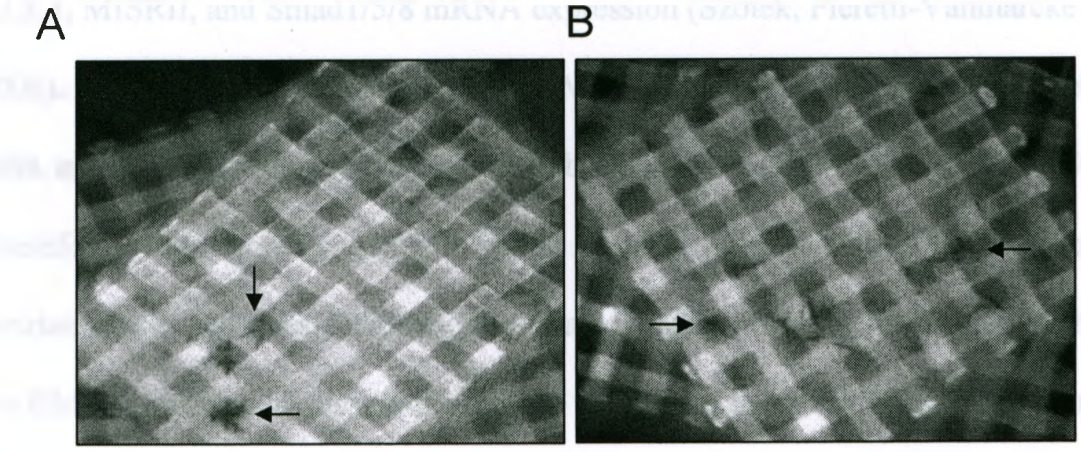
A
B

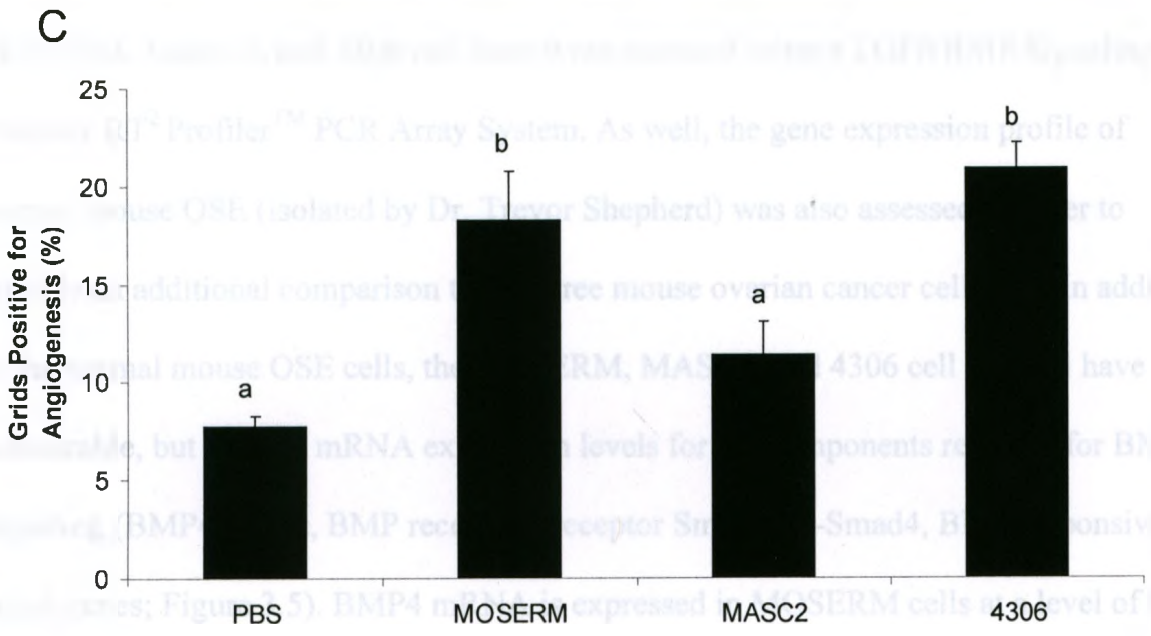
C
Grids Positive for Angiogenesis (%)
25
20
15
10
5
0
a
b
a
b
PBS
MOSERM
MASC2
4306

ALK3, MISRII, and Smad1/5/8 mRNA expression (Szotek, Pieretti-Vanmarcke et al. 2006). However, other aspects of TGFβ/BMP signaling have never been assessed in these cells, and TGFβ/BMP signaling has never been evaluated in MOSERM or MASC2 cells. Therefore, we sought to compare the BMP signaling expression profiles of these mouse ovarian cancer cell lines, and then investigated whether there were correlations between the BMP expression levels and the relative abilities of these cell lines to form tumours on the chick CAM or to induce angiogenesis. The gene expression profiles for the MOSERM, MASC2, and 4306 cell lines were assessed using a TGFβ/BMP Signaling Pathway RT^2 Profiler™ PCR Array System. As well, the gene expression profile of normal mouse OSE (isolated by Dr. Trevor Shepherd) was also assessed in order to provide an additional comparison to the three mouse ovarian cancer cell lines. In addition to the normal mouse OSE cells, the MOSERM, MASC2, and 4306 cell lines all have measurable, but distinct mRNA expression levels for the components required for BMP4 signaling (BMP4 ligand, BMP receptors, receptor Smads, co-Smad4, BMP responsive target genes; Figure 3.5). BMP4 mRNA is expressed in MOSERM cells at a level of 8.3 ± 0.5% relative to the expression levels of a panel of control genes, which was not significantly different than BMP4 expression in 4306 cells of 5.1 ± 1.0%. In mouse OSE cells, BMP4 is expressed at higher levels of 11.0 ± 0.2% when compared to 4306 ($p < 0.01$), but not to MOSERM cells. Interestingly, BMP4 is expressed at 19 ± 0.9% in MASC2 cells, which is significantly higher than MOSERM, 4306, and OSE cells ($p < 0.001$). One of the last steps in the BMP4 signaling pathway is the upregulation of target gene expression, such as the Ids. Id1 mRNA is expressed in MOSERM cells at a level of

Figure 3.5 Expression of BMP pathway signaling components among mouse EOC cell lines and normal mouse OSE cells.

TGFβ/BMP signaling was assessed using a SABiosciences RT^2 Profiler^{TM} PCR Array. Expression of mRNA for each group represents the average of arrays that were completed in duplicate, with error bars representing the standard error of the mean. The expression levels of each gene of interest for MOSERM, MASC2, 4306 and normal mouse OSE cells were normalized to the average expression level of a panel of five housekeeping genes (glucuronidase-beta (Gusb), hypoxanthine guanine phosphoribosyl transferase 1 (Hprt1), heat shock protein 90kDa alpha cystolic-class B member 1 (Hsp90ab1), glyceraldehyde-3-phosphate-dehydrogenase, actin-beta cytoplasmic (Actb)).

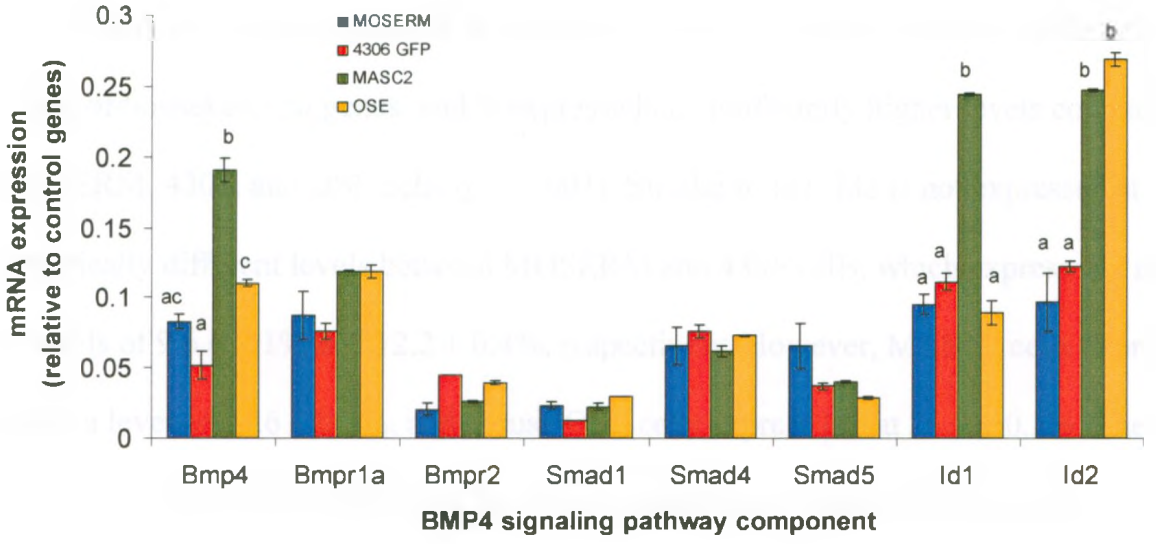
MOSERM
4306 GFP
MASC2
OSE
mRNA expression
(relative to control genes)
0.3
0.25
0.2
0.15
0.1
0.05
0
ac
a
b
c
a
a
b
a
a
b
b
b
Bmp4
Bmpr1a
Bmpr2
Smad1
Smad4
Smad5
Id1
Id2
BMP4 signaling pathway component

9.5 ± 0.7%, at 11.1 ± 0.6% in 4306 cells, and 8.9 ± 0.8% in mouse OSE, with none of these groups having significantly different expression levels from one another. However, Id1 in MASC2 cells is expressed at a level of 24.4 ± 0.1% relative to the expression levels of housekeeping genes, and is expressed at significantly higher levels compared to MOSERM, 4306, and OSE cells ($p < 0.001$). Similar to Id1, Id2 is not expressed at statistically different levels between MOSERM and 4306 cells, which express Id2 mRNA at levels of 9.6 ± 2.1% and 12.2 ± 0.4%, respectively. However, MASC2 cells express Id2 at a level of 24.6 ± 0.1%, and mouse OSE cells express Id2 at 26.9 ± 0.5%. These expression levels in MASC2 cells for Id2 are significantly greater than those for MOSERM or 4306 cells ($p < 0.001$). Other components of the BMP4 signaling pathway that were assessed (ALK3, BMPR2, Smad1, Smad4, Smad5) did not have statistically significant differences among cell lines or normal mouse OSE.

3.6 Ectopic stable expression of constitutively-active ALK3QD receptor in mouse EOC cells

MOSERM-GFP, MASC2-GFP, and 4306-GFP cells were all stably transfected to express the constitutively active type I BMP receptor, ALK3QD (Hoodless, Haerry et al. 1996). This ALK3QD is also HA-tagged so that successful transfections can be visualized by western blot. We originally screened 38 MOSERM clones, 12 MASC2 clones, and 14 4306 clones. From these screens, two independent clones for each of the three cell lines were expanded that were positive for ALK3QD-HA expression (Figure 3.6). The majority of these clones (MOSERM ALK3QD clones 1 and 2, MASC2 ALK3QD clones 1 and 2, 4306 clone 1) exhibited a relatively low level of ALK3QD

Figure 3.6 Changes in BMP signaling as a result of transfection of mouse EOC cell lines with ALK3QD.

Transfected ALK3QD clones are divided into two groups based on their BMP signaling expression levels compared to parental cells. (A) One group of transfected clones exhibits increased downstream BMP signaling relative to parental cells, while the other group (B) exhibits decreased BMP signaling compared to parental cells. (Top panel of A and B) Successful transfections of mouse EOC cell lines with HA-tagged ALK3QD was assessed with anti-HA high affinity. Western blotting was performed by using 90μg of total cellular protein, and equal loading was assessed with anti-actin. (Bottom panel of A and B) The effect of ALK3QD transfections on downstream BMP signaling was assessed using anti-phospho-smad1/5/8, anti-ID1, and anti-ID3. Western blotting was performed with 50μg of total cellular protein, and equal loading was assessed with anti-Smad1 and anti-actin. BMP signaling was considered to be upregulated or downregulated based on a change in phospho-Smad1/5/8 protein expression, as well as a change in at least one of either Id1 or Id3 protein expression.

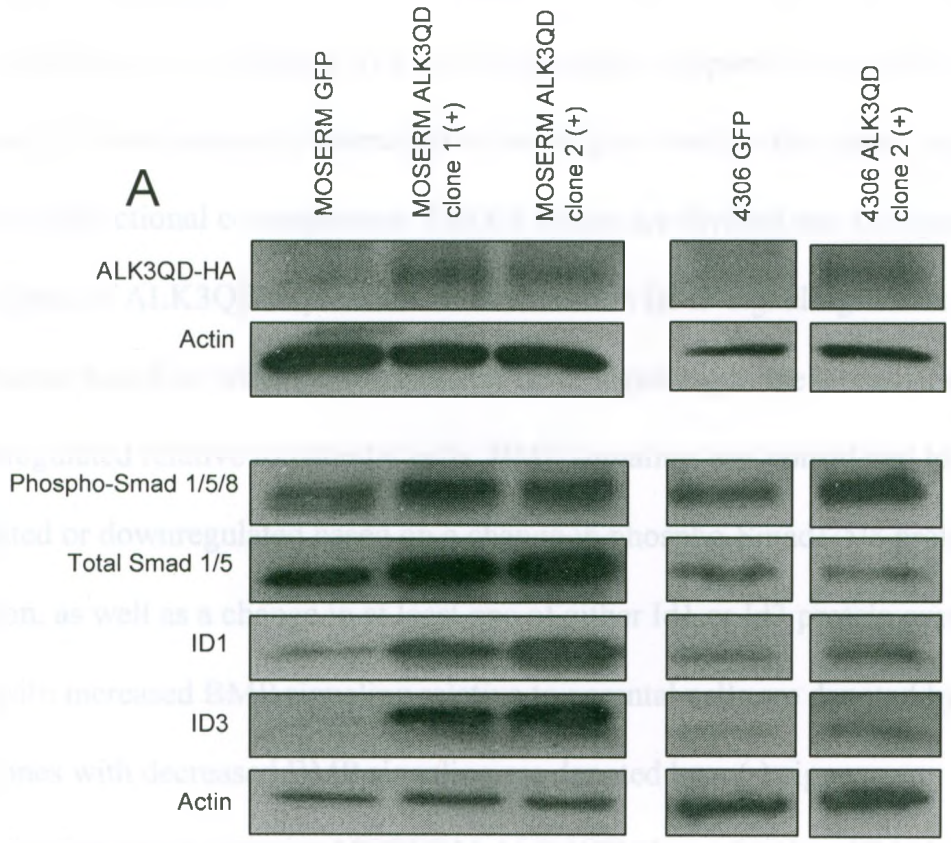
A
MOSERM GFP
MOSERM ALK3QD clone 1 (+)
MOSERM ALK3QD clone 2 (+)
4306 GFP
4306 ALK3QD clone 2 (+)
ALK3QD-HA
Actin
Phospho-Smad 1/5/8
Total Smad 1/5
ID1
ID3
Actin

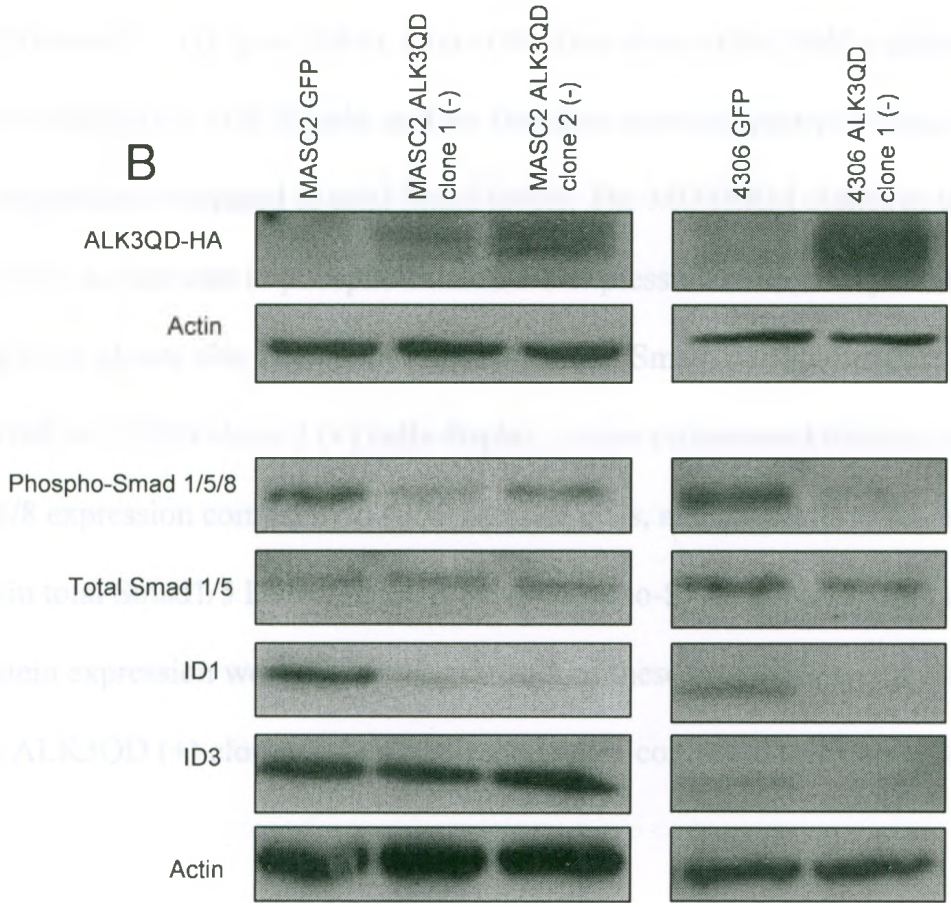
B
MASC2 GFP
MASC2 ALK3QD clone 1 (-)
MASC2 ALK3QD clone 2 (-)
4306 GFP
4306 ALK3QD clone 1 (-)
ALK3QD-HA
Actin
Phospho-Smad 1/5/8
Total Smad 1/5
ID1
ID3
Actin

expression as measured by western blot (top panel of Figure 3.6A and 3.6B), but 4306 clone 2 exhibited much stronger ALK3QD expression compared to the other clones. Therefore, we were especially interested to investigate whether this strong signal would have unique functional consequences. The six clones are divided into two groups based on the effects of ALK3QD expression on downstream BMP signaling. These groups are differentiated based on whether downstream BMP signaling in the clones is upregulated or downregulated relative to parental cells. BMP signaling was considered to be upregulated or downregulated based on a change in phospho-Smad1/5/8 protein expression, as well as a change in at least one of either Id1 or Id3 protein expression. Clones with increased BMP signaling relative to parental cells are denoted by a (+) sign, while clones with decreased BMP signaling are denoted by a (-) sign.

The first group contains MOSERM ALK3QD clones 1 (+) and 2 (+), and 4306 ALK3QD clone 2 (+) (Figure 3.6A). One of the first steps in the BMP signaling pathway is the phosphorylation of R-Smads, and we therefore assessed phospho-Smad1/5/8 protein expression compared to total Smad levels. The MOSERM clones in the first group exhibit an increase in phospho-Smad1/5/8 expression relative to parental cells, although these clones also exhibit an increase in total Smad 1/5 (bottom panel of Figure 3.6A). 4306 ALK3QD clone 2 (+) cells display a more pronounced increase in phospho-Smad1/5/8 expression compared to 4306 parental cells, and do not have any noticeable changes in total Smad1/5 levels. In addition to phospho-Smad1/5/8, Id1 and Id3 target gene protein expression were also assessed. Both of these proteins are expressed at higher levels in ALK3QD (+) clones in this first group when compared to parental cells,

although changes in Id1 and Id3 protein expression are more pronounced in the MOSERM ALK3QD (+) clones than in the 4306 ALK3QD (+) clone.

The second group of clones includes MASC2 ALK3QD clones 1 (-) and 2 (-), and 4306 clone 1 (-) (Figure 3.6B). Both MASC2 ALK3QD clone 1 (-) and 4306 ALK3QD clone 2 (-) display a decrease in phospho-Smad1/5/8 expression compared to parental cells, while MASC2 ALK3QD clone 2 (-) cells display a less apparent decrease in the expression of this protein (bottom panel Figure 6B). Additionally, total Smad1/5 expression does not change between any of the clones and their respective parental cell lines. With respect to the Id proteins, Id1 expression decreases in all three clones relative to parental cells. However, Id3 protein expression does not change among the clones and their parental cells.

3.7 Inverse correlation between BMP signaling expression levels in ALK3QD clones and ability to form tumours on the chick CAM

For each ALK3QD clone, 1 x 10^6 cells were inoculated onto the surface of the chick CAM, and were then incubated for one week at which time tumour formation was assessed. In addition to the ALK3QD clones, parental cells were also inoculated onto the chick CAM. Upon brightfield and fluorescence imaging of tumours formed on the CAM from these clones, MOSERM ALK3QD clone 1 (+) and clone 2 (+) are visibly smaller than tumours formed by the MOSERM parental cell line (Figure 3.7A). Similarly, 4306 ALK3QD clone 2 (+) derived tumours are visibly smaller than those formed by parental 4306 cells. Conversely, tumours that were formed by 4306 ALK3QD clone 1 (-) cells were visibly larger than those formed by parental 4306 cells. Although MASC2, MASC2

Figure 3.7 Differences in size of tumours formed on the chick CAM among ALK3QD stably-transfected mouse EOC cell line clones.

Approximately 1 x 10^6 cells were seeded onto the surface of the CAM for each ALK3QD clone and their respective parental cell lines. (A) Brightfield and fluorescence images were taken of the cell xenograft locations at 20X magnification 7 days after the initial seeding. MOSERM (B) and 4306 (C) tumours were then excised from the surface of the chick CAM, fixed in formalin overnight, and weighed. Error bars represent the standard error of the mean of tumour weights from at least 5 excised tumours per group. Different letters represent statistically significant differences among groups ($p < 0.01$). Scale bars: 2 mm.

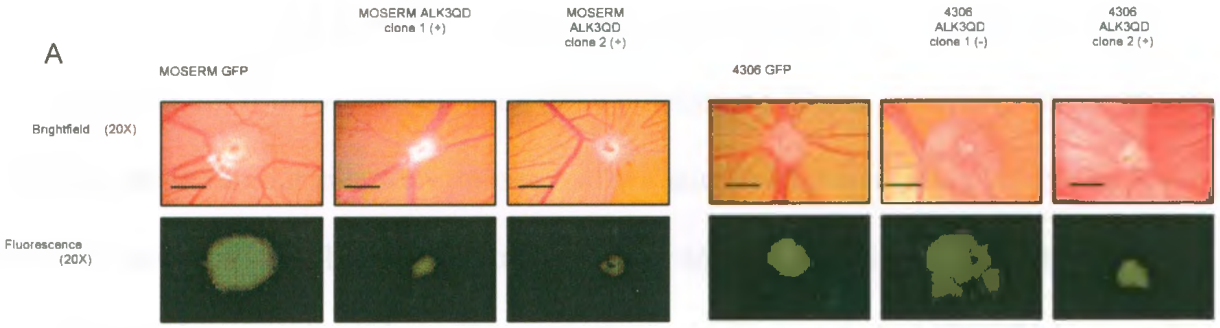
A
MOSERM GFP
MOSERM ALK3QD clone 1 (+)
MOSERM ALK3QD clone 2 (+)
4306 GFP
4306 ALK3QD clone 1 (-)
4306 ALK3QD clone 2 (+)
Brightfield (20X)
Fluorescence (20X)

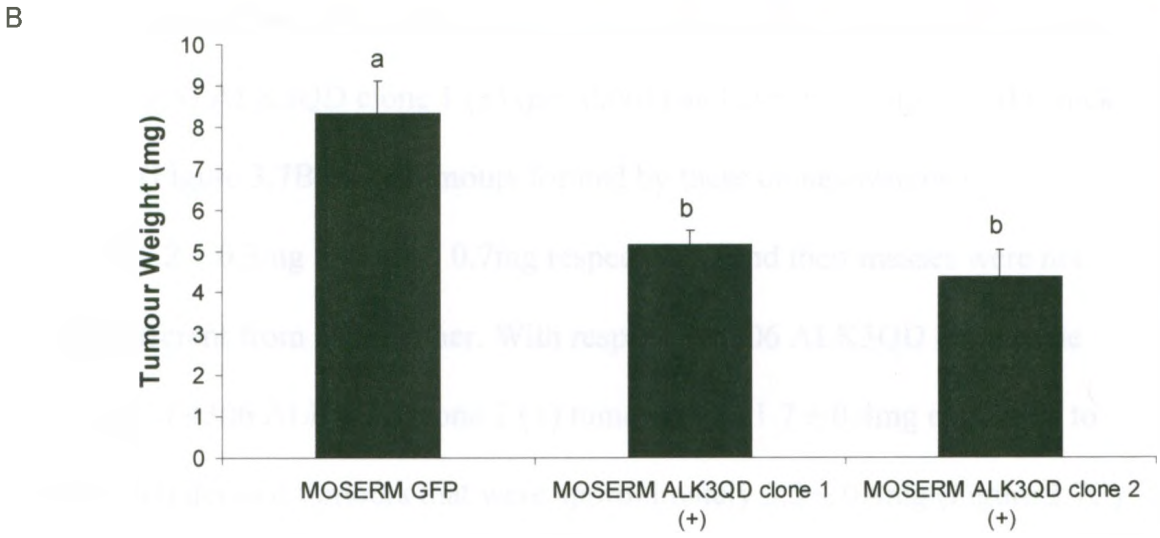
B
Tumour Weight (mg)
0
1
2
3
4
5
6
7
8
9
10
a
b
b
MOSERM GFP
MOSERM ALK3QD clone 1 (+)
MOSERM ALK3QD clone 2 (+)

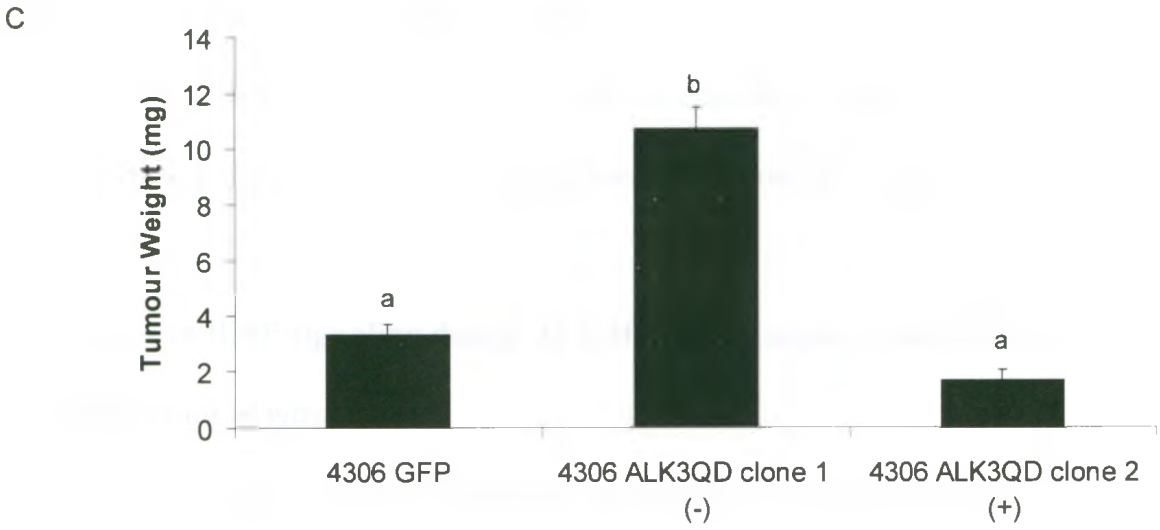
C
Tumour Weight (mg)
0
2
4
6
8
10
12
14
a
b
a
4306 GFP
4306 ALK3QD clone 1 (-)
4306 ALK3QD clone 2 (+)

ALK3QD clone 1 (-) and clone 2 (-) cells were also inoculated onto the surface of the CAM, they did not form visible tumours (data not shown). These qualitative observations of differences in tumour size were subsequently quantified by measuring tumour weight, which was accomplished by excising tumours after imaging, placing in formalin overnight and then weighing them. Tumours that were formed from MOSERM parental cells weighed approximately 8.3 ± 0.8mg, which had a significantly greater mass than both the MOSERM ALK3QD clone 1 (+) ($p < 0.001$) and clone 2 (+) ($p < 0.01$) chick CAM tumours (Figure 3.7B). The tumours formed by these clones weighed approximately 5.2 ± 0.3mg and 4.4 ± 0.7mg respectively, and their masses were not significantly different from one another. With respect to 4306 ALK3QD clones, the average weight of 4306 ALK3QD clone 2 (+) tumours was 1.7 ± 0.4mg compared to 4306 parental cell derived tumours that were approximately 3.3 ± 0.4mg (Figure 3.7C). Although this indicates a trend towards decreased tumour mass in 4306 ALK3QD clone 2 (+) relative to 4306 parental cells, this difference is not statistically significant. Conversely, 4306 ALK3QD clone 1 (-) cells form tumours that weigh approximately 10.7 ± 0.7mg, and have a significantly greater mass than 4306 parental cells ($p < 0.001$).

3.8 Changes in BMP signaling due to ALK3QD expression do not affect cell proliferation *in vitro*

In order to determine which mechanism(s) might be contributing to the differences that are seen between ALK3QD clones and parental cells with respect to their abilities to form tumours on the chick CAM, we decided to first investigate cell proliferation as a potential mechanism. This was accomplished by completing

alamarBlue® assays *in vitro* in full serum over a period of five days, and proliferation was quantified fluorometrically at days 0, 1, 2, 3, and 5 for all mouse EOC cell lines and their respective ALK3QD clones. By day 5, the fluorimetric counts for MOSERM, MOSERM ALK3QD clone 1 (+), and MOSERM ALK3QD clone 2 (+) were not significantly different from one another (Figure 3.8A). As well, there were no significant differences in proliferation between MASC2 parental cells and MASC2 ALK3QD clones (Figure 3.8B). Finally, neither 4306 ALK3QD clone displayed statistically significant differences in proliferation relative to 4306 parental cells (Figure 3.8C).

3.9 Inverse correlation between level of BMP signaling in mouse EOC ALK3QD clones and degree of blood vessel sprouting on the chick CAM

Since altered BMP signaling does not correlate with *in vitro* cell proliferation in mouse EOC cell lines, I next sought to determine whether angiogenesis might be a potential mechanism contributing to the differences that are seen among ALK3QD clones and parental cells with respect to their abilities to form tumours on the chick CAM. Angiogenesis was assessed on the chick CAM using the collagen onplant assay as previously described, and angiogenesis was quantified by expressing the number of grids that are positive for blood vessel sprouting as a percentage of total grids in each mesh. Collagen onplants containing MOSERM cells contributed to new blood vessel sprouting in approximately 20.1 ± 2.0% of grid boxes (Figure 3.9A). This induction of angiogenesis was significantly greater than the PBS control group (11.4 ± 1.3% of grid boxes; $p < 0.01$), the MOSERM ALK3QD clone 1 (+) group (6.0 ± 1.5% of grid boxes; $p < 0.001$), and the MOSERM ALK3QD clone 2 (+) group (11.6 ± 2.4% of grid boxes; $p <$

Figure 3.8 No effect of ALK3QD expression of mouse EOC cell line proliferation *in vitro*.

In order to assess cell proliferation, alamarBlue® assays were performed. 500 cells were seeded into 96 well plates for (A) MOSERM parental cells, MOSERM ALK3QD clone 1 (+) and clone 2 (+), (B) MASC2 parental cells, MASC2 ALK3QD clone 1 (-) and clone 2 (-), (C) 4306 parental cells, 4306 ALK3QD clone 1 (-) and clone 2 (+). Fluorescence units were then measured 12 hours after the initial seeding time in order to ensure equal seeding densities (day 0), and fluorescence units were then subsequently measured again at multiple time points (day 1, day 3, day 5). Each data point represents the average of at least 3 wells.

A

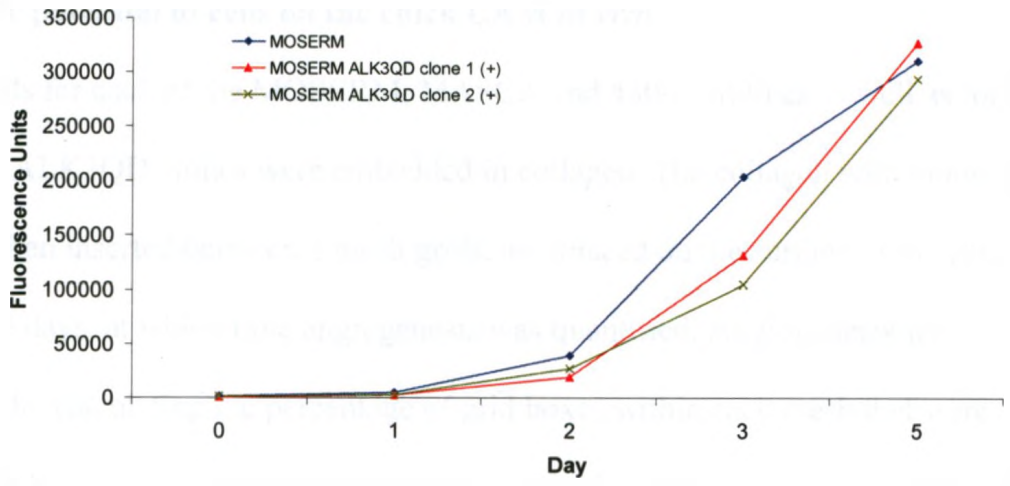
MOSERM
MOSERM ALK3QD clone 1 (+)
MOSERM ALK3QD clone 2 (+)
Fluorescence Units
350000
300000
250000
200000
150000
100000
50000
0
0
1
2
3
5
Day

B

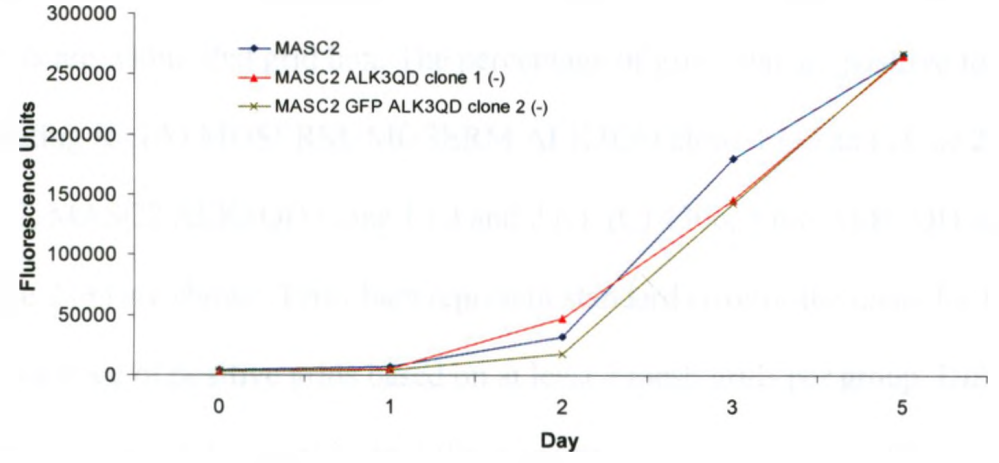
MASC2
MASC2 ALK3QD clone 1 (-)
MASC2 GFP ALK3QD clone 2 (-)
Fluorescence Units
300000
250000
200000
150000
100000
50000
0
0
1
2
3
5
Day

C

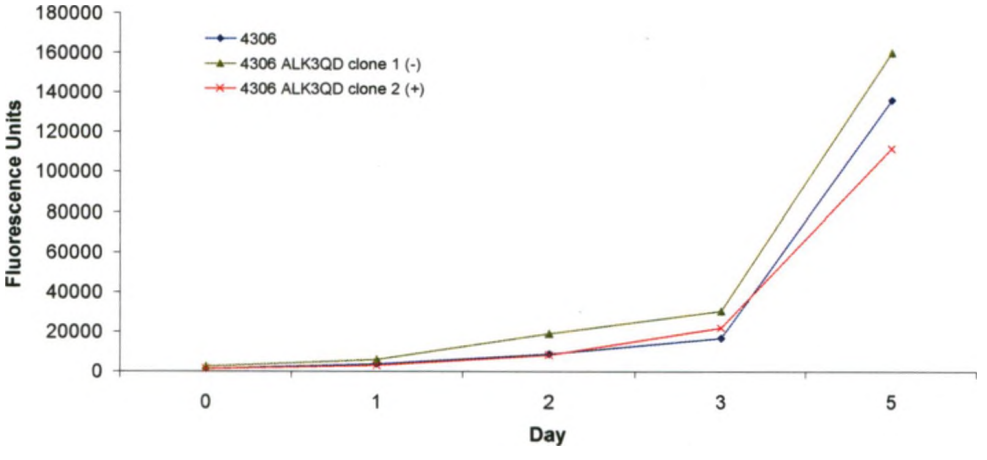
4306
4306 ALK3QD clone 1 (-)
4306 ALK3QD clone 2 (+)
Fluorescence Units
180000
160000
140000
120000
100000
80000
60000
40000
20000
0
0
1
2
3
5
Day

Figure 3.9 ALK3QD expression in mouse EOC cell lines influences the angiogenic potential of cells on the chick CAM *in vivo*.

1×10^5 cells for each of the MOSERM, MASC2, and 4306 cell lines as well as for their respective ALK3QD clones were embedded in collagen. The collagen with mouse EOC cells was then inserted between 2 mesh grids, and placed on the surface of the chick CAM for 3 days, at which time angiogenesis was quantified. Angiogenesis was quantified by calculating the percentage of grid boxes within each mesh that were positive for blood vessel sprouting. Note that if a grid is determined to be positive for blood vessel sprouting, the grid count will only be given a score of one regardless of how many sprouts are within that grid box. The percentage of grids that are positive for blood vessel sprouting for (A) MOSERM, MOSERM ALK3QD clone 1 (+) and clone 2 (+), (B) MASC2, MASC2 ALK3QD clone 1 (-) and 2 (-), (C) 4306, 4306 ALK3QD clone 1 (-) and clone 2 (+) are shown. Error bars represent standard error of the mean for the average percentage of positive grids based on at least 7 mesh grids per group. Different letters represent statistically significant differences between groups ($p < 0.05$).

A

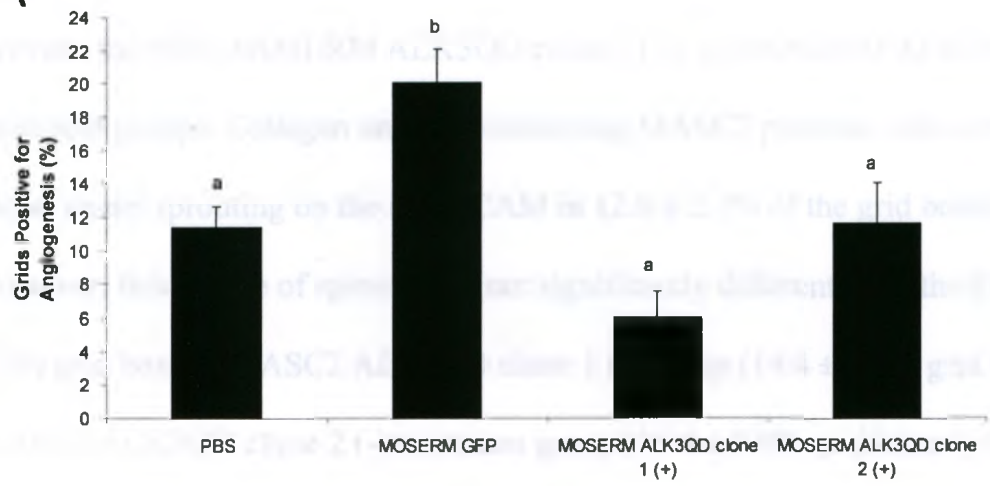
Grids Positive for Angiogenesis (%)
24
22
20
18
16
14
12
10
8
6
4
2
0
a
b
a
a
PBS
MOSERM GFP
MOSERM ALK3QD clone 1 (+)
MOSERM ALK3QD clone 2 (+)

B

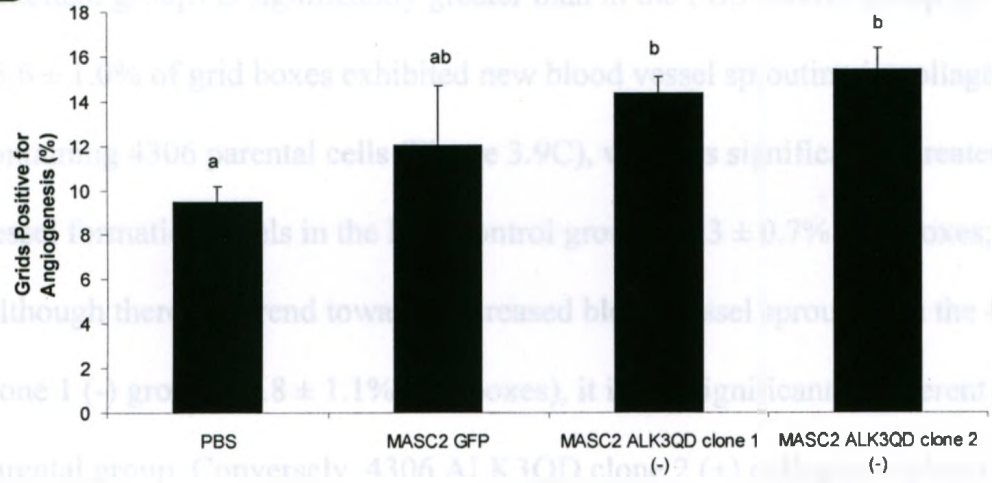
Grids Positive for Angiogenesis (%)
18
16
14
12
10
8
6
4
2
0
a
ab
b
b
PBS
MASC2 GFP
MASC2 ALK3QD clone 1 (-)
MASC2 ALK3QD clone 2 (-)

C

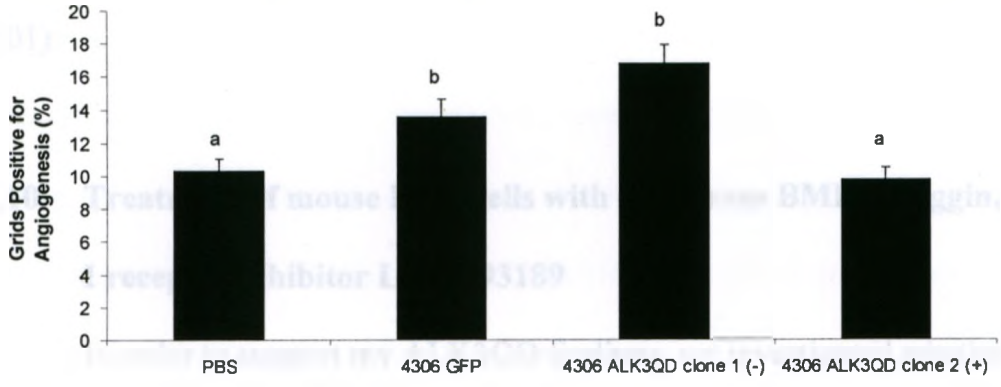
Grids Positive for Angiogenesis (%)
20
18
16
14
12
10
8
6
4
2
0
a
b
b
a
PBS
4306 GFP
4306 ALK3QD clone 1 (-)
4306 ALK3QD clone 2 (+)

0.05). However, there are no statistically significant differences in angiogenic sprouting between the PBS, MOSERM ALK3QD clone 1 (+), or MOSERM ALK3QD clone 2 (+) treatment groups. Collagen onplants containing MASC2 parental cells contributed to new blood vessel sprouting on the chick CAM in 12.0 ± 2.7% of the grid boxes (Figure 3.9B). However, this degree of sprouting is not significantly different from the PBS group (9.5 ± 0.7% grid boxes), MASC2 ALK3QD clone 1 (-) group (14.4 ± 0.7% grid boxes), or the MASC2 ALK3QD clone 2 (-) treatment group (15.4 ± 0.9% grid boxes). Conversely, the degree of angiogenic sprouting in the MASC2 ALK3QD clone 1 (-) and clone 2 (-) treatment groups is significantly greater than in the PBS control group ($p < 0.05$). Finally, 13.6 ± 1.0% of grid boxes exhibited new blood vessel sprouting in collagen onplants containing 4306 parental cells (Figure 3.9C), which is significantly greater than blood vessel formation levels in the PBS control group (10.3 ± 0.7% grid boxes; $p < 0.05$). Although there is a trend towards increased blood vessel sprouting in the 4306 ALK3QD clone 1 (-) group (16.8 ± 1.1% grid boxes), it is not significantly different from the 4306 parental group. Conversely, 4306 ALK3QD clone 2 (+) collagen onplants exhibit new blood vessel sprouting in 9.7 ± 0.7 % of grid boxes, which is significantly decreased compared to both the 4306 parental ($p < 0.05$) and 4306 ALK3QD clone 1 (-) groups ($p < 0.01$).

3.10 Treatment of mouse EOC cells with exogenous BMP4, Noggin, or BMP type I receptor inhibitor LDN-193189

In order to support my ALK3QD findings, we investigated whether short-term changes in BMP pathway signaling expression would have functional consequences on

cell proliferation and angiogenesis. Therefore, the three mouse EOC cell lines were treated with exogenous BMP4, Noggin (extracellular antagonist to inhibit BMP ligand binding) (Groppe, Greenwald et al. 2002) or LDN-193189 (BMP type 1 receptor inhibitor) (Yu, Deng et al. 2008). We first wanted to confirm that exogenous treatment with BMP4, Noggin, or LDN-193189 would affect the BMP signaling pathway, and to determine the duration of these effects. Therefore, cells were treated at the onset of the experiment, and protein was isolated from cells at multiple time points over three days (30 min, 4 hours, 24 hours, 48 hours, and 72 hours). Upon treatment with 10ng/mL BMP4, protein levels of phospho-Smad1/5/8 were increased in all three mouse EOC cell lines within 30 minutes (Figure 3.10A). The increase in phospho-Smad1/5/8 levels in MOSERM cells remained elevated up to the last time point at 72 hours, whereas the effect was diminished in MASC2 and 4306 cells by 24 hours. To a lesser extent, Id1 protein expression was upregulated in MOSERM cells after 4 hours, and remained upregulated at 72 hours. Conversely, there were no consistent changes in Id1 expression in the other cell lines.

After treatment with either 50ng/mL Noggin or 40nM LDN-193189, phospho-Smad1/5/8 protein levels decreased in all three cell lines within 30 minutes (Figures 3.10B and 3.10C). While these effects were sustained over the 72 hours of the experiment in MOSERM cells, phospho-Smad1/5/8 expression began to noticeably increase back towards baseline levels after approximately 24-48 hours in the MASC2 and 4306 cells that were treated with Noggin and LDN-193189. Treatment with either of these BMP signaling inhibitors did not have an effect on Id1 protein expression in MOSERM or

Figure 3.10 Changes in BMP signaling as a result of treatment of mouse EOC cell lines with BMP4, Noggin, or LDN-193189.

Changes in downstream BMP signaling at multiple time points (30min, 4h, 24h, 48h, 72h) after (A) 10ng/mL BMP4 treatment, (B) 50ng/mL Noggin treatment, or (C) 40nM LDN-193189 treatment were assessed using anti-phospho-smad1/5/8 and anti-ID1. Western blotting was performed using 50μg of total cellular protein, and equal loading was assessed with anti-Smad1 and anti-actin. BMP signaling was considered to be upregulated or downregulated based on a change in phospho-Smad1/5/8 protein expression. BMP4 treatment resulted in an upregulation of BMP signaling, while treatment with Noggin or LDN-193189 downregulated BMP signaling.

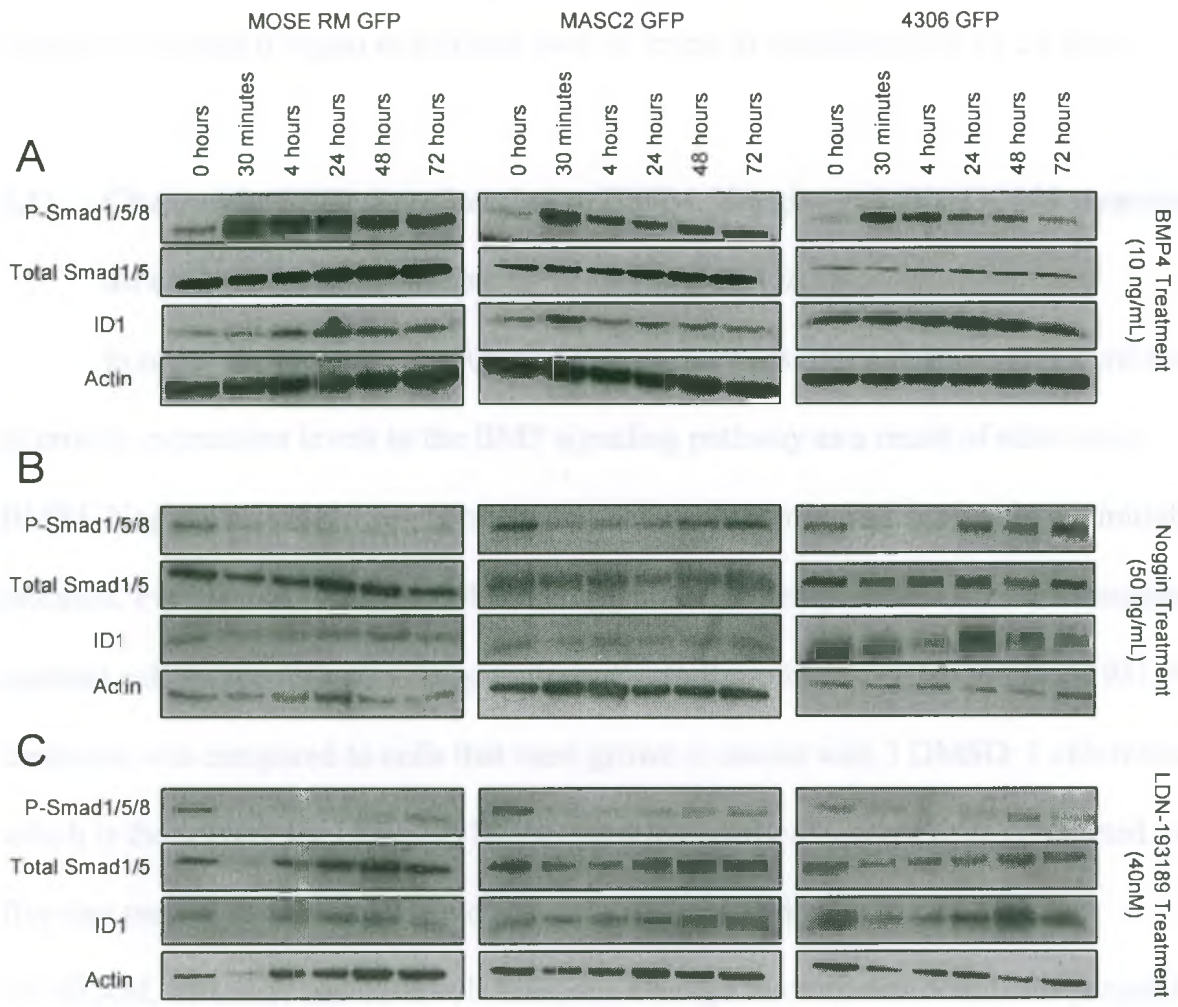
MOSE RM GFP
MASC2 GFP
4306 GFP
0 hours
30 minutes
4 hours
24 hours
48 hours
72 hours
A
P-Smad1/5/8
Total Smad1/5
ID1
Actin
BMP4 Treatment (10 ng/mL)
B
P-Smad1/5/8
Total Smad1/5
ID1
Actin
Noggin Treatment (50 ng/mL)
C
P-Smad1/5/8
Total Smad1/5
ID1
Actin
LDN-193189 Treatment (40nM)

MASC2 compared to untreated cells. Id1 expression did decrease in 4306 cells by 30 minutes, although it began to increase back to levels in untreated cells by 24 hours.

3.11 Changes in BMP signaling due to BMP4, Noggin, or LDN-193189 treatment do not affect cell proliferation or cell survival *in vitro*

In order to determine the functional consequences of the changes that were seen in protein expression levels in the BMP signaling pathway as a result of short-term BMP4, Noggin, or LDN-193189 treatment, cell proliferation and survival were initially assessed. For each cell line, BMP4 and Noggin treated cell proliferation was compared to parental cell line proliferation in growth media. Cell proliferation due to LDN-193189 treatment was compared to cells that were grown in media with 3 DMSO: 1 chloroform, which is the solvent for LDN-193189. *In vitro* alamarBlue® assays were completed over a five day period, and fluorometric counts of wells were taken each day. For the MOSERM, MASC2, and 4306 cell lines, the average fluorometric counts for parental cells, BMP4 treatment, or Noggin treatment were not significantly different from one another at day 5 (Figure 3.11). Similarly, there were no significant differences in the day 5 fluorometric counts for any of the three cell lines between 3 DMSO: 1 chloroform and LDN-193189 treatments.

The ability of each of the three mouse EOC cell lines to survive in serum-free conditions *in vitro* after treatment was also evaluated. As with the *in vitro* cell proliferation assay, cell survival was assessed every 24 hours over 5 days by alamarBlue® fluorometric counts. However, cells were grown in serum-free media instead of media with 5% FBS. Similar to our findings with respect to cell proliferation, changes in the

Figure 3.11 No effect of BMP4, Noggin, or LDN-193189 treatment of mouse EOC cell lines on cell proliferation *in vitro*.

In vitro alamarBlue® assays were performed to assess cell proliferation, which was compared between parental cells, BMP4-treated cells, Noggin-treated cells, LDN193189-treated cells, and cells treated with the solvent for LDN193189 (3 DMSO:1 chloroform). 500 cells in media with 5% FBS were seeded into 96 well plates for (A) MOSERM cells and respective treatments, (B) MASC2 cells and respective treatments, and (C) 4306 cells and respective treatments. Fluorescence units were then measured 12 hours after the initial seeding in order to ensure equal seeding densities (day 0), and fluorescence units were then subsequently measured again at multiple time points (day 1, day 2, day 3, day 4, day 5). Each data point represents the average of at least 3 wells.

A

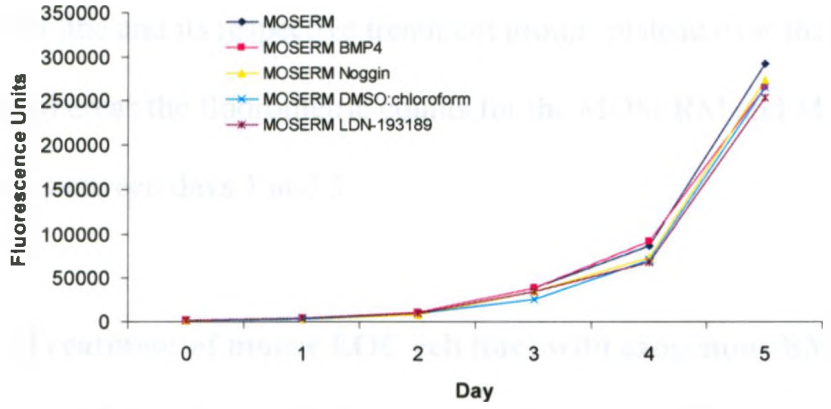
MOSERM
MOSERM BMP4
MOSERM Noggin
MOSERM DMSO:chloroform
MOSERM LDN-193189
Fluorescence Units
350000
300000
250000
200000
150000
100000
50000
0
0
1
2
3
4
5
Day

B

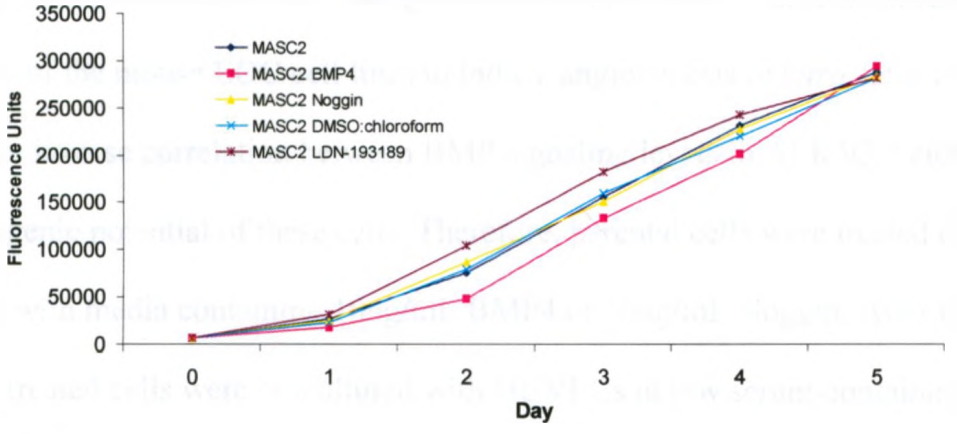
MASC2
MASC2 BMP4
MASC2 Noggin
MASC2 DMSO:chloroform
MASC2 LDN-193189
Fluorescence Units
350000
300000
250000
200000
150000
100000
50000
0
0
1
2
3
4
5
Day

C

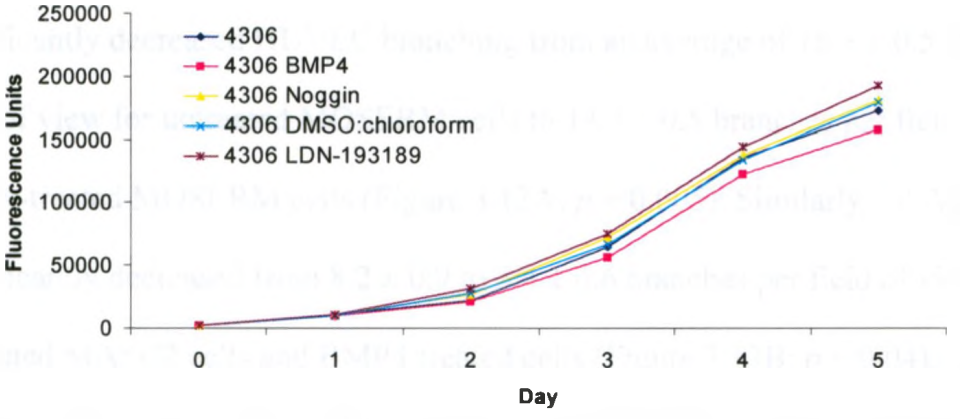
4306
4306 BMP4
4306 Noggin
4306 DMSO:chloroform
4306 LDN-193189
Fluorescence Units
250000
200000
150000
100000
50000
0
0
1
2
3
4
5
Day

ability of cells to survive were not statistically significant among any of the three cell lines for any treatment (Figure 3.12). Interestingly, the fluorescence unit counts for the 4306 cell line and its respective treatment groups plateau over the five day experimental period, whereas the fluorometric counts for the MOSERM and MASC2 cell lines steadily decrease between days 1 and 5.

3.12 Treatment of mouse EOC cell lines with exogenous BMP4 ligand decreases the ability of cells to induce angiogenesis *in vitro*

Since short-term treatment with BMP4, Noggin, or LDN-193189 did not affect cell proliferation or survival, I sought to determine whether these treatments affected the ability of the mouse EOC cell lines to induce angiogenesis *in vitro.* This is because there was an inverse correlation between BMP signaling levels in ALK3QD clones and the angiogenic potential of these cells. Therefore, parental cells were treated overnight for 12 hours with media containing 10ng/mL BMP4 or 50ng/mL Noggin. After this period of time, treated cells were co-cultured with HUVECs in low serum-containing media (1% FBS) on a layer of Matrigel in the wells of 96-well plates. After 6 hours of incubation, multiple images were taken of each well at 100X magnification. Treatment with BMP4 significantly decreased HUVEC branching from an average of 16.5 ± 0.5 branches per field of view for untreated MOSERM cells to 14.3 ± 0.5 branches per field of view in BMP4-treated MOSERM cells (Figure 3.13A; $p = 0.005$). Similarly, HUVEC branching significantly decreased from 8.2 ± 0.9 to 5.4 ± 0.6 branches per field of view between untreated MASC2 cells and BMP4-treated cells (Figure 3.13B; $p = 0.04$). As well, HUVEC branching significantly decreased from HUVECs co-cultured with untreated

Figure 3.12 No effect of BMP4, Noggin, or LDN-193189 treatment of mouse EOC cell lines on cell survival *in vitro*.

In vitro alamarBlue® assays were performed to assess cell survival, which was compared between parental cells, BMP4-treated cells, Noggin-treated cells, LDN193189-treated cells, and cells treated with the solvent for LDN193189 (3 DMSO:1 chloroform). 5000 MOSERM cells, 5000 MASC2 cells, or 10,000 4306 cells in serum-free media were seeded into 96 well plates for (A) MOSERM cells and respective treatments, (B) MASC2 cells and respective treatments, and (C) 4306 cells and respective treatments. Fluorescence units were then measured 12 hours after the initial seeding in order to ensure equal seeding densities (day 0), and fluorescence units were then subsequently measured again at multiple time points (day 1, day 2, day 3, day 4, day 5). Each data point represents the average of at least 3 wells.

A

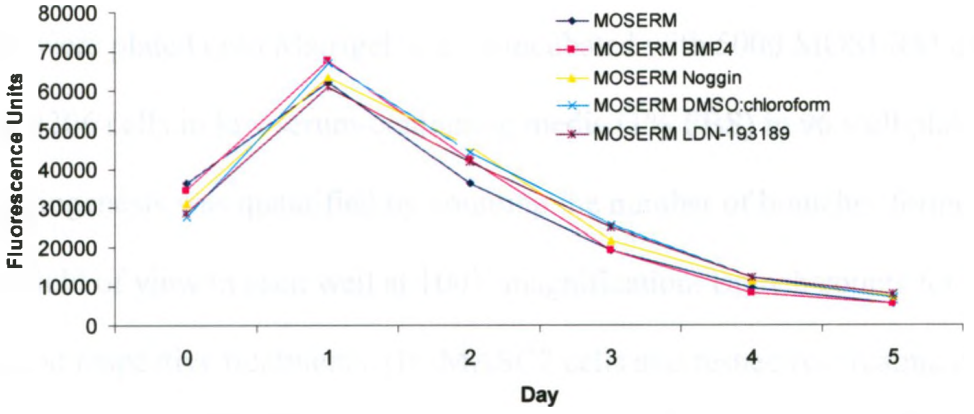
Fluorescence Units
80000
70000
60000
50000
40000
30000
20000
10000
0
0
1
2
3
4
5
Day
MOSERM
MOSERM BMP4
MOSERM Noggin
MOSERM DMSO:chloroform
MOSERM LDN-193189

B

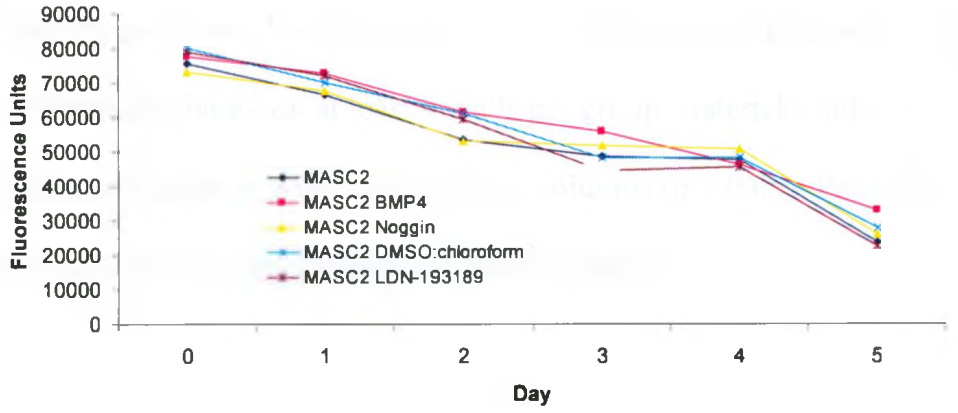
Fluorescence Units
90000
80000
70000
60000
50000
40000
30000
20000
10000
0
0
1
2
3
4
5
Day
MASC2
MASC2 BMP4
MASC2 Noggin
MASC2 DMSO:chloroform
MASC2 LDN-193189

C

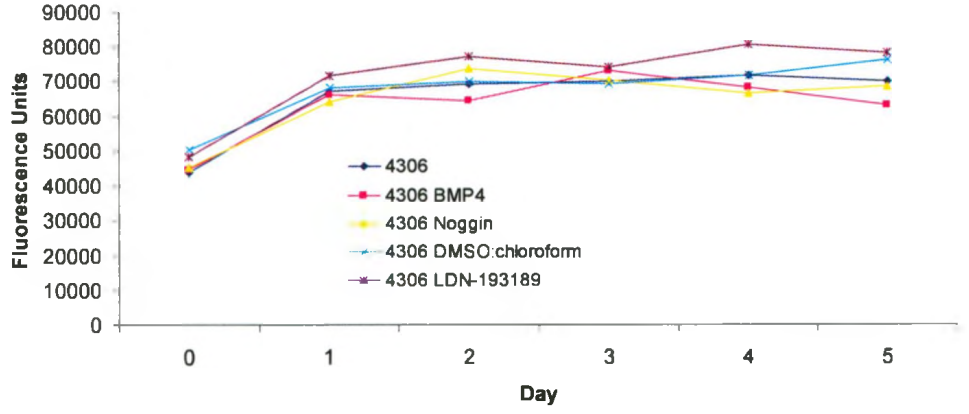
Fluorescence Units
90000
80000
70000
60000
50000
40000
30000
20000
10000
0
0
1
2
3
4
5
Day
4306
4306 BMP4
4306 Noggin
4306 DMSO:chloroform
4306 LDN-193189

Figure 3.13 Short-term treatment of mouse EOC cell lines with BMP4 or Noggin affects ability of cells to induce angiogenesis *in vitro*.

1×10^4 HUVECs were plated onto Matrigel and co-incubated with 5000 MOSERM cells, MASC2 cells, or 4306 cells in low serum-containing media (1% FBS) in 96 well plates. After 6 hours, angiogenesis was quantified by counting the number of branches formed by HUVECs per field of view in each well at 100X magnification. Branch counts for (A) MOSERM cells and respective treatments, (B) MASC2 cells and respective treatments, (C) 4306 cells and respective treatments are shown. Untreated cell branch counts per field of view are represented by black bars, while branch counts for BMP4 or Noggin-treated cells are represented by grey bars. Error bars represent standard error of the mean for the average number of branches based on at least 4 wells per group. Asterisks indicate statistically significant differences within each pair of columns ($p < 0.05$). Pairwise comparisons were made between each treatment and its control.

A

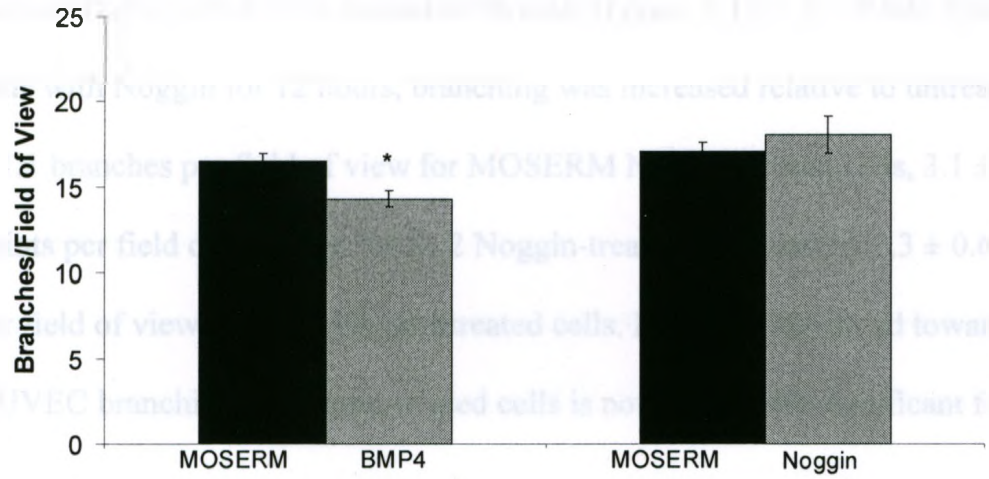
Branches/Field of View
25
20
15
10
5
0
*
MOSERM
BMP4
MOSERM
Noggin

B

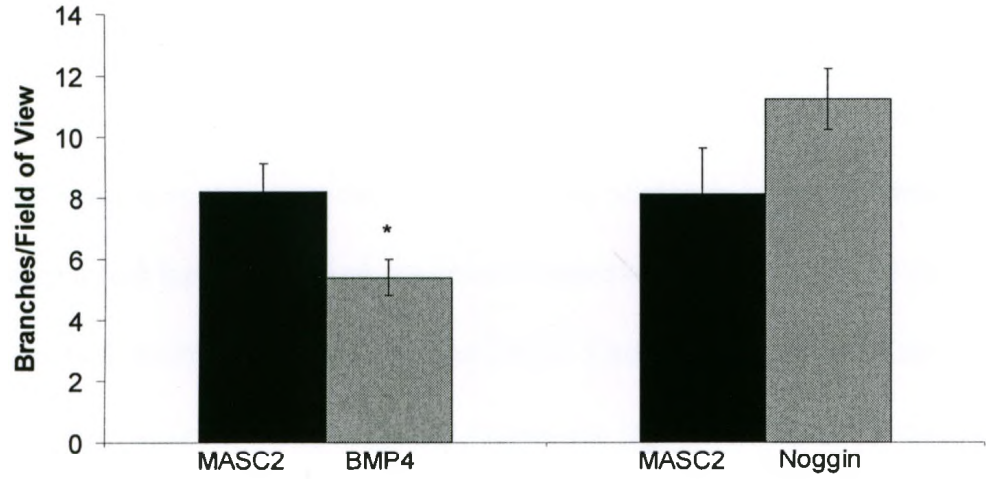
Branches/Field of View
14
12
10
8
6
4
2
0
*
MASC2
BMP4
MASC2
Noggin

C

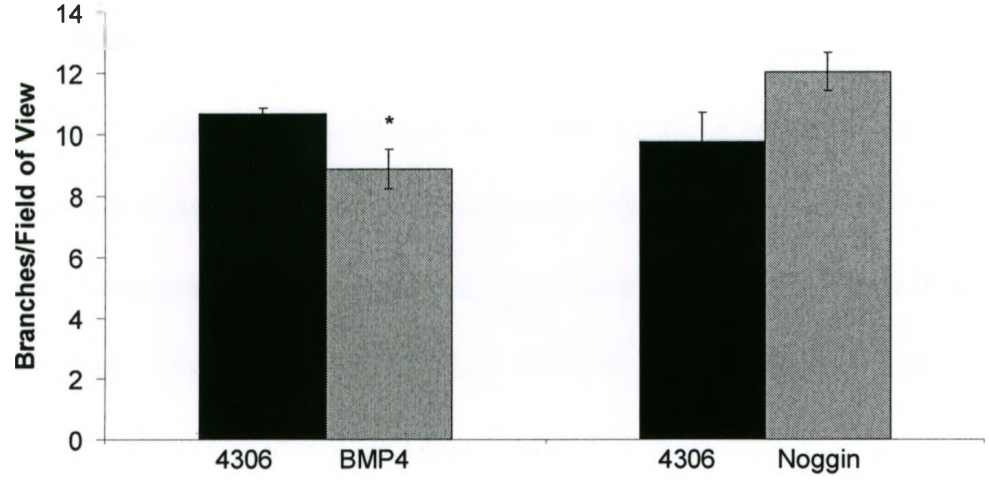
Branches/Field of View
14
12
10
8
6
4
2
0
*
4306
BMP4
4306
Noggin

4306 cells at 10.7 ± 0.2 branches per field of view to 8.9 ± 0.7 branches per field of view in co-cultures with BMP4-treated 4306 cells (Figure 3.13C; $p = 0.04$). Upon treatment of cells with Noggin for 12 hours, branching was increased relative to untreated cells by 1.2 ± 1.1 branches per field of view for MOSERM Noggin-treated cells, 3.1 ± 1.0 branch points per field of view for MASC2 Noggin-treated cells, and by 2.3 ± 0.6 branch points per field of view for 4306 Noggin-treated cells. However, this trend towards increased HUVEC branching in Noggin-treated cells is not statistically significant for any cell line.

CHAPTER FOUR

DISCUSSION

4.1 Summary

Ovarian cancer continues to be a poorly understood disease with respect to the signs and symptoms relating to the early stages of EOC, as well as with respect to the molecular mechanisms that contribute to its progression from a localized tumour that is confined to the ovaries to one that can metastasize to distant sites within the peritoneal cavity (Goff, Mandel et al. 2007). The poor understanding of this disease is highlighted by it having the highest mortality rate of any gynaecological cancer in the developed world, and decreases in this mortality rate have been relatively minimal when compared to other cancers that have seen more successful improvements in mortality rates over the past 15 years such as breast cancer (Canada 2010). Therefore, several key approaches must be employed in order to significantly reduce the high mortality rates that are associated with EOC in the future. One of these approaches is to improve current models of EOC *in vitro* and *in vivo*, or to develop novel model systems that can be efficiently used to study various aspects of EOC progression. Another key approach will be to further our understanding of the role(s) of molecular signaling pathways that have been implicated in other forms of cancer and specifically EOC, such as the BMP signaling pathway (Shepherd and Nachtigal 2003; Moll, Millet et al. 2006; Theriault, Shepherd et al. 2007; Shepherd, Theriault et al. 2008; Ma, Ma et al. 2010; Pils, Wittinger et al. 2010; Shepherd, Mujoomdar et al. 2010; McLean, Gong et al. 2011).

My studies have shown that the relative abilities of the MOSERM, MASC2, and 4306 mouse EOC cell lines to form tumours on the chick CAM correlates with their differential abilities to enhance angiogenesis *in vitro*. Importantly, I was also able to detect these differences in angiogenic potential *in vivo* using the chick CAM collagen gel angiogenesis onplant assay. I have also shown that in addition to normal mouse OSE cells, the MOSERM, MASC2, and 4306 cell lines all express measurable, but distinct levels of *BMP4* and its required intracellular signaling components. ALK3QD clones created from each cell line with increased BMP signaling relative to parental cells formed significantly smaller tumours on the chick CAM, while clones with decreased BMP signaling formed larger tumours on the chick CAM relative to parental cells. Additionally, increased BMP signaling in mouse EOC cell lines leads to decreased HUVEC branching *in vitro*, and decreased blood vessel formation *in vivo* using the chick CAM angiogenesis onplant assay. Conversely, cells with decreased BMP signaling exhibited increased levels of angiogenesis both *in vitro* and *in vivo*.

With respect to EOC mouse cells, there is only one mouse EOC cell line that has been well characterized in multiple studies, which is the ID8 mouse EOC cell line (Pengetnze, Steed et al. 2003). ID8 cells were created from normal mouse OSE cells that spontaneously transformed after repeated passaging *in vitro*. This cell line has multiple benefits because it exhibits an upregulation of Src tyrosine kinase, FAK, and PI3K/AKT signaling activation that in combination increase the rate of growth of ID8 cells, and decrease apoptosis. These signaling pathways have also been shown to be dysregulated in a large percentage of ovarian cancers (Judson, He et al. 1999; Wiener, Windham et al. 2003; Huang, Zhang et al. 2011; Tanaka, Terai et al. 2011). Additionally, ID8 cells are

able to form tumours and ascites when injected into mice with intact immune systems (Roby, Taylor et al. 2000). However, other than this cell line, there are only a couple other mouse EOC cell lines that have been used and partially characterized in the literature (Szotek, Pieretti-Vanmarcke et al. 2006; Goodell, Belisle et al. 2009), although to a lesser extent than ID8 cells. Therefore, the development and characterization of other mouse EOC cell lines will be very beneficial and will contribute to an improved understanding of EOC and its progression. As a result, our lab obtained three mouse ovarian cancer cell lines that I partially characterized both *in vitro* and *in vivo*. The first cell line is the 4306 cell line that overexpresses mutant $Kras^{G12D}$ in addition to having an inactivated *Pten* tumour suppressor gene (Dinulescu, Ince et al. 2005). Secondly, the MOSERM line ectopically expresses the *Ras* and *Myc* oncogenes in addition to a temperature sensitive mutant of SV40 large T antigen (Yao, Li et al. 2006). Thirdly, the MASC2 cell line expresses SV40 large T antigen (Laviolette, Garson et al. 2010). Although the 4306 cell line has been shown to possess an intact Müllerian Inhibiting Substance (MIS) signal transduction pathway (Szotek, Pieretti-Vanmarcke et al. 2006), these three mouse EOC cell lines have otherwise been poorly characterized in the literature. Therefore, our characterization of the MOSERM, MASC2, and 4306 cell lines with respect to their *in vivo* tumour formation abilities on the chick CAM, *in vitro* proliferation, *in vitro* angiogenesis, and angiogenesis on the chick CAM will support the use of these cell lines as additional tools to gain a better understanding of EOC.

Also contributing to our lack of understanding of EOC is a limited number of effective *in vivo* animal model systems that can recapitulate multiple aspects of EOC tumour progression (Pengetnze, Steed et al. 2003). The chick CAM is a useful animal

model system that has been used to study many types of cancer including colon (Kim, Hur et al. 2011), melanoma (Liang, Butterfield et al. 2011), neuroblastoma (Azar, Azar et al. 2011), oral squamous cell carcinoma (Hseu, Wu et al. 2011), pancreatic cancer (Laklai, Laval et al. 2009). In addition, this system can been used to investigate several aspects of tumourigenesis such as primary tumour growth (Gao, Cao et al. 2004; Liang, Butterfield et al. 2011), metastasis (Subauste, Kupriyanova et al. 2009), and angiogenesis (Azar, Azar et al. 2011; Chim, Qin et al. 2011; Liang, Butterfield et al. 2011). With respect to ovarian cancer, the chick CAM can be used to simulate the physiological microenvironment that metastatic EOC cells would be subjected to in the peritoneal cavity when encountering mesothelial surfaces of abdominal organs and a vascularized substratum upon which cells will form secondary metastases (Schmitt and Matei 2011).

The chick CAM has previously been applied to EOC to study the effects of two naturally occurring flavonoids, Kaempferol and Apigenin, on tumour growth and angiogenesis. Both of these flavonoids were shown to decrease angiogenesis in chick CAM assays with human ovarian cancer OVCAR3 cells, while Kaempferol was also shown to limit OVCAR3 tumour growth on the chick CAM (Fang, Zhou et al. 2007; Luo, Rankin et al. 2009). Additionally, malignant ascites fluid (MAF) has been shown to decrease surface capillary formation when it was applied directly to the surface of the chick CAM (Richardson, Gunawan et al. 2002). We have added evidence in addition to these studies that further supports the use of the chick CAM as an effective model system that can be used study tumour formation and angiogenesis in EOC progression. Importantly, other than our collaborations with Dr. John Lewis and his lab, only a few other labs in the world have used the collagen onplant assay on the chick CAM to

quantify angiogenesis (Nguyen, Shing et al. 1994; Seandel, Noack-Kunnmann et al. 2001; Zijlstra, Seandel et al. 2006). Although other chick CAM angiogenesis assays can be useful, they are only qualitative and it can be difficult to distinguish new blood vessel formation from preexisting blood vessels (Staton, Reed et al. 2009). Therefore, our lab is using the novel chick CAM onplant assay that has the ability to detect more subtle changes in angiogenesis by quantifying new blood vessel formation, which may not have been detectable in our studies if traditional chick CAM angiogenesis assays that are more qualitative had been used (Nguyen, Shing et al. 1994).

Angiogenesis is one the essential hallmarks of cancer because tumours require access to a blood supply in order to receive oxygen and nutrients, and to be able to excrete waste products such as carbon dioxide (Hanahan and Folkman 1996). In fact, without the ability to induce a certain level of angiogenesis, tumours cannot grow and survive beyond a size of 1-2 mm in diameter (Bergers and Benjamin 2003). The importance of angiogenesis in the progression of cancer is reflected by the large number of current trials involving anti-angiogenic compounds that are being tested in patients with metastatic ovarian cancer. For example, there are over 25 ongoing phase I, phase II, or phase III clinical trials that involve one or more of the anti-angiogenic agents Bevacizumab, Dasatinib, Imatinib, or Sorafenib as monotherapies or in combination with other drugs (Schmitt and Matei 2011). Due to the importance of angiogenesis in cancer metastasis, it is essential to gain a thorough understanding of the signaling pathways that play an important role in this process. Therefore, I have focused my studies on the role of the BMP signaling pathway on tumour angiogenesis. BMP signaling has been shown to have an important pro-angiogenic role in many cancers such as hepatocellular cancer

(Maegdefrau, Amann et al. 2009) and melanoma (Rothhammer, Bataille et al. 2007), but has also been implicated in having an anti-angiogenic role in others such as lung cancer (Buckley, Shi et al. 2004). However, the role of BMP signaling in the process of angiogenesis has never been previously studied in EOC. Based on my findings, I propose that one of the important mechanism(s) by which increased BMP signaling is able to limit the ability of mouse EOC cells to form tumours on the CAM is by decreasing the angiogenic potential of these cells. Interestingly, my characterization of TGFβ/BMP gene expression in the three mouse EOC cell lines also supports these findings. For example, MASC2 cells exhibit significantly higher expression levels of BMP4, as well as Id1 and Id2. These cells are also unable to form visible tumours on the chick CAM, and do not significantly induce angiogenesis relative to growth media and PBS controls for *in vitro* and *in vivo* angiogenesis assays, respectively. This is compared to MOSERM and 4306 cells that exhibit lower expression levels of BMP signaling genes, are able to form tumours on the chick CAM, and significantly enhance angiogenesis relative to controls both *in vitro* and *in vivo*. Therefore, I propose that MASC2 cells are unable to form tumours on the chick CAM due to the fact that they have a limited ability relative to other mouse EOC cell lines to enhance angiogenesis, and this decreased ability to enhance angiogenesis is partially due to increased BMP signaling.

Although angiogenesis is essential for tumours to metastasize, there are other mechanisms that are also important in cancer progression. Several of these mechanisms have been studied with respect to the BMP4 signaling pathway and its role in EOC progression in several studies. For example, increased BMP4 signaling *in vitro* has been shown to lead to morphological changes in cells that are characteristic of an EMT

transition (Shepherd and Nachtigal 2003; Theriault, Shepherd et al. 2007), a loss of cell adhesion (Shepherd, Mujoomdar et al. 2010), increased motility, and increased invasive potential (Theriault, Shepherd et al. 2007). Similarly, studies that involve decreasing the activity level of the BMP signaling pathway through the use of Noggin and Chordin in EOC cells decreased their migration and invasive potential, as well as increased cell adhesion (Moll, Millet et al. 2006; Theriault, Shepherd et al. 2007). However, a recent conflicting study involving constitutively active BMP signaling with ALK3QD has correlated increased BMP signaling with a decreased ability of EOC cells to form intraperitoneal tumour implantations in addition to decreased ascites formation when injected into mice (Shepherd, Mujoomdar et al. 2010). My findings show that mouse EOC cells with increased levels of BMP signaling form significantly smaller tumours on the chick CAM, which acts to simulate the physiological microenvironment that EOC cells would encounter when metastasizing to the substratum of the peritoneal cavity , and this decreased ability to form secondary tumours is due to a decreased ability to enhance angiogenesis. Therefore, my data supports the previously conflicting study that implicates BMP signaling as an anti-tumourigenic pathway in the later stages of EOC progression. In order to connect these two disparate groups of data, I propose that BMP signaling has unique roles at different stages of ovarian cancer progression. During the early stages of EOC tumour progression, upregulated BMP signaling is advantageous so that EOC cells can lose their adhesion capabilities, and as a result are able to shed from the primary tumour into the peritoneal cavity. However, in later stages of ovarian cancer progression, downregulated BMP signaling is required to promote spheroid formation and the establishment of secondary metastases at distant sites within the peritoneal cavity. The

ability to recruit vasculature is a key component for tumours to be able to establish these secondary metastases. Decreased BMP signaling will therefore improve the ability of tumours to recruit vasculature at these secondary sites, and as a result will be better able to grow and survive upon reattachment.

Due to the complicated nature of the BMP signaling pathway both with respect to its activation and regulation, as well as its multiple roles in various stages of EOC progression, further research will be required in order to gain a more thorough understanding of this pathway in ovarian cancer despite the recent and ongoing advancements in our lab. However, this pathway has important potential future implications for prognostics. For example, elevated BMP4 and potentially BMP2 levels with ovarian cancer could be considered in order to assist with prognoses for patients. This is because decreased BMP levels in patients would be considered to be a negative prognostic factor due to the fact it would correlate with an increased ability of the EOC tumour to further metastasize, and as a result correlate with lower survival outcomes. Additionally, targeting the BMP pathway has potential therapeutic value. For example, in patients with more advanced stages of EOC in which the tumour has already begun to metastasize, therapeutics could possibly be used to increase levels of BMP signaling in EOC cells. This could decrease the ability of additional EOC cells from forming secondary nodules, and could also decrease the survival ability of already metastasized tumours by limiting their abilities to recruit a sufficient blood supply.

4.2 Future directions

BMP signaling as an anti-angiogenic pathway in cancer is a fairly novel concept that has only come to light in the past decade (Buckley, Shi et al. 2004; Stabile, Mitola et al. 2007). Of these studies, there is only one of which we are aware that suggests a potential downstream target of increased BMP signaling that contributes to decreased angiogenesis in cancer. This study by Stabile et al. suggests that in lung cancer, increased BMP4 signaling leads to decreased VEGF protein expression (Stabile, Mitola et al. 2007). Our lab plans to contribute to BMP signaling research in cancer by investigating potential downstream targets of increased BMP signaling that lead to a decreased ability of mouse ovarian cancer cells to enhance angiogenesis. This will be accomplished by comparing the mRNA or protein expression levels of well known pro-angiogenic factors such as VEGF as well as angiogenesis inhibitors such as TSP-1 in our ALK3QD-transfected clones, BMP4-treated cells, Noggin-treated cells, or LDN-193189-treated cells. Expression levels will then be compared to the untreated parental mouse EOC cell lines. An alternative approach will be to use RNA or protein-based array screens that are specifically designed to evaluate a large number of angiogenic growth factors and related proteins. We also plan to conduct future experiments in order to provide additional evidence that angiogenesis is responsible for the differential abilities of the three mouse EOC cell lines to form tumours on the chick CAM. Based on my current data, I hypothesize that MASC2 cells would be able to form tumours on the chick CAM if the angiogenic potential of these cells was significantly increased. Therefore, MASC2 cells will be transfected in order to overexpress a major pro-angiogenic factor such as VEGF,

after which time these transfected cells will be inoculated onto the surface of the chick CAM to assess tumour growth.

My studies have further supported the use of the chick CAM as an effective model system that can be used to study EOC. Although there has been one study that has investigated the effects of whole MAF from patients with ovarian cancer on angiogenesis by inoculating this fluid onto the surface of the CAM (Richardson, Gunawan et al. 2002), there have been no studies of which we are aware that have used the chick CAM to study primary human EOC cells specifically. Therefore, my findings relating to the role of BMP signaling in mouse EOC cells on the chick CAM now provides an initial starting point from which our lab will be able to assess the effect of altered BMP signaling on tumour growth and angiogenesis in primary human EOC cells using this model system. These primary human EOC cells will be directly isolated from patient ascites fluid by using a protocol that was previously developed by Dr. Trevor Shepherd (Shepherd, Theriault et al. 2006). Additionally, the ease of use and large-scale applicability of the chick CAM model system provides unique opportunities in the future to rapidly test novel therapeutic compounds, specifically compounds targeting BMP signaling pathway in EOC that can be directly tested in this model system. For example, anti-angiogenic agents that would act by enhancing BMP signaling and therefore decrease the angiogenic potential of metastatic EOC tumours could be applied to the chick CAM, which could then lead to mouse and human trials, and eventually to improved therapeutic outcomes for patients.

REFERENCES

Akiyoshi, S., H. Inoue, et al. (1999). "c-Ski acts as a transcriptional co-repressor in transforming growth factor-beta signaling through interaction with smads." J Biol Chem **274**(49): 35269-77.

Allen, H. J., C. Porter, et al. (1987). "Isolation and morphologic characterization of human ovarian carcinoma cell clusters present in effusions." Exp Cell Biol **55**(4): 194-208.

Antoniou, A., P. D. Pharoah, et al. (2003). "Average risks of breast and ovarian cancer associated with BRCA1 or BRCA2 mutations detected in case Series unselected for family history: a combined analysis of 22 studies." Am J Hum Genet **72**(5): 1117-30.

Argento, M., P. Hoffman, et al. (2008). "Ovarian cancer detection and treatment: current situation and future prospects." Anticancer Res **28**(5B): 3135-8.

Arihiro, K. and K. Inai (2001). "Expression of CD31, Met/hepatocyte growth factor receptor and bone morphogenetic protein in bone metastasis of osteosarcoma." Pathol Int **51**(2): 100-6.

Armstrong, D. K., B. Bundy, et al. (2006). "Intraperitoneal cisplatin and paclitaxel in ovarian cancer." N Engl J Med **354**(1): 34-43.

Audeh, M. W., J. Carmichael, et al. (2010). "Oral poly(ADP-ribose) polymerase inhibitor olaparib in patients with BRCA1 or BRCA2 mutations and recurrent ovarian cancer: a proof-of-concept trial." Lancet **376**(9737): 245-51.

Auerbach, R., L. Kubai, et al. (1974). "A simple procedure for the long-term cultivation of chicken embryos." Dev Biol **41**(2): 391-4.

Auersperg, N., A. S. Wong, et al. (2001). "Ovarian surface epithelium: biology, endocrinology, and pathology." Endocr Rev **22**(2): 255-88.

Auf, G., A. Jabouille, et al. (2010). "Inositol-requiring enzyme 1alpha is a key regulator of angiogenesis and invasion in malignant glioma." Proc Natl Acad Sci U S A **107**(35): 15553-8.

Azar, W. J., S. H. Azar, et al. (2011). "IGFBP-2 Enhances VEGF Gene Promoter Activity and Consequent Promotion of Angiogenesis by Neuroblastoma Cells." Endocrinology.

Batlle, E., E. Sancho, et al. (2000). "The transcription factor snail is a repressor of E-cadherin gene expression in epithelial tumour cells." Nat Cell Biol **2**(2): 84-9.

Benezra, R., R. L. Davis, et al. (1990). "The protein Id: a negative regulator of helix-loop-helix DNA binding proteins." Cell **61**(1): 49-59.

Benezra, R., S. Rafii, et al. (2001). "The Id proteins and angiogenesis." Oncogene **20**(58): 8334-41.

Beppu, H., F. Ichinose, et al. (2004). "BMPR-II heterozygous mice have mild pulmonary hypertension and an impaired pulmonary vascular remodeling response to prolonged hypoxia." Am J Physiol Lung Cell Mol Physiol **287**(6): L1241-7.

Bergers, G. and L. E. Benjamin (2003). "Tumorigenesis and the angiogenic switch." Nat Rev Cancer **3**(6): 401-10.

Bieniasz, M., K. Oszajca, et al. (2009). "The positive correlation between gene expression of the two angiogenic factors: VEGF and BMP-2 in lung cancer patients." Lung Cancer **66**(3): 319-26.

Bilici, A., T. Salepci, et al. (2010). "Neoadjuvant chemotherapy followed by interval cytoreductive surgery in patients with unresectable, advanced stage epithelial ovarian cancer: a single centre experience." Arch Gynecol Obstet **282**(4): 417-25.

Blanco Calvo, M., V. Bolos Fernandez, et al. (2009). "Biology of BMP signalling and cancer." Clin Transl Oncol **11**(3): 126-37.

Blitz, I. L. and K. W. Cho (2009). "Finding partners: how BMPs select their targets." Dev Dyn **238**(6): 1321-31.

Bradford, M. M. (1976). "A rapid and sensitive method for the quantitation of microgram quantities of protein utilizing the principle of protein-dye binding." Anal Biochem **72**: 248-54.

Bragdon, B., O. Moseychuk, et al. (2011). "Bone morphogenetic proteins: a critical review." Cell Signal **23**(4): 609-20.

Buckley, S., W. Shi, et al. (2004). "BMP4 signaling induces senescence and modulates the oncogenic phenotype of A549 lung adenocarcinoma cells." Am J Physiol Lung Cell Mol Physiol **286**(1): L81-6.

Canada, C. C. S. N. C. I. o. (2010). Canadian Cancer Statistics 2010. Canadian Cancer Statistics 2010.

Chambers, A. F., A. C. Groom, et al. (2002). "Dissemination and growth of cancer cells in metastatic sites." Nat Rev Cancer **2**(8): 563-72.

Cheng, Y. J., J. W. Tsai, et al. (2011). "Id1 promotes lung cancer cell proliferation and tumor growth through Akt-related pathway." Cancer Lett.

Chim, S. M., A. Qin, et al. (2011). "EGFL6 promotes endothelial cell migration and angiogenesis through the activation of ERK." J Biol Chem.

Cho, K. R. (2009). "Ovarian cancer update: lessons from morphology, molecules, and mice." Arch Pathol Lab Med **133**(11): 1775-81.

Cho, K. R. and M. Shih Ie (2009). "Ovarian cancer." Annu Rev Pathol **4**: 287-313.

Connolly, D. C. (2009). "Animal models of ovarian cancer." Cancer Treat Res **149**: 353-91.

Connolly, D. C., R. Bao, et al. (2003). "Female mice chimeric for expression of the simian virus 40 TAg under control of the MISIIR promoter develop epithelial ovarian cancer." Cancer Res **63**(6): 1389-97.

Coppola, D., B. Saunders, et al. (1999). "The insulin-like growth factor 1 receptor induces transformation and tumorigenicity of ovarian mesothelial cells and down-regulates their Fas-receptor expression." Cancer Res **59**(13): 3264-70.

Cragun, J. M. (2011). "Screening for ovarian cancer." Cancer Control **18**(1): 16-21.

Davies, B. R., N. Auersperg, et al. (1998). "Transfection of rat ovarian surface epithelium with erb-B2/neu induces transformed phenotypes in vitro and the tumorigenic phenotype in vivo." Am J Pathol **152**(1): 297-306.

Deckers, M. M., R. L. van Bezooijen, et al. (2002). "Bone morphogenetic proteins stimulate angiogenesis through osteoblast-derived vascular endothelial growth factor A." Endocrinology **143**(4): 1545-53.

Deng, H., R. Makizumi, et al. (2007). "Bone morphogenetic protein-4 is overexpressed in colonic adenocarcinomas and promotes migration and invasion of HCT116 cells." Exp Cell Res **313**(5): 1033-44.

Deng, H., T. S. Ravikumar, et al. (2009). "Overexpression of bone morphogenetic protein 4 enhances the invasiveness of Smad4-deficient human colorectal cancer cells." Cancer Lett **281**(2): 220-31.

Deryugina, E. I. and J. P. Quigley (2008). "Chapter 2. Chick embryo chorioallantoic membrane models to quantify angiogenesis induced by inflammatory and tumor cells or purified effector molecules." Methods Enzymol **444**: 21-41.

Deryugina, E. I. and J. P. Quigley (2008). "Chick embryo chorioallantoic membrane model systems to study and visualize human tumor cell metastasis." Histochem Cell Biol **130**(6): 1119-30.

Dings, R. P., X. Chen, et al. (2006). "Design of nonpeptidic topomimetics of antiangiogenic proteins with antitumor activities." J Natl Cancer Inst **98**(13): 932-6.

Dinulescu, D. M., T. A. Ince, et al. (2005). "Role of K-ras and Pten in the development of mouse models of endometriosis and endometrioid ovarian cancer." Nat Med **11**(1): 63-70.

Downer, J. B., L. A. Jones, et al. (2001). "Effect of administration route on FES uptake into MCF-7 tumors." Nucl Med Biol **28**(4): 397-9.

Erickson, G. F. and S. Shimasaki (2003). "The spatiotemporal expression pattern of the bone morphogenetic protein family in rat ovary cell types during the estrous cycle." Reprod Biol Endocrinol **1**: 9.

Ernst, A., S. Hofmann, et al. (2009). "Genomic and expression profiling of glioblastoma stem cell-like spheroid cultures identifies novel tumor-relevant genes associated with survival." Clin Cancer Res **15**(21): 6541-50.

Fang, J., Q. Zhou, et al. (2007). "Apigenin inhibits tumor angiogenesis through decreasing HIF-1alpha and VEGF expression." Carcinogenesis **28**(4): 858-64.

Fathalla, M. F. (1971). "Incessant ovulation--a factor in ovarian neoplasia?" Lancet **2**(7716): 163.

Feeley, B. T., S. C. Gamradt, et al. (2005). "Influence of BMPs on the formation of osteoblastic lesions in metastatic prostate cancer." J Bone Miner Res **20**(12): 2189-99.

Flesken-Nikitin, A., K. C. Choi, et al. (2003). "Induction of carcinogenesis by concurrent inactivation of p53 and Rb1 in the mouse ovarian surface epithelium." Cancer Res **63**(13): 3459-63.

Fogel, M., P. Gutwein, et al. (2003). "L1 expression as a predictor of progression and survival in patients with uterine and ovarian carcinomas." Lancet **362**(9387): 869-75.

Forootan, S. S., Y. C. Wong, et al. (2007). "Increased Id-1 expression is significantly associated with poor survival of patients with prostate cancer." Hum Pathol **38**(9): 1321-9.

Friedli, A., E. Fischer, et al. (2009). "The soluble form of the cancer-associated L1 cell adhesion molecule is a pro-angiogenic factor." Int J Biochem Cell Biol **41**(7): 1572-80.

Gao, F., M. L. Cao, et al. (2004). "Brain hyaluronan binding protein inhibits tumor growth." Chin Med J (Engl) **117**(7): 1072-8.

Gao, Q., W. Tong, et al. (2010). "Effects of bone morphogenetic protein-2 on proliferation and angiogenesis in oral squamous cell carcinoma." Int J Oral Maxillofac Surg **39**(3): 266-71.

Gardner, G. J. and E. L. Jewell (2011). "Current and future directions of clinical trials for ovarian cancer." Cancer Control **18**(1): 44-51.

Gazzerro, E. and E. Canalis (2006). "Bone morphogenetic proteins and their antagonists." Rev Endocr Metab Disord **7**(1-2): 51-65.

Giacomini, D., M. Paez-Pereda, et al. (2006). "Bone morphogenetic protein-4 inhibits corticotroph tumor cells: involvement in the retinoic acid inhibitory action." Endocrinology **147**(1): 247-56.

Gilks, C. B. and J. Prat (2009). "Ovarian carcinoma pathology and genetics: recent advances." Hum Pathol **40**(9): 1213-23.

Goff, B. A., L. S. Mandel, et al. (2007). "Development of an ovarian cancer symptom index: possibilities for earlier detection." Cancer **109**(2): 221-7.

Goodell, C. A., J. A. Belisle, et al. (2009). "Characterization of the tumor marker muc16 (ca125) expressed by murine ovarian tumor cell lines and identification of a panel of cross-reactive monoclonal antibodies." J Ovarian Res **2**(1): 8.

Grcevic, D., R. Kusec, et al. (2010). "Bone morphogenetic proteins and receptors are over-expressed in bone-marrow cells of multiple myeloma patients and support myeloma cells by inducing ID genes." Leuk Res **34**(6): 742-51.

Greenaway, J., J. Henkin, et al. (2009). "ABT-510 induces tumor cell apoptosis and inhibits ovarian tumor growth in an orthotopic, syngeneic model of epithelial ovarian cancer." Mol Cancer Ther **8**(1): 64-74.

Groppe, J., J. Greenwald, et al. (2002). "Structural basis of BMP signalling inhibition by the cystine knot protein Noggin." Nature **420**(6916): 636-42.

Gu, Z., E. M. Reynolds, et al. (1999). "The type I serine/threonine kinase receptor ActRIA (ALK2) is required for gastrulation of the mouse embryo." Development **126**(11): 2551-61.

Gutwein, P., A. Stoeck, et al. (2005). "Cleavage of L1 in exosomes and apoptotic membrane vesicles released from ovarian carcinoma cells." Clin Cancer Res **11**(7): 2492-501.

Hagedorn, M., S. Javerzat, et al. (2005). "Accessing key steps of human tumor progression in vivo by using an avian embryo model." Proc Natl Acad Sci U S A **102**(5): 1643-8.

Hamada, S., K. Satoh, et al. (2007). "Bone morphogenetic protein 4 induces epithelial-mesenchymal transition through MSX2 induction on pancreatic cancer cell line." J Cell Physiol **213**(3): 768-74.

Han, E. S., P. Lin, et al. (2009). "Current status on biologic therapies in the treatment of epithelial ovarian cancer." Curr Treat Options Oncol **10**(1-2): 54-66.

Hanahan, D. and J. Folkman (1996). "Patterns and emerging mechanisms of the angiogenic switch during tumorigenesis." Cell **86**(3): 353-64.

Hanahan, D. and R. A. Weinberg (2011). "Hallmarks of cancer: the next generation." Cell **144**(5): 646-74.

Haubold, M., A. Weise, et al. (2010). "Bone morphogenetic protein 4 (BMP4) signaling in retinoblastoma cells." Int J Biol Sci **6**(7): 700-15.

Hay, E., J. Lemonnier, et al. (2001). "Bone morphogenetic protein-2 promotes osteoblast apoptosis through a Smad-independent, protein kinase C-dependent signaling pathway." J Biol Chem **276**(31): 29028-36.

He, C. and X. Chen (2005). "Transcription regulation of the vegf gene by the BMP/Smad pathway in the angioblast of zebrafish embryos." Biochem Biophys Res Commun **329**(1): 324-30.

Hebert, J. M., M. Hayhurst, et al. (2003). "BMP ligands act redundantly to pattern the dorsal telencephalic midline." Genesis **35**(4): 214-9.

Heinke, J., L. Wehofsits, et al. (2008). "BMPER is an endothelial cell regulator and controls bone morphogenetic protein-4-dependent angiogenesis." Circ Res **103**(8): 804-12.

Hjertner, O., H. Hjorth-Hansen, et al. (2001). "Bone morphogenetic protein-4 inhibits proliferation and induces apoptosis of multiple myeloma cells." Blood **97**(2): 516-22.

Hocevar, B. A., T. L. Brown, et al. (1999). "TGF-beta induces fibronectin synthesis through a c-Jun N-terminal kinase-dependent, Smad4-independent pathway." Embo J **18**(5): 1345-56.

Hoodless, P. A., T. Haerry, et al. (1996). "MADR1, a MAD-related protein that functions in BMP2 signaling pathways." Cell **85**(4): 489-500.

Hseu, Y. C., C. R. Wu, et al. (2011). "Inhibitory effects of Physalis angulata on tumor metastasis and angiogenesis." J Ethnopharmacol **135**(3): 762-71.

Huang, J., L. Zhang, et al. (2011). "Frequent genetic abnormalities of the PI3K/AKT pathway in primary ovarian cancer predict patient outcome." Genes Chromosomes Cancer **50**(8): 606-18.

Hussein, S. M., E. K. Duff, et al. (2003). "Smad4 and beta-catenin co-activators functionally interact with lymphoid-enhancing factor to regulate graded expression of Msx2." J Biol Chem **278**(49): 48805-14.

Iantosca, M. R., C. E. McPherson, et al. (1999). "Bone morphogenetic proteins-2 and -4 attenuate apoptosis in a cerebellar primitive neuroectodermal tumor cell line." J Neurosci Res **56**(3): 248-58.

Imamura, T., M. Takase, et al. (1997). "Smad6 inhibits signalling by the TGF-beta superfamily." Nature **389**(6651): 622-6.

Izzi, L. and L. Attisano (2004). "Regulation of the TGFbeta signalling pathway by ubiquitin-mediated degradation." Oncogene **23**(11): 2071-8.

Jacobs, I. J. and U. Menon (2004). "Progress and challenges in screening for early detection of ovarian cancer." Mol Cell Proteomics **3**(4): 355-66.

Jatoi, A., K. F. Giordano, et al. (2005). "Targeting and palliating malignant ascites: an overview of an upcoming clinical trial from the north central cancer treatment group." Support Cancer Ther **3**(1): 59-62.

Jelovac, D. and D. K. Armstrong (2011). "Recent progress in the diagnosis and treatment of ovarian cancer." CA Cancer J Clin **61**(3): 183-203.

Jemal, A., R. Siegel, et al. (2008). "Cancer statistics, 2008." CA Cancer J Clin **58**(2): 71-96.

Johnson, K. A. (2009). "The standard of perfection: thoughts about the laying hen model of ovarian cancer." Cancer Prev Res (Phila) **2**(2): 97-9.

Judson, P. L., X. He, et al. (1999). "Overexpression of focal adhesion kinase, a protein tyrosine kinase, in ovarian carcinoma." Cancer **86**(8): 1551-6.

Kane, R., C. Godson, et al. (2008). "Chordin-like 1, a bone morphogenetic protein-4 antagonist, is upregulated by hypoxia in human retinal pericytes and plays a role in regulating angiogenesis." Mol Vis **14**: 1138-48.

Karst, A. M. and R. Drapkin (2010). "Ovarian cancer pathogenesis: a model in evolution." J Oncol **2010**: 932371.

Ketolainen, J. M., E. L. Alarmo, et al. (2010). "Parallel inhibition of cell growth and induction of cell migration and invasion in breast cancer cells by bone morphogenetic protein 4." Breast Cancer Res Treat **124**(2): 377-86.

Kido, M. and M. Shibuya (1998). "Isolation and characterization of mouse ovarian surface epithelial cell lines." Pathol Res Pract **194**(10): 725-30.

Kim, T. H., E. G. Hur, et al. (2011). "NRF2 blockade suppresses colon tumor angiogenesis by inhibiting hypoxia-induced activation of HIF-1alpha." Cancer Res **71**(6): 2260-75.

Kiyono, M. and M. Shibuya (2003). "Bone morphogenetic protein 4 mediates apoptosis of capillary endothelial cells during rat pupillary membrane regression." Mol Cell Biol **23**(13): 4627-36.

Kiyono, M. and M. Shibuya (2006). "Inhibitory Smad transcription factors protect arterial endothelial cells from apoptosis induced by BMP4." Oncogene **25**(54): 7131-7.

Konishi, I., H. Kuroda, et al. (1999). "Review: gonadotropins and development of ovarian cancer." Oncology **57 Suppl 2**: 45-8.

Kubota, Y., H. K. Kleinman, et al. (1988). "Role of laminin and basement membrane in the morphological differentiation of human endothelial cells into capillary-like structures." J Cell Biol **107**(4): 1589-98.

Laklai, H., S. Laval, et al. (2009). "Thrombospondin-1 is a critical effector of oncosuppressive activity of sst2 somatostatin receptor on pancreatic cancer." Proc Natl Acad Sci U S A **106**(42): 17769-74.

Langenfeld, E. M. and J. Langenfeld (2004). "Bone morphogenetic protein-2 stimulates angiogenesis in developing tumors." Mol Cancer Res **2**(3): 141-9.

Laviolette, L. A., K. Garson, et al. (2010). "17beta-estradiol accelerates tumor onset and decreases survival in a transgenic mouse model of ovarian cancer." Endocrinology **151**(3): 929-38.

Lechleider, R. J., J. L. Ryan, et al. (2001). "Targeted mutagenesis of Smad1 reveals an essential role in chorioallantoic fusion." Dev Biol **240**(1): 157-67.

Levanon, K., C. Crum, et al. (2008). "New insights into the pathogenesis of serous ovarian cancer and its clinical impact." J Clin Oncol **26**(32): 5284-93.

Liang, G., C. Butterfield, et al. (2011). "Beta-35 is a transferrin-derived inhibitor of angiogenesis and tumor growth." Biochem Biophys Res Commun **409**(3): 562-6.

Liu, B., D. Tian, et al. (2010). "Effect of bone morphogenetic protein 4 in the human brain glioma cell line U251." Cell Biochem Biophys **58**(2): 91-6.

Lombardo, Y., A. Scopelliti, et al. (2011). "Bone morphogenetic protein 4 induces differentiation of colorectal cancer stem cells and increases their response to chemotherapy in mice." Gastroenterology **140**(1): 297-309.

Luo, H., G. O. Rankin, et al. (2009). "Kaempferol inhibits angiogenesis and VEGF expression through both HIF dependent and independent pathways in human ovarian cancer cells." Nutr Cancer **61**(4): 554-63.

Lyden, D., A. Z. Young, et al. (1999). "Id1 and Id3 are required for neurogenesis, angiogenesis and vascularization of tumour xenografts." Nature **401**(6754): 670-7.

Ma, Y., L. Ma, et al. (2010). "Expression of bone morphogenetic protein-2 and its receptors in epithelial ovarian cancer and their influence on the prognosis of ovarian cancer patients." J Exp Clin Cancer Res **29**: 85.

Mackey, J. R. and P. M. Venner (1996). "Malignant ascites: demographics, therapeutic efficacy and predictors of survival." Can J Oncol **6**(2): 474-80.

Maegdefrau, U., T. Amann, et al. (2009). "Bone morphogenetic protein 4 is induced in hepatocellular carcinoma by hypoxia and promotes tumour progression." J Pathol **218**(4): 520-9.

Massague, J. (2008). "TGFbeta in Cancer." Cell **134**(2): 215-30.

Mathura, J. R., Jr., N. Jafari, et al. (2000). "Bone morphogenetic proteins-2 and -4: negative growth regulators in adult retinal pigmented epithelium." Invest Ophthalmol Vis Sci **41**(2): 592-600.

McLean, K., Y. Gong, et al. (2011). "Human ovarian carcinoma-associated mesenchymal stem cells regulate cancer stem cells and tumorigenesis via altered BMP production." J Clin Invest.

Medeiros, F., M. G. Muto, et al. (2006). "The tubal fimbria is a preferred site for early adenocarcinoma in women with familial ovarian cancer syndrome." Am J Surg Pathol **30**(2): 230-6.

Mehrara, E., E. Forssell-Aronsson, et al. (2007). "Specific growth rate versus doubling time for quantitative characterization of tumor growth rate." Cancer Res **67**(8): 3970-5.

Mern, D. S., J. Hasskarl, et al. (2010). "Inhibition of Id proteins by a peptide aptamer induces cell-cycle arrest and apoptosis in ovarian cancer cells." Br J Cancer **103**(8): 1237-44.

Mishina, Y., A. Suzuki, et al. (1995). "Bmpr encodes a type I bone morphogenetic protein receptor that is essential for gastrulation during mouse embryogenesis." Genes Dev **9**(24): 3027-37.

Mitchell, D., E. G. Pobre, et al. (2010). "ALK1-Fc inhibits multiple mediators of angiogenesis and suppresses tumor growth." Mol Cancer Ther **9**(2): 379-88.

Mitola, S., E. Moroni, et al. (2008). "Angiopoietin-1 mediates the proangiogenic activity of the bone morphogenic protein antagonist Drm." Blood **112**(4): 1154-7.

Moll, F., C. Millet, et al. (2006). "Chordin is underexpressed in ovarian tumors and reduces tumor cell motility." Faseb J **20**(2): 240-50.

Montesano, R. (2007). "Bone morphogenetic protein-4 abrogates lumen formation by mammary epithelial cells and promotes invasive growth." Biochem Biophys Res Commun **353**(3): 817-22.

Montesano, R., R. Sarkozi, et al. (2008). "Bone morphogenetic protein-4 strongly potentiates growth factor-induced proliferation of mammary epithelial cells." Biochem Biophys Res Commun **374**(1): 164-8.

Moser, M. and C. Patterson (2005). "Bone morphogenetic proteins and vascular differentiation: BMPing up vasculogenesis." Thromb Haemost **94**(4): 713-8.

Moustakas, A. and C. H. Heldin (2009). "The regulation of TGFbeta signal transduction." Development **136**(22): 3699-714.

Mutch, D. G. (2002). "Surgical management of ovarian cancer." Semin Oncol **29**(1 Suppl 1): 3-8.

Nagy, J. A., S. H. Chang, et al. (2010). "Heterogeneity of the tumor vasculature." Semin Thromb Hemost **36**(3): 321-31.

Nakamura, K., T. Shirai, et al. (1999). "p38 mitogen-activated protein kinase functionally contributes to chondrogenesis induced by growth/differentiation factor-5 in ATDC5 cells." Exp Cell Res **250**(2): 351-63.

Naora, H. and D. J. Montell (2005). "Ovarian cancer metastasis: integrating insights from disparate model organisms." Nat Rev Cancer **5**(5): 355-66.

Nguyen, M., Y. Shing, et al. (1994). "Quantitation of angiogenesis and antiangiogenesis in the chick embryo chorioallantoic membrane." Microvasc Res **47**(1): 31-40.

Nishanian, T. G., J. S. Kim, et al. (2004). "Suppression of tumorigenesis and activation of Wnt signaling by bone morphogenetic protein 4 in human cancer cells." Cancer Biol Ther **3**(7): 667-75.

Norton, J. D. (2000). "ID helix-loop-helix proteins in cell growth, differentiation and tumorigenesis." J Cell Sci **113 (Pt 22)**: 3897-905.

Norton, J. D. and G. T. Atherton (1998). "Coupling of cell growth control and apoptosis functions of Id proteins." Mol Cell Biol **18**(4): 2371-81.

Ossowski, L. and E. Reich (1980). "Experimental model for quantitative study of metastasis." Cancer Res **40**(7): 2300-9.

Ozols, R. F., M. A. Bookman, et al. (2004). "Focus on epithelial ovarian cancer." Cancer Cell **5**(1): 19-24.

Paez-Pereda, M., D. Giacomini, et al. (2003). "Involvement of bone morphogenetic protein 4 (BMP-4) in pituitary prolactinoma pathogenesis through a Smad/estrogen receptor crosstalk." Proc Natl Acad Sci U S A **100**(3): 1034-9.

Pekarik, V., D. Bourikas, et al. (2003). "Screening for gene function in chicken embryo using RNAi and electroporation." Nat Biotechnol **21**(1): 93-6.

Pengetnze, Y., M. Steed, et al. (2003). "Src tyrosine kinase promotes survival and resistance to chemotherapeutics in a mouse ovarian cancer cell line." Biochem Biophys Res Commun **309**(2): 377-83.

Pesce, S. and R. Benezra (1993). "The loop region of the helix-loop-helix protein Id1 is critical for its dominant negative activity." Mol Cell Biol **13**(12): 7874-80.

Pi, X., R. Ren, et al. (2007). "Sequential roles for myosin-X in BMP6-dependent filopodial extension, migration, and activation of BMP receptors." J Cell Biol **179**(7): 1569-82.

Piccirillo, S. G., B. A. Reynolds, et al. (2006). "Bone morphogenetic proteins inhibit the tumorigenic potential of human brain tumour-initiating cells." Nature **444**(7120): 761-5.

Pils, D., M. Wittinger, et al. (2010). "BAMBI is overexpressed in ovarian cancer and co-translocates with Smads into the nucleus upon TGF-beta treatment." Gynecol Oncol **117**(2): 189-97.

Qiu, H., B. Yang, et al. (2010). "WSS25 inhibits growth of xenografted hepatocellular cancer cells in nude mice by disrupting angiogenesis via blocking bone morphogenetic protein (BMP)/Smad/Id1 signaling." J Biol Chem **285**(42): 32638-46.

Raida, M., J. H. Clement, et al. (2005). "Bone morphogenetic protein 2 (BMP-2) and induction of tumor angiogenesis." J Cancer Res Clin Oncol **131**(11): 741-50.

Ren, R., P. C. Charles, et al. (2007). "Gene expression profiles identify a role for cyclooxygenase 2-dependent prostanoid generation in BMP6-induced angiogenic responses." Blood **109**(7): 2847-53.

Ribatti, D., A. Vacca, et al. (1996). "The chick embryo chorioallantoic membrane as a model for in vivo research on angiogenesis." Int J Dev Biol **40**(6): 1189-97.

Richardson, M., J. Gunawan, et al. (2002). "Malignant ascites fluid (MAF), including ovarian-cancer-associated MAF, contains angiostatin and other factor(s) which inhibit angiogenesis." Gynecol Oncol **86**(3): 279-87.

Roby, K. F., C. C. Taylor, et al. (2000). "Development of a syngeneic mouse model for events related to ovarian cancer." Carcinogenesis **21**(4): 585-91.

Rothhammer, T., F. Bataille, et al. (2007). "Functional implication of BMP4 expression on angiogenesis in malignant melanoma." Oncogene **26**(28): 4158-70.

Rothhammer, T., I. Poser, et al. (2005). "Bone morphogenic proteins are overexpressed in malignant melanoma and promote cell invasion and migration." Cancer Res **65**(2): 448-56.

Satoh, K., S. Hamada, et al. (2008). "Up-regulation of MSX2 enhances the malignant phenotype and is associated with twist 1 expression in human pancreatic cancer cells." Am J Pathol **172**(4): 926-39.

Schmitt, J. and D. Matei (2011). "Targeting angiogenesis in ovarian cancer." Cancer Treat Rev.

Seandel, M., K. Noack-Kunnmann, et al. (2001). "Growth factor-induced angiogenesis in vivo requires specific cleavage of fibrillar type I collagen." Blood **97**(8): 2323-32.

Shen, F. Z., J. Wang, et al. (2010). "Low-dose metronomic chemotherapy with cisplatin: can it suppress angiogenesis in H22 hepatocarcinoma cells?" Int J Exp Pathol **91**(1): 10-6.

Shepherd, T. G., M. L. Mujoomdar, et al. (2010). "Constitutive activation of BMP signalling abrogates experimental metastasis of OVCA429 cells via reduced cell adhesion." J Ovarian Res **3**: 5.

Shepherd, T. G. and M. W. Nachtigal (2003). "Identification of a putative autocrine bone morphogenetic protein-signaling pathway in human ovarian surface epithelium and ovarian cancer cells." Endocrinology **144**(8): 3306-14.

Shepherd, T. G., B. L. Theriault, et al. (2006). "Primary culture of ovarian surface epithelial cells and ascites-derived ovarian cancer cells from patients." Nat Protoc **1**(6): 2643-9.

Shepherd, T. G., B. L. Theriault, et al. (2008). "Autocrine BMP4 signalling regulates ID3 proto-oncogene expression in human ovarian cancer cells." Gene **414**(1-2): 95-105.

Shield, K., M. L. Ackland, et al. (2009). "Multicellular spheroids in ovarian cancer metastases: Biology and pathology." Gynecol Oncol **113**(1): 143-8.

Shon, S. K., A. Kim, et al. (2009). "Bone morphogenetic protein-4 induced by NDRG2 expression inhibits MMP-9 activity in breast cancer cells." Biochem Biophys Res Commun **385**(2): 198-203.

Sirard, C., J. L. de la Pompa, et al. (1998). "The tumor suppressor gene Smad4/Dpc4 is required for gastrulation and later for anterior development of the mouse embryo." Genes Dev **12**(1): 107-19.

Sneddon, J. B., H. H. Zhen, et al. (2006). "Bone morphogenetic protein antagonist gremlin 1 is widely expressed by cancer-associated stromal cells and can promote tumor cell proliferation." Proc Natl Acad Sci U S A **103**(40): 14842-7.

Spanjol, J., G. Djordjevic, et al. (2010). "Role of bone morphogenetic proteins in human prostate cancer pathogenesis and development of bone metastases: immunohistochemical study." Coll Antropol **34 Suppl 2**: 119-25.

Stabile, H., S. Mitola, et al. (2007). "Bone morphogenic protein antagonist Drm/gremlin is a novel proangiogenic factor." Blood **109**(5): 1834-40.

Staton, C. A., M. W. Reed, et al. (2009). "A critical analysis of current in vitro and in vivo angiogenesis assays." Int J Exp Pathol **90**(3): 195-221.

Su, D., S. Zhu, et al. (2009). "BMP4-Smad signaling pathway mediates adriamycin-induced premature senescence in lung cancer cells." J Biol Chem **284**(18): 12153-64.

Subauste, M. C., T. A. Kupriyanova, et al. (2009). "Evaluation of metastatic and angiogenic potentials of human colon carcinoma cells in chick embryo model systems." Clin Exp Metastasis **26**(8): 1033-47.

Szotek, P. P., R. Pieretti-Vanmarcke, et al. (2006). "Ovarian cancer side population defines cells with stem cell-like characteristics and Mullerian Inhibiting Substance responsiveness." Proc Natl Acad Sci U S A **103**(30): 11154-9.

Tanaka, Y., Y. Terai, et al. (2011). "Prognostic effect of epidermal growth factor receptor gene mutations and the aberrant phosphorylation of Akt and ERK in ovarian cancer." Cancer Biol Ther **11**(1): 50-7.

Thawani, J. P., A. C. Wang, et al. (2010). "Bone morphogenetic proteins and cancer: review of the literature." Neurosurgery **66**(2): 233-46; discussion 246.

Theriault, B. L., T. G. Shepherd, et al. (2007). "BMP4 induces EMT and Rho GTPase activation in human ovarian cancer cells." Carcinogenesis **28**(6): 1153-62.

Valdimarsdottir, G., M. J. Goumans, et al. (2002). "Stimulation of Id1 expression by bone morphogenetic protein is sufficient and necessary for bone morphogenetic protein-induced activation of endothelial cells." Circulation **106**(17): 2263-70.

Vogt, R. R., R. Unda, et al. (2006). "Bone morphogenetic protein-4 enhances vascular endothelial growth factor secretion by human retinal pigment epithelial cells." J Cell Biochem **98**(5): 1196-202.

Wagner, D. O., C. Sieber, et al. (2010). "BMPs: from bone to body morphogenetic proteins." Sci Signal **3**(107): mr1.

Waite, K. A. and C. Eng (2003). "From developmental disorder to heritable cancer: it's all in the BMP/TGF-beta family." Nat Rev Genet **4**(10): 763-73.

Wiener, J. R., T. C. Windham, et al. (2003). "Activated SRC protein tyrosine kinase is overexpressed in late-stage human ovarian cancers." Gynecol Oncol **88**(1): 73-9.

Winnier, G., M. Blessing, et al. (1995). "Bone morphogenetic protein-4 is required for mesoderm formation and patterning in the mouse." Genes Dev **9**(17): 2105-16.

Wu, R., N. Hendrix-Lucas, et al. (2007). "Mouse model of human ovarian endometrioid adenocarcinoma based on somatic defects in the Wnt/beta-catenin and PI3K/Pten signaling pathways." Cancer Cell **11**(4): 321-33.

Yang, H. Y., H. L. Liu, et al. (2010). "Expression and prognostic value of Id protein family in human breast carcinoma." Oncol Rep **23**(2): 321-8.

Yang, X., L. H. Castilla, et al. (1999). "Angiogenesis defects and mesenchymal apoptosis in mice lacking SMAD5." Development **126**(8): 1571-80.

Yao, D. S., L. Li, et al. (2006). "[The mouse ovarian surface epithelium cells (MOSE) transformation induced by c-myc/K-ras in]." Zhonghua Zhong Liu Za Zhi **28**(12): 881-5.

Yu, P. B., D. Y. Deng, et al. (2008). "BMP type I receptor inhibition reduces heterotopic [corrected] ossification." Nat Med **14**(12): 1363-9.

Zhao, H., O. Ayrault, et al. (2008). "Post-transcriptional down-regulation of Atoh1/Math1 by bone morphogenic proteins suppresses medulloblastoma development." Genes Dev **22**(6): 722-7.

Zietarska, M., C. M. Maugard, et al. (2007). "Molecular description of a 3D in vitro model for the study of epithelial ovarian cancer (EOC)." Mol Carcinog **46**(10): 872-85.

Zijlstra, A., M. Seandel, et al. (2006). "Proangiogenic role of neutrophil-like inflammatory heterophils during neovascularization induced by growth factors and human tumor cells." Blood **107**(1): 317-27.

Appendix A: Chick CAM Animal Use Ethics Approval

Principal investigator: Dr. John Lewis

Animal use protocol application title: Migration-mediated intravasation and tumour cell metastasis in cancer

Animal use protocol application number: 2007-087